DESIGN AND EVALUATION OF COMPOSITE CAR-FRONT SUBFRAME RAILS IN A SEDAN AND ITS CORRESPONDING OCCUPANT CRASH INJURY RESPONSE

A Thesis by

Kumar Nijagal Honnagangaiah

Bachelor of Engineering, Bangalore University, India, 2001

Submitted to the Department of Mechanical Engineering
and the faculty of Graduate School of
Wichita State University in partial fulfillment of
the requirements for the degree of
Master of Science

May 2006

DESIGN AND EVALUATION OF COMPOSITE CAR-FRONT SUBFRAME RAILS IN A SEDAN AND ITS CORRESPONDING OCCUPANT CRASH INJURY RESPONSE

The following faculty members have examined the final copy of thesis for form and content and recommend that it be accepted in partial fulfillment of the requirements for the degree of Master of Science, with a major in Mechanical Engineering.

_____
Hamid M. Lankarani, Committee Chair

_____
Ramazan Asmatulu, Committee Member

_____
Krishna K Krishnan, Committee Member

DEDICATION

To My Parents

Smt Sarvamangala Honnagangaiah and Sri Nijagal Honnagangaiah

ACKNOWLEDGEMENTS

I would like to express my sincere gratitude to my graduate advisor, Dr. Hamid M. Lankarani, who has been instrumental in guiding me towards the successful completion of this thesis. I would also like to thank Dr. Ramazan Asmatulu and Dr. Krishna K. Krishnan for reviewing my thesis and making valuable suggestions.

I would like to express my gratefulness to my parents and my brothers Siddalinga Swamy. N.H and Sateesh. N.H, who have always supported my vision and have given me timely guidance, support and inspiration until now in every aspect of my education. Without their support, my stay and studies at Wichita State University would not have been possible.

I am indebted to National Institute for Aviation Research (NIAR) for supporting me financially throughout my Master's degree. I would like to acknowledge the support of my colleagues at NIAR, especially the managers Tiong Keng Tan, Tim Ng, and Kim Leng in the completion of this thesis.

Special thanks to Ashwin Sheshadri, Krishna N Pai, Divakara Basavaraju, Avinash Deshpande, Raghu Yedehalli, Vikram Krishnamurthy, Santosh Ankola, Santosh Reddy and Praveen Shivalli and all my friends in encouragement and suggestions throughout my Masters degree.

ABSTRACT

Today occupant safety is of a prime concern to every car manufacturer. New standards are being set for the safety of the occupant in different crash scenarios like frontal head on collision, angle impacts, side impacts, rear impacts and rollover. Among these standards, frontal impact is one of the fatal crash scenarios that lead to death of scores of people in the United States and across the globe. The automotive mid-rail is the main load carrying/energy-absorbing component in a event of frontal vehicle crash. In the contemporary world, fuel consumption also poses a serious issue that has to be considered. With these constraints in consideration, a lighter and stronger composite material is used in car front rail than steel. Using this material would help in reducing the fuel efficiency without sacrificing the safety of the vehicle.

In this research, section modeling of rails is designed to replace the present rail model and the injury sustained by the occupant is recorded. An attempt is made to use Carbon fiber/Epoxy and Glass fiber/epoxy composite materials for the rails. In addition, parametric study is carried out on the rail to find out the maximum possible energy absorbing parameters. It was found that carbon/epoxy rail with a pertinent orientation and thickness was absorbing more energy than the present steel rail. Energy absorption, displacement and the acceleration of the original and section model is compared and discussed in detail.

The Ford Taurus model is first validated using the LS-DYNA finite element software package and then dynamic analysis is performed on the original model and the section model according to the Federal Motor Vehicle Safety Standard (FMVSS) 208, the

New Car Assessment Program (NCAP) and the Insurance Institute for Highway Safety (IIHS) regulations. The vehicle displacements, Energy absorption and deceleration levels are compared for the steel, carbon-fiber epoxy and glass-fiber epoxy model. The occupant injuries are then evaluated for the full width rigid barrier test at 30 mph and 35 mph using the MADYMO, occupant modeling software package. With the new composite model and the section model the injury levels including, the head, neck and chest injuries are evaluated and compared. It is demonstrated that the new composite rail with carbon/epoxy is more effective than the present steel rail.

TABLE OF CONTENTS

TABLE OF CONTENTS (Continued)

CHAPTER **PAGE**

TABLE OF CONTENTS (Continued)

CHAPTER PAGE

LIST OF TABLES

TABLE **PAGE**

LIST OF FIGURES

FIGURE **PAGE**

LIST OF FIGURES (Continued)

FIGURE **PAGE**

CHAPTER 1

INTRODUCTION

1.1 Motivation

Automotive structures are developed to sustain impact loading in diverse crash conditions, such as, frontal perpendicular, angular, offset, pole impacts and side collisions. In addition, other non-crash functional requirements, such as, vibration, durability and fatigue life cycle are also integral part of vehicle design. However with growing focus on safety new vehicles are expected to be crash tested under newer and more demanding crash conditions, such as, the vehicle to vehicle 30 degree oblique offset impact under consideration by NHTSA. This shift may result into body structure designs with higher strength, stiffness and higher mass. At the same time environmental and fuel economy requirements dictate that vehicle design be lighter and compact resulting in smaller crush space. When crush space is limited, the body structure, typically designated to dissipate major share of impact energy, require thicker sheet metal and/or higher strengths alloys translating to added weight.

1.2 Crashworthiness

During an accident, the capability of vehicle structure to absorb the energy is defined as crashworthiness. In the present age lot of the people (around 30,000) die due to vehicle-to-vehicle frontal collisions. The vehicle must be designed such that, at higher speeds its occupants do not experience a net deceleration greater than 20 g.. Crashworthy structure should be designed in such a way that, structure as to absorb impact energy in a controlled manner, thereby bringing the passenger compartment to rest without the occupant being subjected to high decelerations, which can cause serious internal injury , particularly brain damage.

The need for increased crashworthiness, and lighter compact design, demands the development of more efficient body-in-white, chassis, suspension and power train components. Sub-frame and underbody cross-members provide significant rigidity to the vehicle front-end allowing longitudinal member to crush efficiently.

Crashworthiness is the ratio of the mean crush stress (S) to the density of the composite material (D).

ES = Mean Crush Stress/ Density of the composite material = S/D

Design Engineers of the vehicles should keep in mind while designing that, the structures in the vehicles should absorb the maximum energy during the impact. In the force v/s deflection curve, the area under the curve shows the energy absorption. The structure should be designed in such way that the area under the curve should be maximum during the vehicle impact which in turn reduces the injury of the occupants.

In the present day accidents happen every hour around the world and most of these are very dangerous. Frontal-Impact crash is the one of the most severe crash scenario. Figure 1 shows the comparison of different crash scenarios involved. It can be observed that the frontal impact is higher than all other impacts.

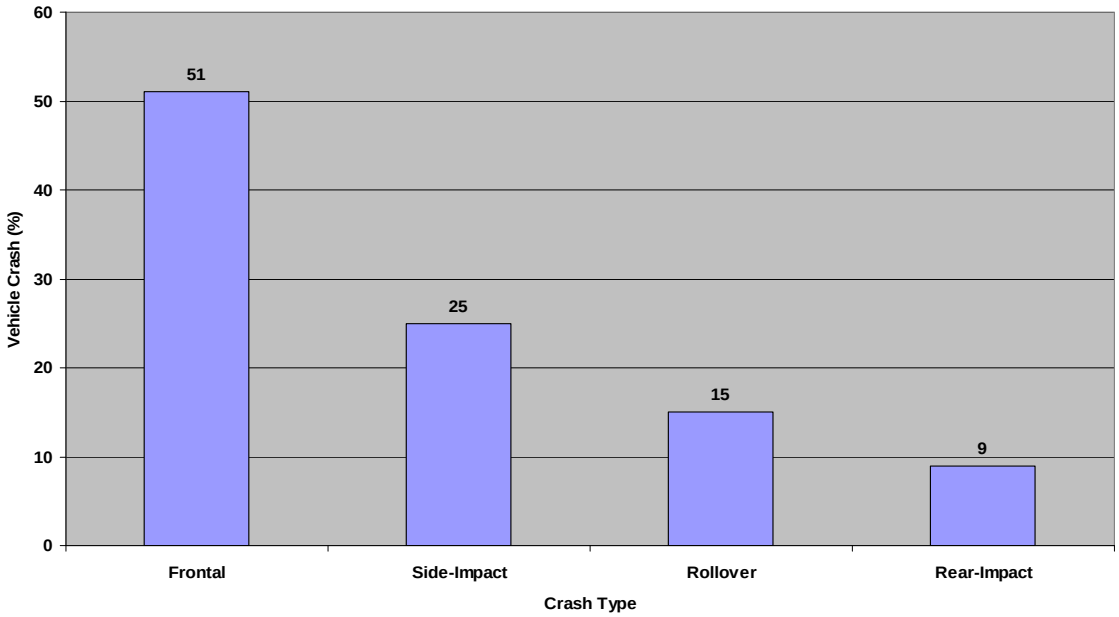

Figure 1. Vehicle crashes by crash type [9].

1.3 Composite Materials in Crashworthiness

In the design of modern vehicles, it is more important to reduce the weight of the structures, which mainly use internal-combustion engines, to reduce exhaust gas and improve fuel combustion ratio. Every day the price of the fuel and the requirement of the fuel is increasing randomly, eventually emission of chemicals from the vehicle exhaust pollute the environment and increase the global temperature. Composite Materials helps in reducing the weight of the structure thus bringing down the fuel used.

Composites are engineered materials that have been designed to provide significantly higher specific stiffness and specific strength (stiffness or strength divided by material density)—that is, higher structural efficiency—relative to previously available structural materials. In composite materials, strength and stiffness are provided by the high-strength, high-modulus reinforcements [1].

Fiber-reinforced composite materials have been widely used in various transportation vehicle structures because of their high specific strength, modulus and high

damping capability. If composite materials are applied to vehicles, it is expected that not only the weight of the vehicle is decreased but also that noise and vibration are reduced. In addition to that composites have a very high resistance to fatigue and corrosion.

To reduce the overall weight and improve the fuel economy of vehicles, more and more metal parts are replaced by polymer composite materials. Compared to metals, in compression, most composites are generally characterized by a brittle rather than ductile response to load. While metal structure collapse under crush or impact by buckling and folding which involves extensive plastic deformation, composites fail through a sequence of fracture mechanisms involving fiber fracture, matrix crazing and cracking, fiber-matrix debonding, delamination and inter-ply separation. The actual mechanisms and sequence of damage are highly dependent on the geometry of the structure, lamina orientation, type of trigger and crush speed, all of which can be suitably designed to develop high energy absorbing mechanisms.

1.4 Test Methodologies

There are different methodologies which can be carried out for crash testing [7].

1.4.1 Quasi-static testing

In quasi-static testing, the test specimen is crushed at a constant speed. Quasi-static tests may not be an actual simulation of the crash condition because in an actual crash condition, the structure is subjected to a decrease in crushing speed, from an initial impact speed, finally to rest.

The following are some advantages of quasi-static testing.

- Quasi-static tests are simple and easy to control.
- To follow the crushing process, Impact tests require very expensive equipment,

as the whole process occurs in a split second. Hence, quasi-static tests are used to study the failure mechanisms in composites, by selection of appropriate crush speeds.

The following is a major disadvantage of quasi-static testing.

- Quasi-static tests may not be a true simulation of the actual crash conditions since certain materials are strain rate sensitive.

1.4.2 Impact testing

The crushing speed decreases from the initial impact speed to rest as the specimen absorbs the energy.

The following is a major advantage of impact testing

- It is a true simulation of the crash condition since it takes into account the stress rate sensitivity of materials.

The following is a major disadvantage of impact testing.

- In Impact testing, the crushing process takes place in a fraction of a second. Therefore, it is recommended that crushing be studied with high-speed camera [10].

1.4.3 Crushing modes and mechanisms

1.4.3.1 Catastrophic failure modes

Catastrophic failure modes are not of interest to the design of crashworthy structures. This type of failure occurs because of the following events:

- When unstable intralaminar or interlaminar crack growth occurs.

- In long thin walled tubes because of column instability.
- In tubes composed of brittle fiber reinforcement, when the lamina bundles do not bend or fracture due to interlaminar cracks being less than a ply thickness.

Catastrophic failure is characterized by a sudden increase in load to a peak value followed by a low post failure load. As a result of this, the actual magnitude of energy absorbed is much less and the peak load is too high to prevent injury to the passengers. [7]

1.4.3.2 Progressive failure modes

Progressive failure can be achieved by providing a trigger at one end of the tube. This initiates a failure at a specific location within the structure. The most widely used method of triggering is to chamfer one end of the tube. A number of trigger geometries such as bevels, grooves and holes that have been investigated in laboratory specimens are not as easy to use in vehicle structures

The following are the advantages of progressive failure in the design of crashworthy structures.

- The energy absorbed in progressive crushing is larger than the energy absorbed in catastrophic failure.
- A structure designed to react to loads produced by progressively failing energy absorbers are lighter than structures designed to react to loads produced by catastrophically failing energy absorbers. [7]

The following are the different types of progressive failure modes:

1.4.3.3 Transverse shearing or Fragmentation mode

- The fragmentation mode is characterized by a wedge-shaped laminate cross section with one or multiple short interlaminar and longitudinal cracks that form partial lamina bundles (Figure 1)
- Brittle fiber reinforcement tubes exhibit this crushing mode.
- The main energy absorption mechanisms is fracturing of lamina bundles
- When fragmentation occurs, the length of the longitudinal and interlaminar cracks is less than that of the lamina.
- Mechanisms like interlaminar crack growth and fracturing of lamina bundles control the crushing process for fragmentation. [7]

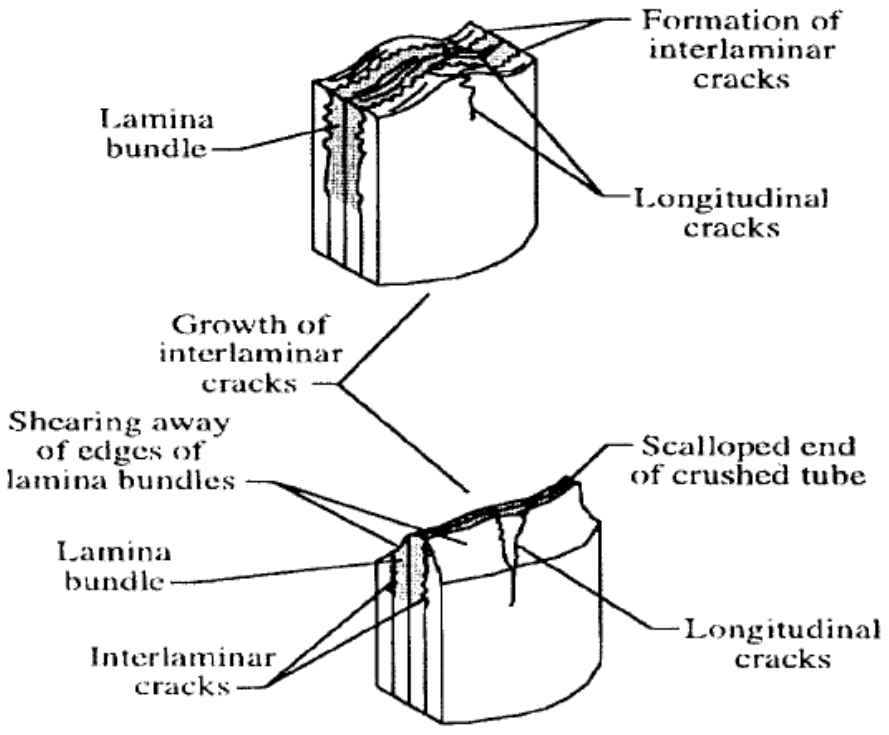

Figure 2. Fragmentation crushing mode [2].

1.4.3.4 *Lamina bending or Splaying mode*

- Very long interlaminar, intralaminar, and parallel to fiber cracks characterizes the splaying mode. The lamina bundles do not fracture. (Figure 2)
- Brittle fiber reinforcement tubes exhibit this crushing mode.
- The main energy absorbing mechanism is matrix crack growth. Two secondary energy absorption mechanisms related to friction occur in tubes that exhibit splaying mode.
- Mechanisms like interlaminar, intralaminar and parallel to fiber crack growth control the crushing process for splaying. [7]

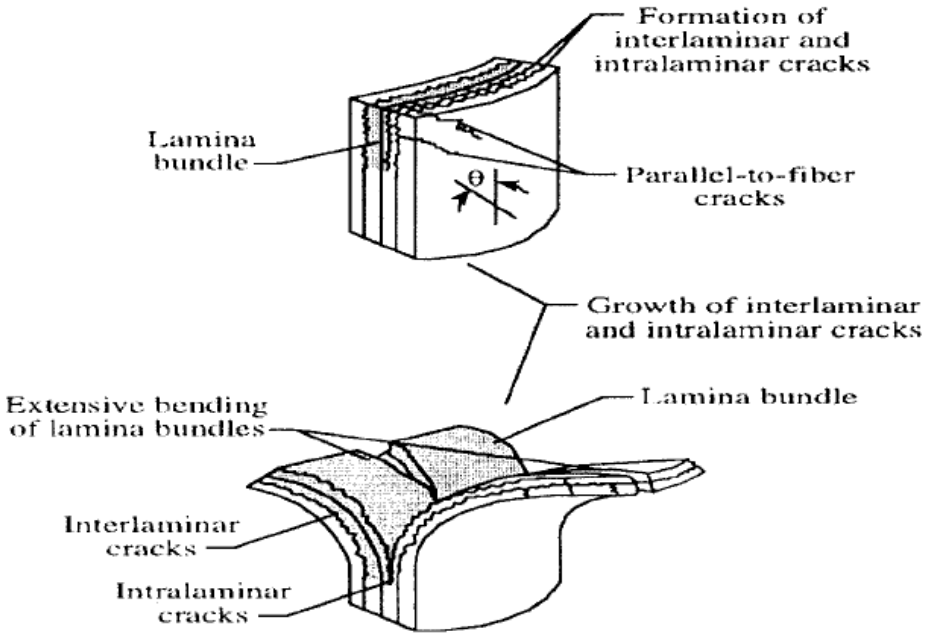

Figure 3. Splaying crushing mode [2].

1.4.3.5 Brittle fracturing

- The brittle fracturing crushing mode is a combination of fragmentation and splaying crushing modes (Figure 3).

- Brittle fiber reinforcement tubes exhibit this crushing mode.
- The main energy absorption mechanism is fracturing of lamina bundles.
- When brittle fracturing occurs, the lengths of the interlaminar cracks are between 1 and 10 laminate thickness.

1.4.3.6 Local buckling or Progressive folding

- The progressive folding mode is characterized by the formation of local buckles (Figure 4).
- This mode is exhibited by both brittle and ductile fiber reinforced composite material.
- Mechanisms like plastic yielding of the fiber and/or matrix control the crushing process for progressive folding. [7]

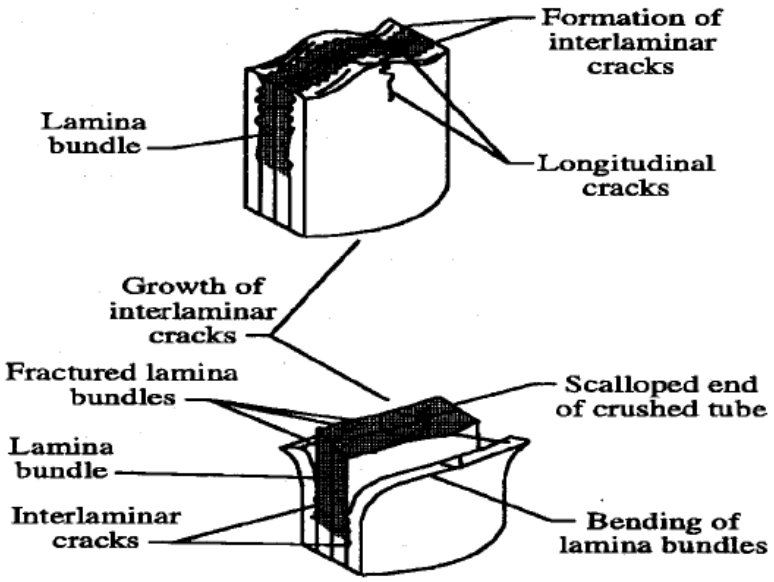

Figure 4. Brittle fracturing crushing mode [2].

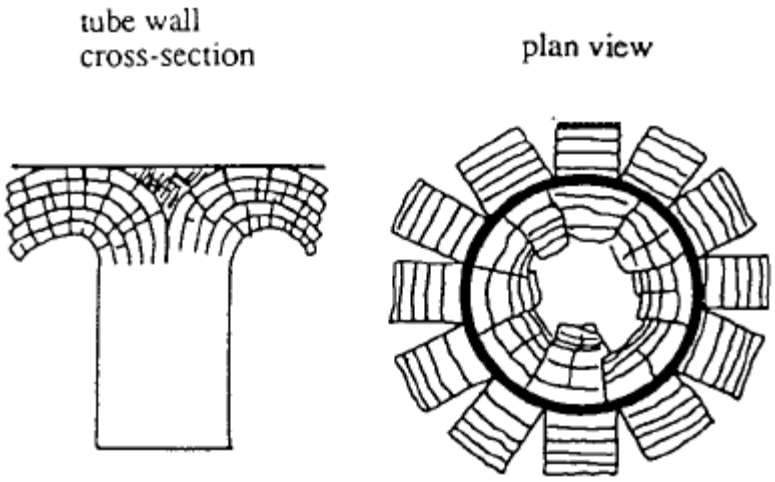

Figure 5. Progressive crushing mode [23].

1.5 Injury Criteria

An injury criterion can be defined as a biomechanical index of exposure severity, which indicates the potential for impact induced injury by its magnitude. There are several kinds of injury criteria's that are related to the human body. These are basically the impact loads acting on the human body. Some of the criteria's pertinent to the frontal Impact are discussed here.

1.5.1 Gaddis severity index (GSI)

Gaddis Severity Index for the head is given as:

$$GSI = \int_{t0}^{te} R(t)^{2.5}\, dt$$

where R (t) = resultant linear acceleration in g's in the centre of gravity of head,

t0 = starting time of the simulation in seconds,

te = end time of simulation in seconds,

t = time in seconds.

1.5.2 Head injury criterion (HIC)

The Head Injury Criteria is defined as:

$$HIC = \max_{T0 \le t_1 \le t_2 \le TE} \left[\frac{1}{t_2 - t_1} \int_{t_1}^{t_2} R(t)dt \right]^{2.5} (t_2 - t_1)$$

where T0 = start time of simulation

TE = end time of simulation

R(t) = is the resultant head acceleration in g's measured at head's center of gravity over the time interval $T0 \le t \le TE$

t_1 and t_2 are the initial and final times (in sec) of the interval during which the HIC attains a maximum value.

A value of 1000 is specified for the HIC as concussion tolerance level in frontal (contact) impact. For practical reasons, the maximum time interval (t2-t1) that is considered to give appropriate HIC values was set to 36 ms. This time interval greatly affects the HIC calculations and recently, this time interval has been proposed to be further reduced to 16 ms in order to restrict the use of HIC to hard head contact impacts..

1.5.3 Thoracic trauma index (TTI)

The TTI is the acceleration criterion based on accelerations of the lower thoracic spine and the ribs. The TTI can be used as an indicator for the side impact performance of passenger cars. The specific benefit of the TTI is that it can be used to address the entire population of vehicle occupants because the age and the weight of the cadaver is included. The TTI is defined by Morgan:

$$TTI = 1.4 * AGE + 0.5 * (RIB_g + T12\ ) * MASS/MSTD$$

Where AGE = age of the test subject in years,

RIB_g = maximum absolute value of acceleration in g's of the 4^{th} and 8^{th} rib on the struck side,

$T12_g$ = maximum absolute acceleration values in g's of the 12^{th} thoracic vertebra, in lateral direction,

MASS = test subject mass in kg

MSTD = standard reference mass of 75 kg.

There is also a definition for the TTI that could be used for dummies without a specific age, called the TTI (d). It is defined for 50^{th} percentile dummies with a mass of 75 kg:

$$TTI(d) = 0.5 * (RIB_g + T12_g)$$

The dynamic performance requirement, as stated in FMVSS 214 regulations of 1990, is that the TTI (d) level shall not exceed 85 g for passenger cars with four side doors and 90 g for two side doors.

1.5.4 Viscous injury response (VC)

The Viscous response, denoted as VC, is the maximum value of a time function formed by the product of velocity of deformation (V) and the instantaneous compression function (C):

$$VC = \max\left(\frac{dD(t)}{dt}\frac{D(t)}{SZ}\right)$$

where D (t) is deflection and SZ is prescribed size (the initial torso thickness for frontal impacts or half the torso width for side impacts). Analysis of data from experiments on human cadavers show that a frontal impact which produces a VC value of 1.3 m/s has a 50% chance of causing severe thoracic injuries (AIS $\geq$ 4).

1.5.5 Combined thoracic index (CTI)

The Combine Thoracic Index (CTI) is a measure of the injuries of the thorax. It is a combination of the maximum chest deflection D_{max} and the 3 ms clip maximum value of the resultant upper spine acceleration A_{max}. The equation for the calculation of the CTI is given by:

$$CTI = \left(A_{\max} / A_{\text{int}}\right) + \left(D_{\max} / D_{\text{int}}\right)$$

where A_{int} and D_{int} are constants that depend on the dummy.

1.5.6 Tibia index (TI)

The Tibia Index is a measure of injury to tibia. The equation for the calculation of TI is given by

$$TI = \left|F_Z / \left(F_C\right)_Z\right| + \left|M_R / \left(M_C\right)_R\right|$$

Where

F_Z = compressive axial force in joint ζ-direction

$(F_C)_Z$ = critical compressive force and should be taken to be 35.9 KN

M_X = bending moment about the joint ξ-axis

M_Y = bending moment about the joint η-axis

$M_R = \sqrt{\left(M_X\right)^2 + \left(M_Y\right)^2}$

The Tibia Index can be calculated for the top and bottom of each tibia. For each joint, the corresponding axial force F_Z is used.

1.5.7 Tibia compressive force criterion (TCFC)

The Tibia Compressive Force Criterion (TCFC) is a measure of injury to the tibia. It is the compressive force F_Z expressed in kN, transmitted axially by the tibia load cell. The TCFC injury calculation is applied to the joint constraint force in the bracket joint located at a tibia load cell. It is assumed that the coordinate systems of this joint are oriented in agreement with SAE J221 / 1 because as axial force, the component of the constraint force in the joint ζ-direction is used.

1.6 NHTSA/Crashworthiness

National Highway Safety Bureau was responsible for all the safety acts before NHTSA took over as the successor. The National Highway Traffic Safety Administration (NHTSA), which is part of the U.S. Department of Transportation, is responsible to conduct the motor vehicle safety act and highway act of 1966. Title 49 in chapter 301 of the U.S codes is used to record the entire motor vehicle safety act, motor vehicle information & cost savings act. The US department of safety standards (NHTSA) sets performance standards for vehicles and its equipments. By setting the performance standards to vehicles, percentages of deaths and injuries during vehicle crashes can be reduced. NHTSA has done lot of research to improve the vehicle safety and it always tries to bring awareness in the peoples mind about the safety belts, airbags and child safety seats.

1.7 FMVSS 208 Regulations

FMVSS 208 regulations are the standards that are used to protect the occupants of vehicles during crashes. These regulations sets standards on restraint systems and sets

standards on forces and accelerations measured on dummies in test crashes. These regulations help to reduce no. of deaths and injuries during vehicle crashes and are applied to cars, buses and trucks.

1.8 New Car Assessment Program(NCAP)

The NHTSA New Car Assessment Program (NCAP) uses a rigid barrier and the full width of vehicle is crashed into the rigid barrier at 35 mph. Since the full frontal width is crashed in the rigid barrier the deformation of the vehicle is in somewhat defined pattern. This procedure is used by National Highway Traffic Safety Administration and OSA for full width frontal impact collisions. IIHS in the United States has standardized the procedure for frontal offset crash test that is adopted by The Euro NCAP and Australian NCAP. NCAP program is used to evaluate occupant restraint systems like airbags and seatbelts.

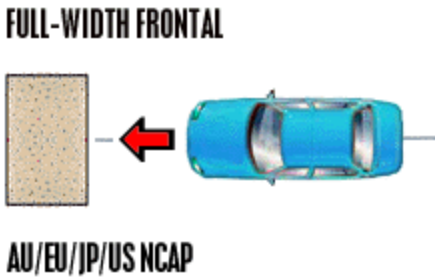

Figure 6. Full Frontal Crash Test at 35 mph [9].

1.9 IIHS Test Procedure

Unlikely in full frontal test which uses rigid barrier, Insurance Institute of Highway Safety uses a deformable barrier for the impact analysis. The test is carried out with 40 % offset angle of the vehicle with vehicle speeds of 40mph. The deformable barrier, made

of aluminum honeycomb, absorbs some of the energy and the 40 % offset of the vehicle leads to transfer of entire impact on just one corner of the vehicle. As a result the vehicle crushes more and such tests impart higher injuries to the occupant due to higher intrusions in the occupant compartment. In vehicle to vehicle crashes, it is unlikely that the vehicle will deform in axial direction, hence the deformable barrier with 40 % offset for the vehicle represents the real life scenario .In order to evaluate the vehicle condition and effect on dummies after the impact, the dummies are placed in both passenger and driver's seat. In this test, two vehicles are travelling at 40 mph and impact the barrier as shown in **Figure 7**. This test helps to evaluate the vehicle deformation and the injury sustained to vehicle occupants due to very high vehicle intrusions from the impact.

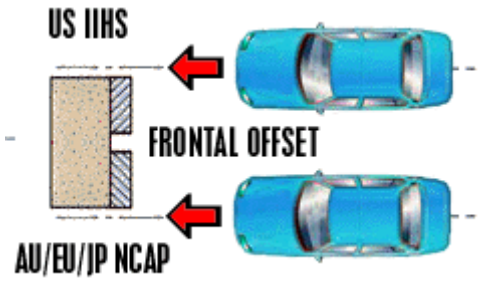

Figure 7. Offset frontal crash Test at 40 mph [9].

1.10 Car Front Sub-Frame Rails

The Automotive Sub-Frame-rail is the main load carrying, Energy absorbing component during frontal and angled impacts. Mid-rails generally have non-uniform cross-sections, contain various crush initiators and include several holes [5]. Generally, the cross-section shape of the side rails is square, rectangular, or hourglass tube. The four side rails can absorb 70% of the impact energy through the progressive plastic deformation of metals when the vehicle crashes.

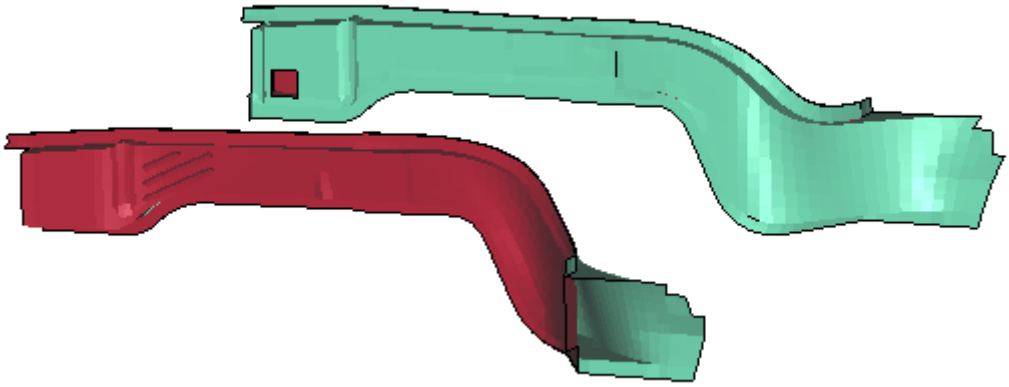

Figure 8. Car front sub-frame Rails.

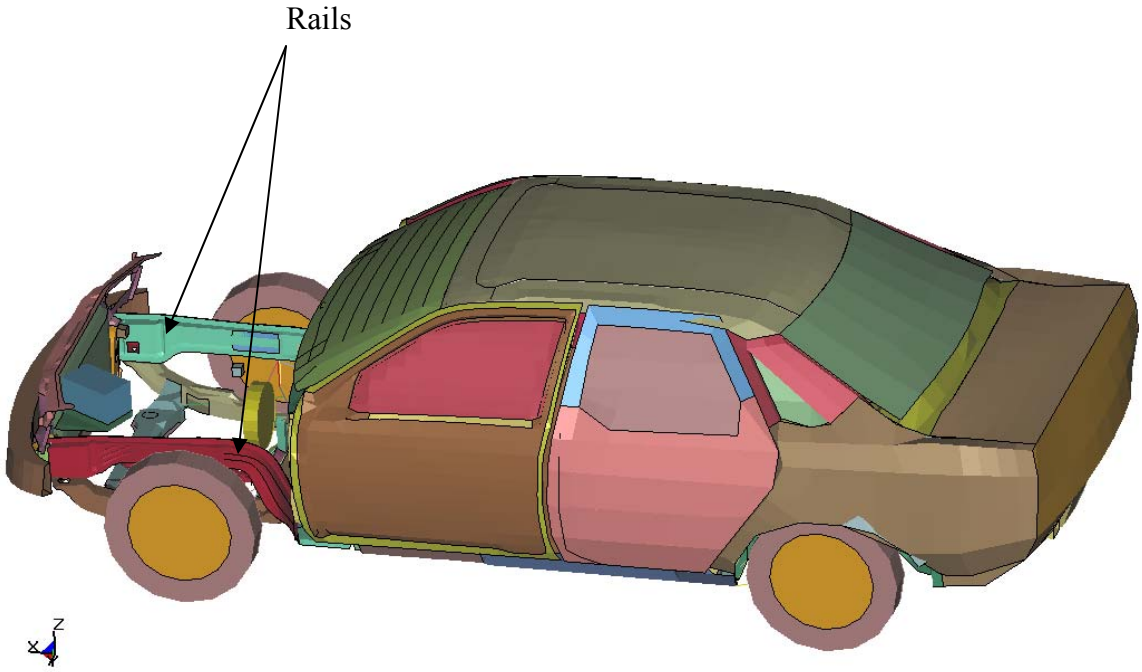

Figure 9. Rails in the Car.

For the structural analysis of the Car Front sub-frame rail, Finite Element Method is used since it is the most widely used computational method in the automotive industry.

By considering the car front rail as a component, the rail does not perform precisely the same in a crash as it does in the full vehicle. This is because of the complex

boundary conditions in an actual car. Crashworthiness of a structure is complicated system and individual performance of components donot necessarily compare across platforms. However , the general trends and energy absorption capabilities of component analysis are indicative of actual performance for each platform and are extensively used for design and analysis [5].

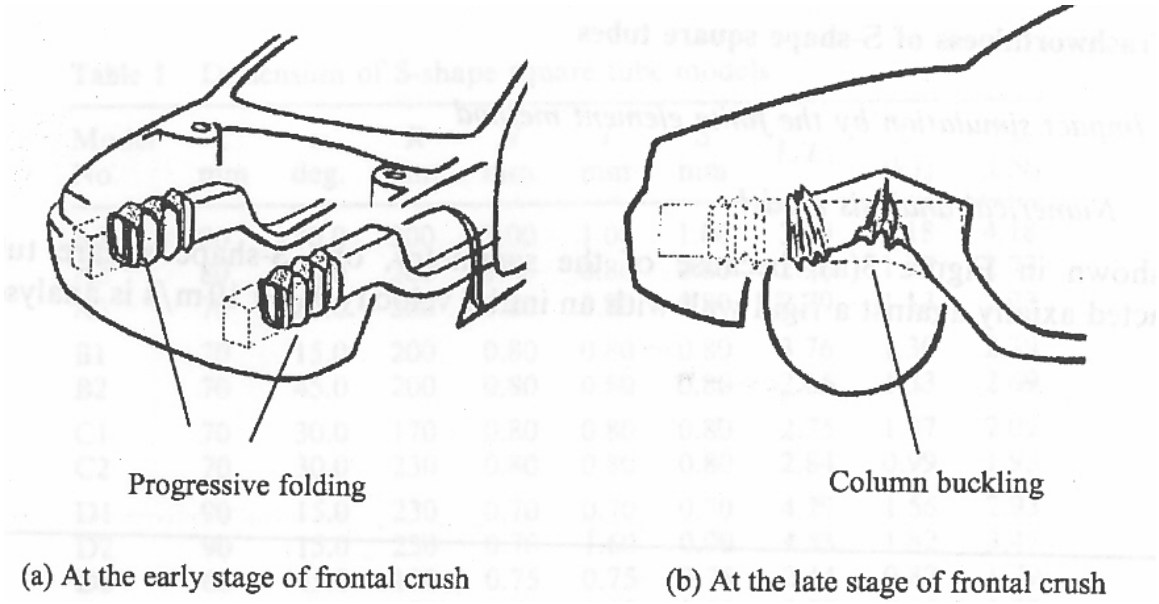

Figure 10. Ideal Deformation of the front member [4].

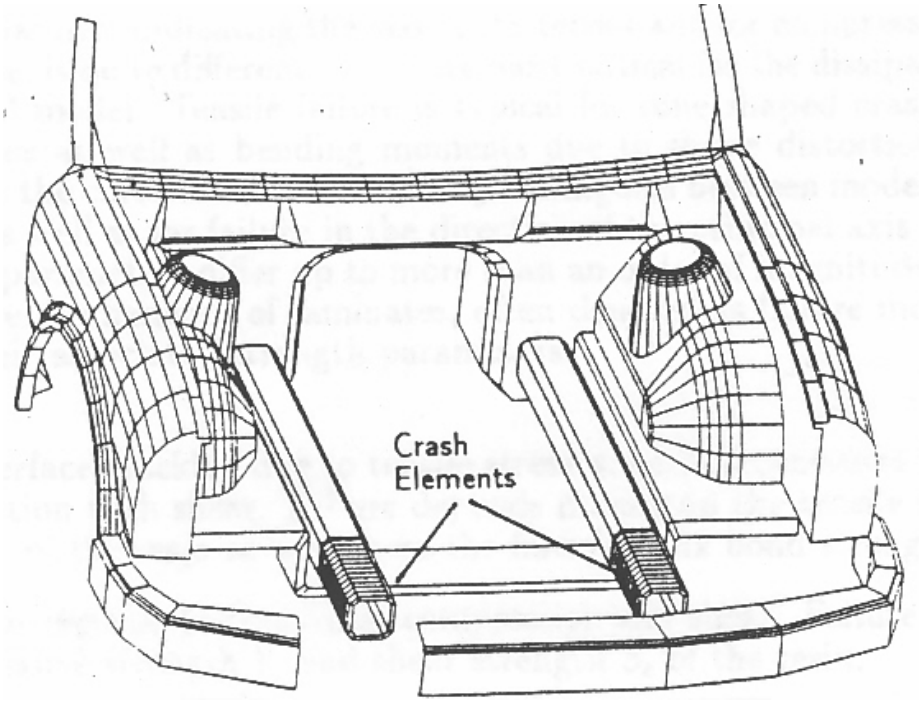

Figure 11. use of crash elements in automobiles [4].

CHAPTER 2

OBJECTIVE AND METHODOLOGY

2.1 Objective

In this study, the main objective of this research work is to replace the current car front sub-frame rail with the better design and using a composite material instead of steel and study its effect on occupant kinematics and occupant injuries. The basic idea behind this research is that, if we replace current steel rails with composite rails, there will be more amount of energy absorbed after impact thus reducing the forces transmitted the occupant cabin and reducing the amount of intrusions in the cabin and over all crush of the vehicle. Efforts are made to reduce the weight of the car without sacrificing the safety of the occupant.

This modified vehicle is tested for full frontal test according to NCAC experimental test for 30mph, NCAP for 35mph full frontal rigid barrier test as well as for 40 % offset impact test according to IIHS for 40mph. All these tests are done using LS-DYNA and the occupant dynamic response and injuries shall be further evaluated with the aid of MADYMO.

2.2 Methodology

In this study, an attempt is made to design an energy absorbing car front rails that would reduce the injuries sustained by the occupant Due to high energy absorbing capability, high strength, crushing stability, and easy manufacture of fiber reinforced composites made them to widely use in vehicles and aircraft.

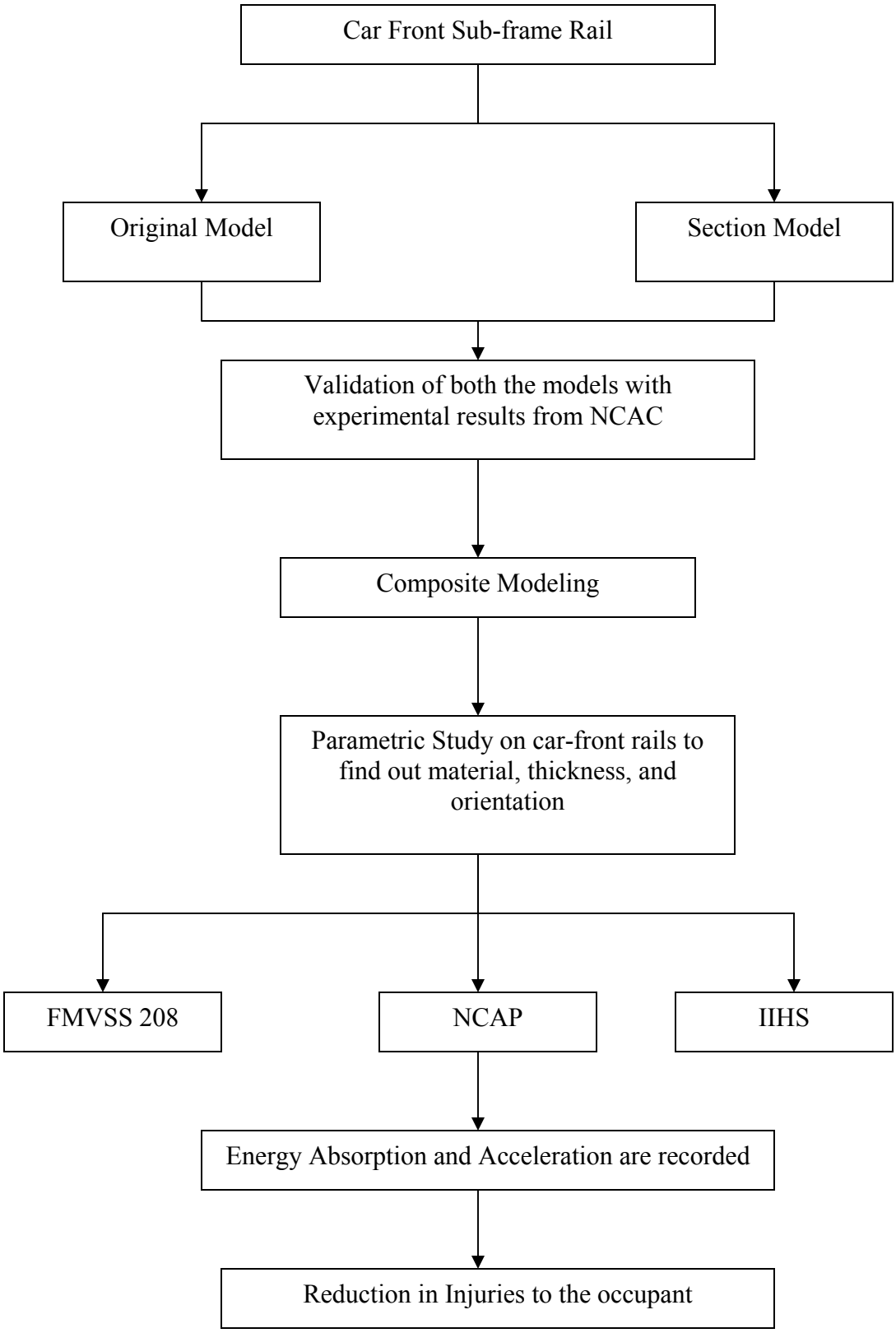
Car Front Sub-frame Rail
Original Model
Section Model
Validation of both the models with experimental results from NCAC
Composite Modeling
Parametric Study on car-front rails to find out material, thickness, and orientation
FMVSS 208
NCAP
IIHS
Energy Absorption and Acceleration are recorded
Reduction in Injuries to the occupant

Points below depict the methodology carried out in this research.

- This study starts with the section modeling of car front rails with different strength of steels used for different section.
- Both the original model and section model are validated with the experimental results from National crash analysis centre.
- Composite modeling of the car-front sub-frame rails
- Parametric study is carried out on the rails, which included changing the material, layers, orientation and thickness. Finally, the maximum energy sustained by the rail with the pertinent material, layers orientation and thickness is used for composite modeling.
- Composites used for both the original model and section model are simulated according to FMVSS 208, NCAP and IIHS test specifications.
- Energy absorption and Accelerations is note down for all the cases.
- Finally, the acceleration pulse values are input to the Madymo model and Injuries sustained by the dummy were compared.

CHAPTER 3

LITERATURE REVIEW

Previous researches have shown that the efficient design and increase use of composite materials into the automotive parts directly influences the car safety, weight reduction and gas emission, because the efficient design can absorb more deformation and composite materials have high specific strength (strength to density) and high specific stiffness (stiffness/density). They also have very high impact load absorbing and damping properties.

3.1 Related work in Car Front Rails

Designing structures that meet crashworthiness goals is a critical task in the design of transportation systems, such as cars, trucks, planes, helicopters and ships. The objective of designing a crashworthy structure is to absorb energy through material deformation while protecting passengers and cargo during crash event. One of the most important contributes to the crashworthiness of structure is the thin-walled column composed of various cross-sections. Reid research provides guidelines to design engineers that material properties have influence on crashworthiness of structures. From this research engineers will get an idea about design reviews and get confidence in design proposals where testing is not generally possible [5]. Many research works on the side rail made of composite materials have been reported. Thornton investigated the axial collapse of circular tubes made of Carbon, Kevlar, and glass fiber-reinforced composite materials [19]. He also suggested the trigger mechanism to prevent catastrophic failure of brittle composite structures and to induce stable and progressive failure of them.

Although the trigger mechanism can induce stable failure in the composite tube, it is known to be difficult to fabricate the composite tube with various kinds of trigger [12].

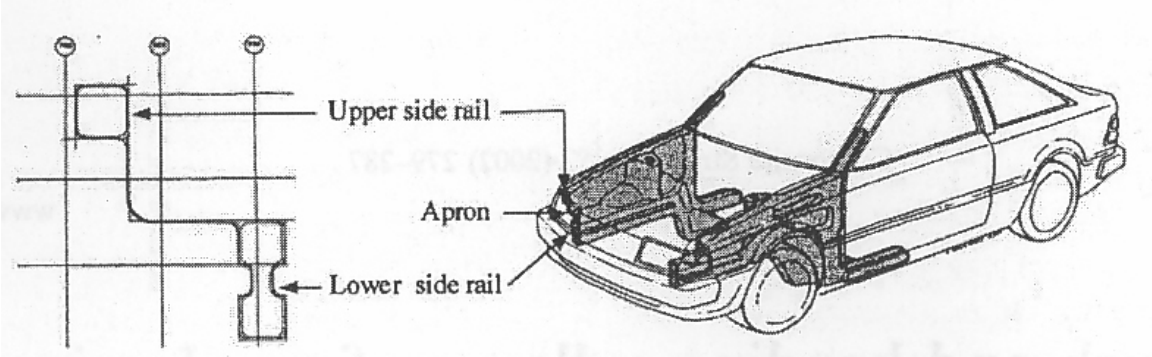

Figure 12. Composite front structure [12].

Mamalis have done research on crashworthy behaviour of an automotive hourglass cross-section frame rail. Frame rail is made of glass fiber/vinylester composite, designed for use in the apron construction of the car in order to improve the crashworthiness at this location of the car, when subjected to axial and dynamic loading. Comparison between theory and experiments concerning crushing loads and energy absorption was good, indicating , therefore that the proposed theoretical model may be efficient for predicting the energy absorbing capacity of the collapsed shell [11].

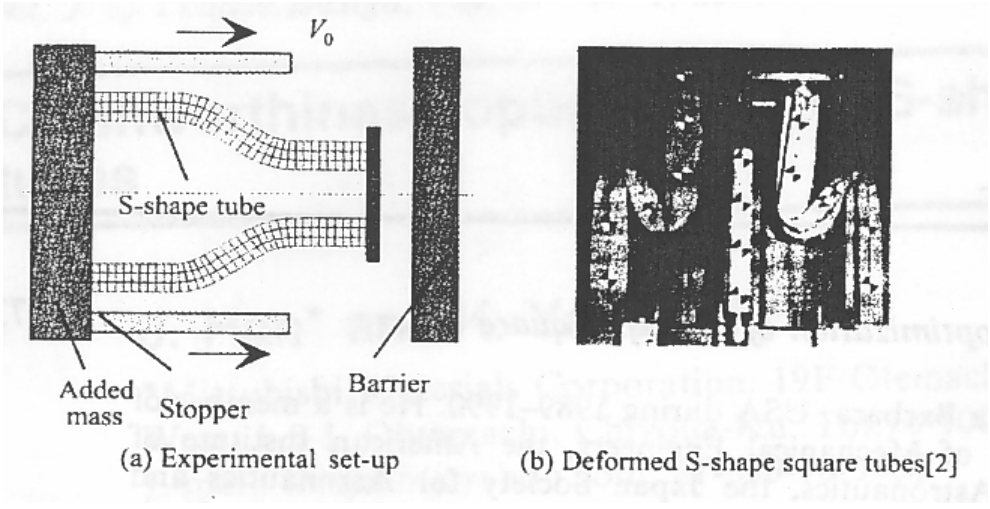

Figure 13. Experimental setup and crushing observation [11].

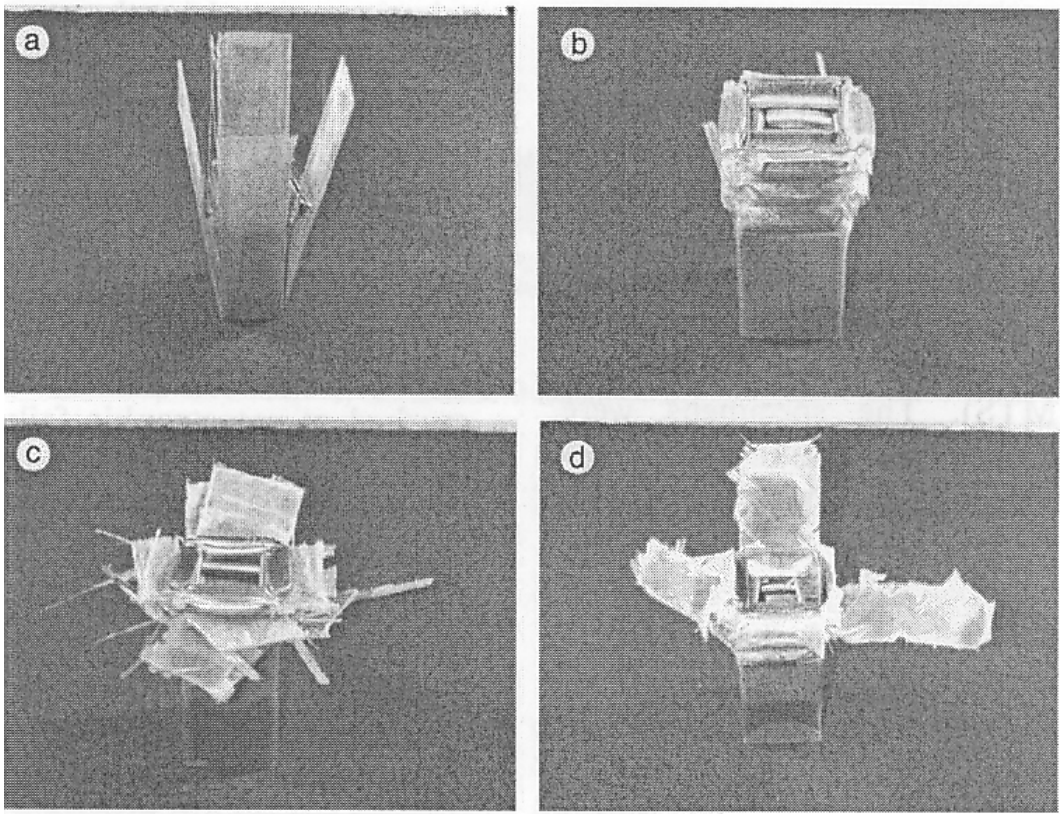

Figure 14. Axial crushing of hybrid composite tubes [11].

3.2 Composites Materials

3.2.1 Composite in automobile parts

Increasing legal and market demands for safety, the weight of the car body will most likely increase in the future. At the same time, environmental demands will become stronger and lower weight will play an important part in meeting them. In the European Union, the car manufacturers have agreed to an overall 25% increase in fuel efficiency by the year 2005 compared to 1990 [10].

Fuel efficiency of the vehicle directly depends on the weight of the vehicle. The carbon fiber composite body structure is 57% lighter than steel structure of the same size and providing the superior crash protection, improved stiffness and favorable thermal and acoustic properties. [15]

Composite materials may find the exciting opportunity in the automotive industry as a means of increasing fuel efficiency. With 75 percent of fuel consumption relating directly to vehicle weight, the automotive industry can expect an impressive 6 to 8 percent improvement in fuel usage with mere 10 percent reduction in vehicle weight. This translates into reduction of around 20 kilogram of carbon dioxide per kilogram of weight reduction over the vehicle's lifetime [16].

For the first time FRP's were introduced to the formula-1 in 1980 by McLaren team. Since then the crashworthiness of the racing cars has improved beyond all recognition. Carbon fiber composite has been used to manufacture the body, which is low weight, high rigidity and provided the high crash safety standards

The report from the United states and Canada predicted that plastics and composites would be widely used applied to body panels, bumper systems, flexible components, trims, drive shaft and transport parts of cars. In addition, rotors manufactured using RTM (Resin Transfer Moldings) for air compressor or superchargers of cars have been used to substitute for metal rotors which are difficult to machine [12].

3.2.2 Impact damage response on composite materials [17]

A significant amount of research has focused on investigating the damage, crashworthiness, and behavior of dynamic loading under impact. Impact damage in composites occurs when a foreign object causes through the thickness and/or in-plane fracture in the material. The damaged areas can be investigated visually or by using optical or electron microscopy, ultrasonic C-scanning, and acoustic imaging.

Impact damage in composite plates is associated with these major failure modes: delamination, matrix cracking, and fiber breakage. Matrix cracking and delamination are

properties of the resin matrix, whereas the fiber breakage is more responsive to the fiber specifications and characteristics and is usually caused by higher energy impacts [17].

3.2.3 Matrix cracking

Matrix cracking in an impacted composite is caused by tensile stress and by stress concentrations at the fiber-matrix interface. A higher tensile stress results in a longer and denser cracking pattern. The total energy absorbed by matrix cracking is equal to the product of the surface energy and the small area produced by the crack. Larger crack areas are normally caused by crack branching, in which case the cracks run in the direction normal to the general direction of fracture. In many cases, the surface area created by such cracks is much larger than the area parallel to the primary cracks, increasing the fracture energy significantly. This, in effect, can increase the toughness of composites or the total energy of damage absorbed during impact.

3.2.4 Delamination

Different orientation of the plies can promote delamination of two adjacent plies due to the stiffness mismatch at their interface. The delamination areas are influenced directly by changes in the energy of impact. The cracks, which can initiate delaminations, can propagate through the plies and may be arrested as the crack tips reach the fiber–matrix interface in the adjacent plies. [17]

3.2.5 Fiber breakage

Fiber breakage can be a direct result of crack propagation in the direction perpendicular to the fibers. If sustained, the fiber breakage will eventually grow to form a complete separation of the laminate. Reaching the fracture strain limit in a composite component results in fiber breakage. For the same impact energy, higher capacity of

fibers to absorb energy results in less fiber breakage and a higher residual tensile strength. Secondary matrix damage, which occurs after initial fiber failure, is also reduced allowing residual compressive strength to increase [17].

3.2.6 Energy absorption in various composite materials

Composites absorb more energy than steel or aluminum. Steel has higher young's modulus, yet fails to absorb higher energy absorption. In composites, there are different kinds of fibers having different stiffness. For instance, carbon fibers are stronger than glass, yet glass fiber withstand load for a longer time than carbon fibers. The energy absorption capability of the composite materials offers a unique combination of reduced weight and improves crashworthiness of the vehicle structures [18].

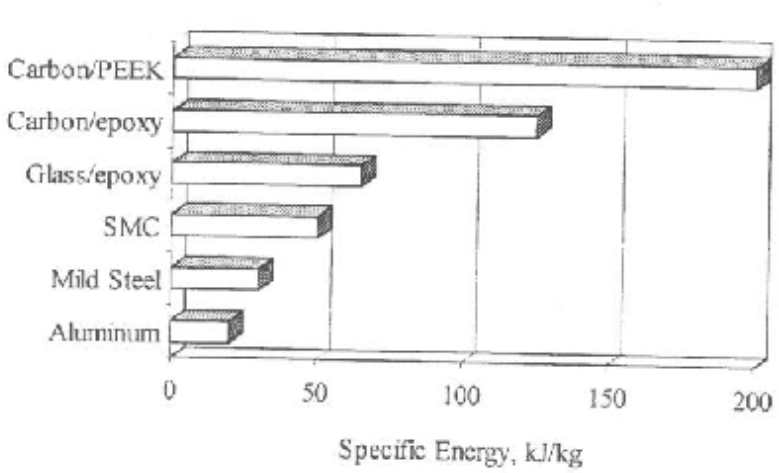

Figure 15. Specific energy of different materials [18].

3.2.7 Properties effecting energy absorption of composite material

In the past, crushing of tube was the method of testing composite specimens and this was primarily used to determine the energy absorption performance of composite materials.

3.2.7.1 Fiber

Farley [10], reports that, in tests conducted on comparable specimens, carbon fiber reinforced tubes absorb higher energy than those of glass or aramid fibers. This is supported by the data in Table 1. The reasons for this are related to the physical properties of the fibers, overall failure mechanisms and fiber-matrix bond strengths. [20]

Farley [10] observed that glass and carbon fiber reinforced thermoset tubes progressively crush in fragmentation and splaying modes. Aramid (Kevlar and Dyneema) fiber reinforced thermoset tubes, on the other hand, crush by a progressive folding mode. Similar results were obtained when impact and static compression tests were carried on Graphite/epoxy, Kevlar/epoxy and Glass/epoxy composite tube specimens respectively. The graphite/epoxy and glass/epoxy angle-ply tubes exhibited brittle failure modes consisting of fiber splitting and ply delamination, whereas the Kevlar/epoxy angle-ply tubes collapsed in a buckling mode. The lower strain to failure of the glass and carbon fibers, which fail at about 1% strain, compared to aramid fibers, which fail at about 8% strain attributes to this difference in behavior. [7]

Table 1. Specific Energy Absorption of different composite materials [20].

Fiber-Matrix	Lay up	Thickness to diameter ratio	Specific Energy absorption
Carbon-Epoxy	$[0/\pm15]_3$	0.033	99
Carbon-Epoxy	$[\pm45]_3$	0.021	50
Aramid-Epoxy	$[\pm45]_8$	0.066	60
Aramid-Epoxy	$[0/\pm15]_2$	0.02	9
Glass-Epoxy	$[0/\pm75]_2$	0.069	53
Glass-Epoxy	$[0/\pm15]_2$	0.06	30
1015 Steel		0.06	42
6061 Al		0.06	44

Results of static crushing tests of graphite reinforced composite tubes were conducted to study the effects of fiber and matrix strain failure on energy absorption helped in drawing the following conclusion: ‘‘To obtain the maximum energy absorption from a particular fiber, the matrix material in the composite must have a greater strain at failure than the fiber’’. The graphite/epoxy tubes had specific energy absorption values greater than that of Kevlar/epoxy and glass/epoxy tubes having similar ply constructions. This is attributed to the lower density of carbon fibers compared to glass and Kevlar fibers. [7]

Research was done on PEEK matrix composite tubes reinforced with AS4 carbon fiber, IM7 carbon fiber and S2 glass fiber respectively. The tubes crushed progressively by the splaying mode. The S2/PEEK tubes displayed approximately 20% lower E_S than the AS4/PEEK and IM7/PEEK tubes though the mean crush stress of S2/PEEK tubes is comparable to that of AS4/PEEK and IM7/PEEK tubes. This is a direct result of the lower density of carbon fiber reinforced materials than the glass reinforced material, since the specific energy absorption is defined as the ratio of the mean crush stress and density of the composite. [7]

A finite element analysis was carried out to model the crushing process of continuous-fiber-reinforced tubes by Farley et al. [10]. The analysis is compared with experiments on graphite/epoxy and Kevlar/epoxy tubes. The method obtained a reasonable agreement between the analysis and the experiment. Thornton et al. [29] examined the energy absorption capability in graphite/epoxy, Kevlar/epoxy and glass/epoxy composite tubes. The composite tubes collapsed by fracture and folding mechanisms. The load–compression curves for the graphite/epoxy and the glass/epoxy

tubes had similar characteristics but the Kevlar/epoxy composite tubes collapsed by buckling. [7]

In addition, it can be observed from Table 2 that the carbon fibers have high specific energy absorption because of the low density and high strength of the constituent carbon fibers. If aramid fibers are considered, these have low specific energy absorption than those of carbon. This is because of the reason that the compressive strength of aramid fiber composites is around 20% of the tensile strength. In addition, due to ductile nature, aramid fibers undergo progressive folding failure mechanism. This absorbs energy less efficiently than brittle fracture.

Table 2. Physical properties of different fibers types [20].

Fiber	**Density (kg/m^3)**	**Axial Young's Modulus (GN/m^3)**	**Tensile Strength (MN/ m^3)**
Carbon Fiber (HighModulus)	1950	380	2400
Carbon Fiber (High Strength)	1750	230	3400
Aramid Fiber	1450	130	3000
Glass Fiber	2560	76	2000

3.2.7.2 *Matrix material*

The following points can be worth noted about the matrix.

- $G_{1C,}$ higher interlaminar facture toughness, of the thermoplastic matrix material causes an increase in the energy absorption of the composite.
- Increase in the matrix failure strain results in higher energy absorption in brittle fiber reinforcements

- Change in stiffness has very little effect on the energy absorption.

Thornton & Jeryan report that specific energy absorption is a linear function of the tensile strength and tensile modulus of the matrix resin, and that it increases with the order phenolic < polyester < epoxy for glass fiber tubes. While this observation may be reasonable, it is not conclusively verified by direct reference to material property data (Table 2) because of the spread in reported values. [20]

Table 3. Mechanical Properties of resin systems [20].

Fiber	**Density (kg/m^3)**	**Young's Modulus (GN/m^2)**	**Tensile Strength (MN/m^2)**
Epoxy	1100-1400	2.1-6.0	35-90
Polyester	1100-1500	1.3-4.5	45-85
Phenolic	1300	4.4	50-60

Carbon fiber reinforced composite tubes with different kinds of thermoplastic matrices were studied. The specific energy of thermoplastic tubes follow the order PAS<PI<PEI< PEEK. In a similar study, energy absorption of carbon/PEI (C/PEI), carbon/polyimide (C/PI), carbon/polyarylsulfore (C/PAS), carbon/PEEK (C/PEEK), were investigated and compared with that of carbon/epoxy and glass/polyester. Carbon/thermoplastic tubes demonstrated superior energy absorbing capabilities (E_S=128–194 kJ/kg) than carbon/epoxy (E_S=110 kJ/kg) or glass/polyester (E_S=80 kJ/kg) structures. [7]

3.2.7.3 Fiber & Matrix combination

The studies described above tend to relate the energy absorption capability of an FRP to the individual properties of its constituent fibers and matrix. It was proposed that energy absorption is substantially dependent on the relative (rather than the absolute)

properties of the fibers and matrix. In particular, he reports that the relative values of fiber and matrix failure strain significantly affect energy absorption. It is suggested that to achieve maximum energy absorption from an FRP, a matrix material with a higher failure strain than the fiber reinforcement should be used. This ensures crushing by high-energy fragmentation. [20]

3.2.7.4 Effect of orientation & lay-up

The orientation of the fibers in a given layer, and the relative orientation of successive layers within a laminate, can significantly affect a component's mechanical properties.

Energy absorption capability varies with ply orientation. Variations in specific energy absorption were observed in tests on $[0/\pm\theta]_3$ carbon/epoxy tubes for $15^o<\theta<45^o$. Specific energy absorption fell quite markedly over this range. This would suggest that carbon fibers absorb most energy when their orientation tends towards that of the loading. However, it was noted that a laminate consisting entirely of 0^o fibers would be unlikely to have good energy absorption characteristics. In particular, the absence of an outer hoop (90^o) layer in laminated tubes can lead to very low energy absorption.

In pertinent to aramid/epoxy tubes it was observed that observed smaller variations in energy absorption capability for $[0/\pm\theta]_3$. Specific energy absorption generally increased with increasing θ over the range $45^o<\theta<90^o$. No significant variation was observed for $15^o<\theta<45^o$. This trend is opposite to that observed for carbon-epoxy tubes. [20]

CHAPTER 4

COMPUTER AIDED ENGINEERING TOOLS

Due to increasing cost on conducting real-time crash simulations, CAE tools are very widely used in auto industry. As a result, automakers have reduced product development cost and time while improving safety, comfort, and durability of the vehicles they produce. The predictive capability of CAE tools has progressed to the point where much of the design verification is now done using computer simulations rather than physical prototype testing. Tools used in this study are briefly explained below.

4.1 Msc Patran

MSC Patran is one of the versatile software's that deals with design and finite-element analysis. It is a finite element modeler used to perform a variety of CAD/CAE tasks including modeling, meshing, and post processing for FEM solvers LSDYNA, NASTRAN, ABAQUS Etc. MSC Patran can be used to access any kind of geometrical format standards. In addition to that patran overcomes the traditional barriers like topological incompatibilities and mixed tolerances This has the ability to import geometry from any CAD system and various data exchange standards.

Meshing of any part can be done in simple way using patran which includes powerful tool like solid meshing and editing of elements. Post-processing part of the Msc Patran as good tools which enables to check the deformations, Stresses and correlations.

4.2 Ls-dyna

LS-DYNA is non-linear finite element processor which can be used to solve any kind of Static /Dynamic problems. LS-DYNA users spread all over the world and mostly used to solve complex crash analysis and Manufacturing forming problems.

. Explicit analysis can be used to simulate geomtries which are complex and deforms badly. Explicit analysis requires fewer time step than implicit analysis. Explicit analysis method is more accurate , more faster than the implicit analysis method while doing benchmark analysis (metal forming) and crash analysis

LS-DYNA has more than 100 material models, which includes Elastic, Plastic, Foams, Composites and many more.

LS-DYNA has the capability to do fully automated contact analysis, which is very simple to use and also validated. Penalty method and Constraint method are the two methods that are used to give contacts in LS-DYNA. Many applications that use these methods are Occupant safety analysis, crashworthiness studies and many component analysis. Some of the contacts that are generally used in most of the problems are Surface to surface contact. Some of the examples where contacts are used are, one in metal forming between rigid punch and rigid die and another example between vehicle occupant dummies & airbags/panels.

Following are different kinds of analysis that can be done using LS_DYNA:

- Vehicle crash analysis which includes occupant safety analysis
- Metal forming analysis and optimization
- Simulation of bird strike to aircrafts
- Composite Analysis.

4.3 Madymo

Dynamic behavior of mechanical systems can be simulated using MADYMO (MAthematical DYnamical MOdels) software. When this software was developed, it was used to study passive safety. Now it is used to study active safety and biomechanics.

MADYMO is a combination of Finite Element Technique and Fully Integrated Multibody. This Software is combination of many things in program. It offers the capability of mutibody, for the simulation of systems, which are joined by complicated kinematic joints and the FE techniques.

The outputs that can be collected from MADYMO are force data, acceleration data, torques data and kinematic data. In addition to that MADYMO helps to calculate Head Injury Criteria (HIC), femur and tibia loads, Viscous Injury Response (VC), Gadd Severity Index (GSI) and Thoracic Trauma Index (TTI). The results from the MADYMO can be accessed using many post-processing programs [22].

4.4 Easi Crash Dyna (ECD)

EASI CRASH DYNA is the first fully integrated simulation environment specially designed for crash engineering requiring large manipulation capability. It can directly read files in IGES, NASTRAN, PAM-CRASH, MADYMO and LSDYNA data. ECD has unique features, which enable the crash simulation more realistic and more accurate. These are

Pre-Processing Features

- Fully automatic meshing and automatic weld creation
- Rapid graphical assembly of system models
- FE-Dummy and Rigid body dummy structuring, positioning and orientation
- Material database access and manipulation
- Graphical creation, modification and deletion of contacts, materials, constraints and I/O controls

- Automatic detection and correction of initial penetration
- Replacing the component from one model to another model

Post-Processing Features

- Highly optimized loading and animation of DYNA results for design
- Superposition of results for design
- User friendly and complete plotting for processing simulation and test data comparisons
- Quick access to stress energies and displacements without reloading the file
- Dynamic inclusion/exclusion of parts during animation and visualization
- Import and super-imposition of test results with simulation results
- Synchronization between animation and plots, between simulation result file and test result file

EASI-Plot Features

- User friendly complete plotting tool for processing simulation and test data
- Easy access to engineering functions
- Plot file re-generation using template and session file

4.5 Easi-Crash Mad

EASi-CRASH is based on EASi's 10+ years of practical experience in crash simulations. It greatly enhances the simulation process by allowing concurrent access to the model and simulation results. Animation, visualization and synchronized curve plotting make EASi-CRASH MAD a high performance CAE environment.

Pre-processing features

- Graphical creation, modification and deletion of multi-bodies and FE entities

- FE meshing and manipulation capabilities
- Graphical display, browsing and editing of MADYMO entities through browser interface (MADYMO explorer)
- Supports INCLUDE files
- Card Image representation of MADYMO input deck
- Quick JOINT definition and orientation
- Easy dummy positioning
- Rapid contact creation, modification and preview through Contact spreadsheet
- High speed generation of MADYMO and FE seat belt using automated belt routing techniques
- Supports advanced airbag modeling (CFD)

Post-processing features

- Simultaneous access to both model and result files
- Associate model option to display kn3 file as a data file
- Export of model and results (kn3) display in GIF and JPEG format
- Simultaneous animation and visualization of stresses, displacements and time history plots with synchronize option
- Multi-mode (wire frame, shaded, transparent and silhouette) operation during animation and visualization
- Ability to superimpose two animation files for design comparison
- Camera option to focus and study the behavior of an object
- Penetration visualization between multi-bodies
- Allows creation of trajectory for multi-bodies and FE nodes

CHAPTER 5

DYNAMIC CRASH ANALYSIS OF FORD TAURUS

5.1 Study of Finite element Ford Taurus model

Use of finite element vehicle model for crash analysis is increasing progressively in industry. The main reason being repeatability of tests and reduction in cost of production. With the increase in the use of FE models, the models are improving in terms of accuracy, robustness, fidelity and size.

The Ford Taurus model which we have used for our analysis is a four-door sedan with 5 meters length and 2.76 m wheelbase. It is developed by National Crash Analysis Center. Figure 15 shows the finite element model of Ford Taurus Model.

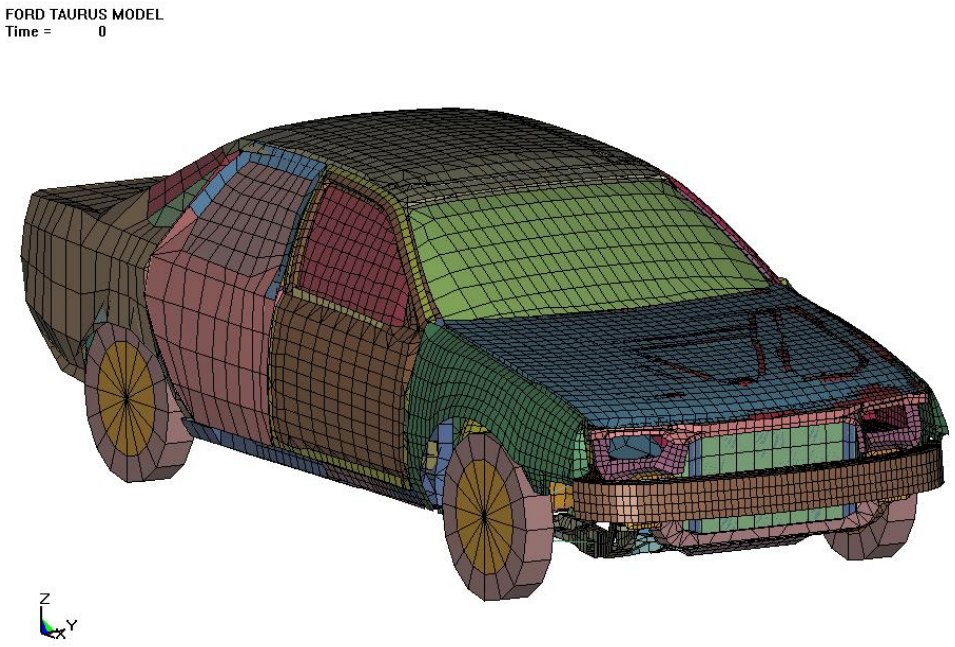

Figure 16. FE Model of Ford Taurus Vehicle.

Usually in frontal impacts the vehicle undergoes heavy deformations on the front end whereas the central and the rear portions hardly undergo any deformation. Since these

models are developed for frontal impacts, the front portion of the vehicle is meshed finely and the middle and the rear portions of the vehicle are coarsely meshed. Some parts are modeled as beam elements and joined with spot welds. Such modeling does not affect the accuracy of the model as long as the mass and inertia distribution is consistent with actual model.

5.1.1 Development of the fe models

The FE Ford Taurus model is developed by a method called as digitizing. In this method the real time vehicle model is disassembled into different groups like front inner, front outer, frame, cabin, doors, rear trunk, etc. Three dimensional geometric data of each component is then obtained by using a passive digitizing arm connected to the computer. The digitized data is stored in IGES format using some CAD software. This IGES data is then imported in pre-processors like PATRAN or HYPERMESH and meshed accordingly. The output file obtained from the pre-processors is then submitted to the processor LS-DYNA to check the accuracy of the model. Considerable details are included in the FE models like the suspension characteristics, radiator, engine, frame rails, etc are digitized in detail minimizing any loss in the part's geometry.

5.1.2 Detailed description of finite element model

The finite element model of the vehicle is made of 123 parts. All the parts represent the different parts of the vehicle. 104 parts are made of shell elements, 18 parts are made of beam elements to represent the steel bars in the vehicle. One part is made of brick elements that represent the radiator. Two different types of shell elements are used, triangular and quadrilateral. The shell elements are assigned with isotropic elastic plastic material, the stress strain relationship being defined by eight stress strain points. Beam

elements are assigned with isotropic elastic material and the solid elements are assigned with honeycomb material with constant stress element formulation. The parts are joined by rigid body constrained options and spot welds. The contacts between different parts are modeled as single surface-sliding interface also known as automatic contact for the beam, shell and solid element with arbitrary segment orientation. Table 4 gives the summary of the vehicle model.

Table 4. Summary of vehicle model.

Number of Parts	123
Number of Nodes	26729
Number of Shell Elements	27873
Number of Solid Elements	340
Number of Beam Elements	140

5.2 Frontal Crash Analysis of Ford Taurus Model

The FE Ford Taurus model is tested against the full width rigid barrier at 30mph according the NHTSA Experimental test that is FMVSS 208 regulations. The analysis is done using LS-DYNA. The rigid wall is modeled as rigid plane using the card of RIGIDWALL_PLANAR.

5.2.1 LS-DYNA Simulations

The full frontal rigid barrier analysis is carried out in LS-DYNA for 120 milliseconds. The accelerometers are placed at eight locations in the vehicle. The contacts are defined by geometric interface. The distance between the vehicle and the barrier is kept to the minimum in order to minimize the simulation time. There is considerable

deformation of hood, bumper and engine compartment as can be seen below. Figure 16 shows the animation sequence of the full frontal rigid barrier crash test carried out 30mph.

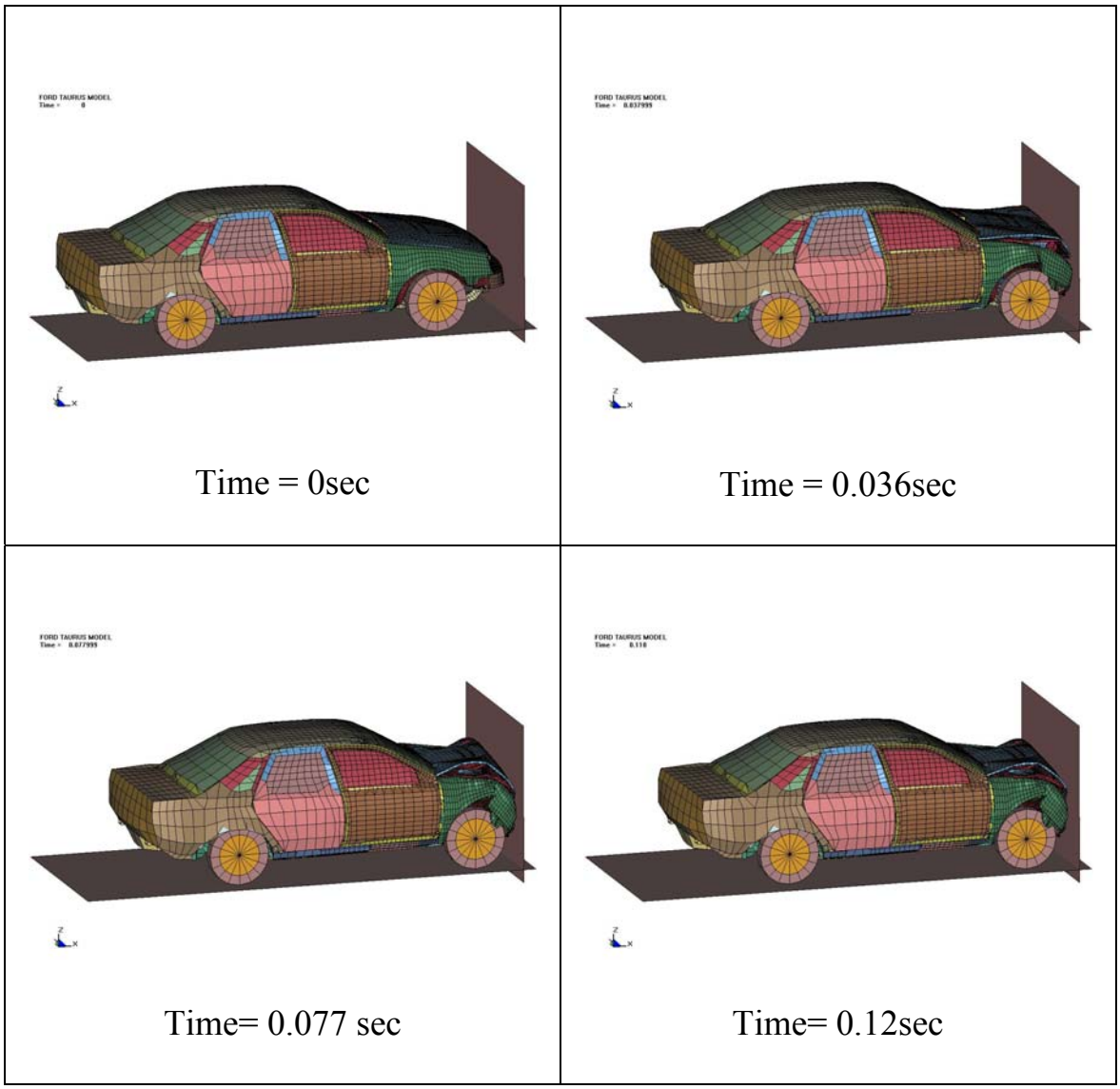

Figure 17. Animation sequence for full width rigid barrier test.

5.2.2 Model validation

The accuracy of simulation is evaluated by comparing the simulation test results with the actual test results. In order for the simulation be fairly accurate the profile of the acceleration data obtained from the simulation should closely match the profile of the

acceleration data obtained from actual sled test results. Here we have compared the x-acceleration data of the some of the accelerometers at different position in the car. Figure 17 shows the engine x-acceleration comparison of the simulation and the test result.

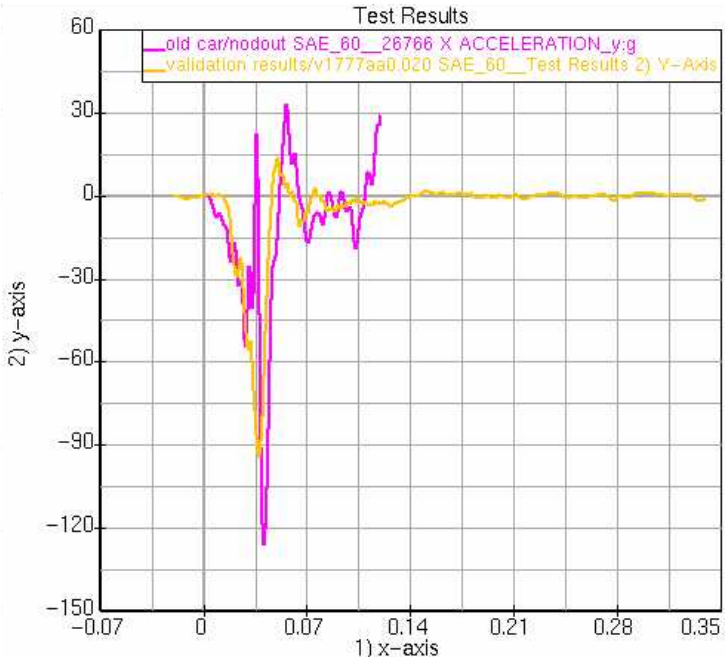

Figure 18. Comparison of acceleration levels for the actual test and LS-DYNA simulation at Engine Bottom.

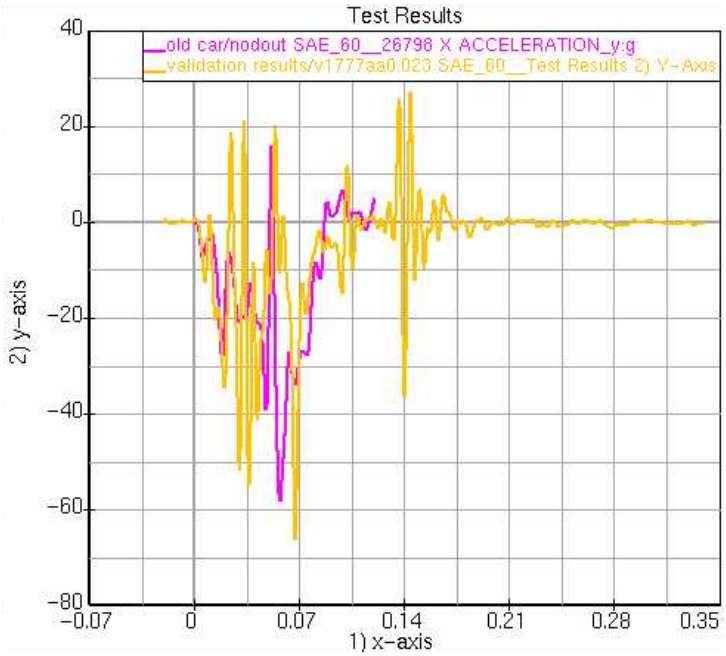

Figure 19. Comparison of acceleration levels for the actual test and LS-DYNA simulation at C.G of the car.

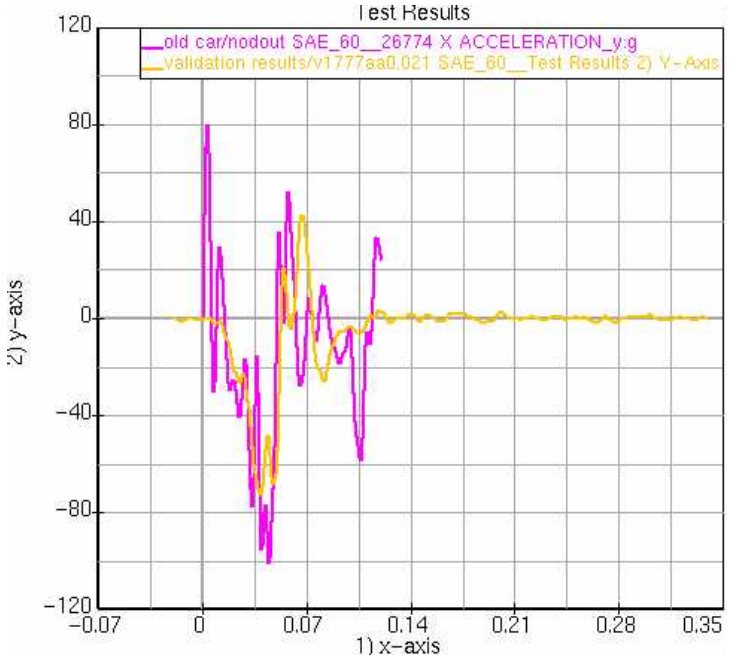

Figure 20. Comparison of acceleration levels for the actual test and LS-DYNA simulation at Right brake caliper.

From the above figure we can clearly see that the acceleration profile obtained from simulation closely matches with the acceleration profile obtained from the actual sled test results. The accelerometers are located on the engine and are defined as rigid bodies assigned with time-history to that particular set of nodes of rigid body.

5.3 IIHS 40 % Offset Frontal Crash Test

In full width rigid barrier test the impact force is distributed over the entire width of the vehicle. As a result there are fewer amounts of intrusions resulting in more integrity of the occupant compartment. Also the deceleration levels are very high in full width rigid barrier test. Unlikely in offset frontal crash tests the impact force is distributed over just 40 percent of the vehicle as can be seen in figure 20. In case of offset tests the intrusion in the occupant compartment are very high. Hence the offset tests are more demanding for structural analysis and full width tests are more demanding for restraint analysis. The

offset test has been carried out at 40 mph with 40 percent overlap of the vehicle on the deformable barrier.

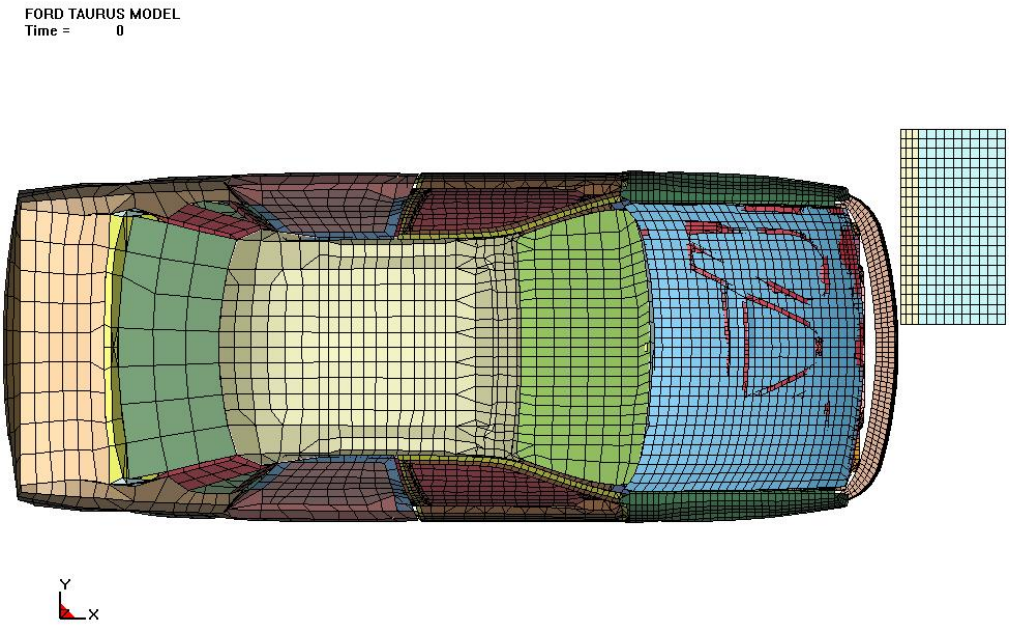

Figure 21. Test setup for Offset Crash Analysis.

5.3.1 Test condition

The test vehicle is aligned with the deformable barrier such that the right edge of the barrier face is offset to the left of the vehicle centerline by 10 percent of vehicle's width (figure 21).

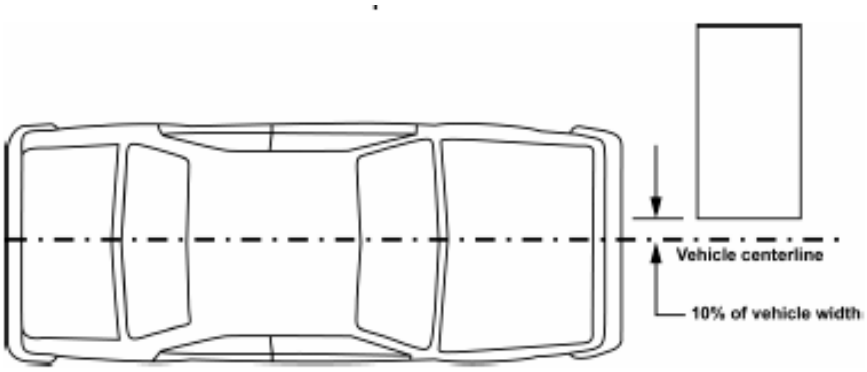

Figure 22. IIHS Offset test setup [9].

The vehicle width is defined and measured as indicated in SAE J1100-Motor vehicle Dimensions, which states, “The maximum dimension is between the widest part on the vehicle excluding exterior mirrors, flexible mud flaps, and marker lamps, but including bumpers, moldings, sheet metal protrusions, or dual wheels, if standard equipment.” The vehicle is accelerated by propulsion system at an average of 0.3 g until it reaches the test speed and then is released from propulsion system 25 cm before the barrier. The onboard breaking system, which applies the vehicle’s service brakes on all four wheels, is activated 1.5 seconds after the vehicle is released from the propulsion system.

5.3.2 Barrier composition and preparation

The barrier is composed of three elements: base unit, extension and deformable face (figure 22).

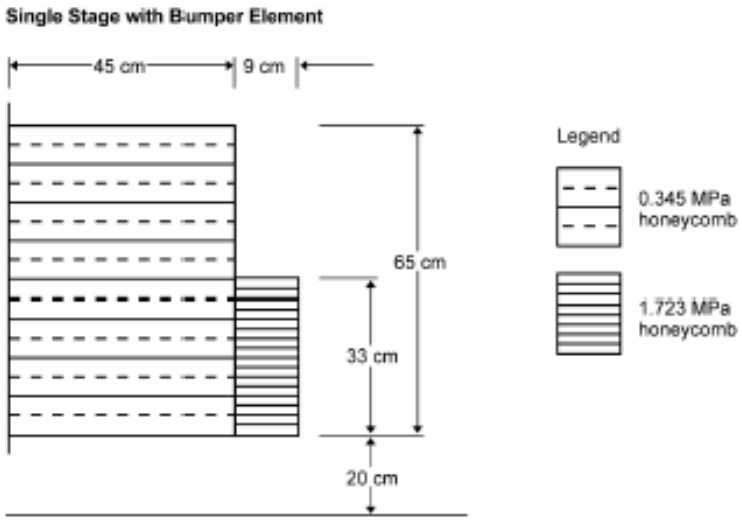

Figure 23. Deformable Barrier face profile and Dimensions [9].

The base unit is 184 cm high, 366 cm wide and 542 cm deep. It is composed of laminated steel and reinforced concrete with total mass of 145,150 kg. The extension is 91 cm high, 183 cm wide and 125 cm deep. It is made of structural steel and has a 1.9 cm thick piece

of plywood attached to the 4.5 cm thick face plate. The deformable face is 1m wide and consists of bumper element of 1.723 MPa honeycomb material attached to a base of 0.345 MPa honeycomb.

5.3.3 LS-DYNA simulations of offset impact test

The offset impact test was carried out at 40 mph using LS-DYNA. The deformable barrier was developed according to the specification mentioned above using HYPERMESH. The simulation was carried out for 120 milliseconds. The distance between the barrier and the car is kept minimum, in order to reduce the simulation time. Figure 23 shows the animation sequence for 40 percent offset test.

5.4 Time History Plots

In the offset crash test, since total impact energy is absorbed by 40% of the frontal structures, the intrusions are found to be more as compared to the full frontal test. For the offset crash test, the acceleration time histories at three important locations in the car model are recorded. The accelerometers are located at the top of the engine, on the instrument panel, between the front seats. In the offset the decelerations at various locations of the car model show low peaks when compared to the full-width. The engine top and front floor between the seats, decelerations are low when compared to the full-width. Figure 24 to Figure 26 show the acceleration curves.

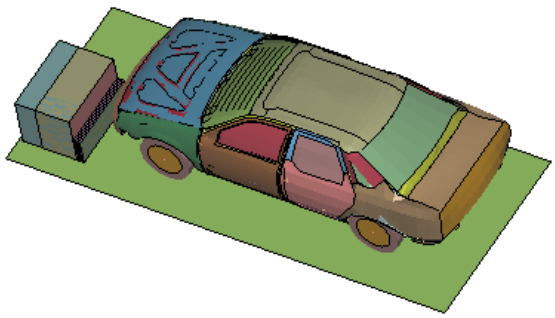

Time = 0sec

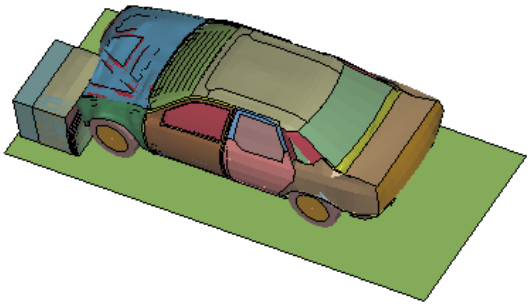

Time = 0.036sec

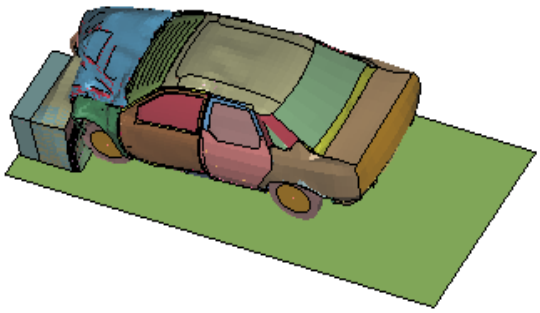

Time= 0.072sec

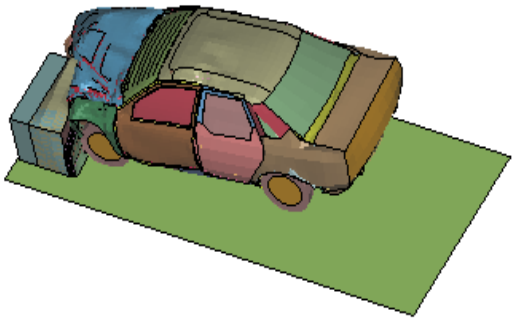

Time= 0.12sec

Figure 24. Animation sequence for IIHS 40 % offset test.

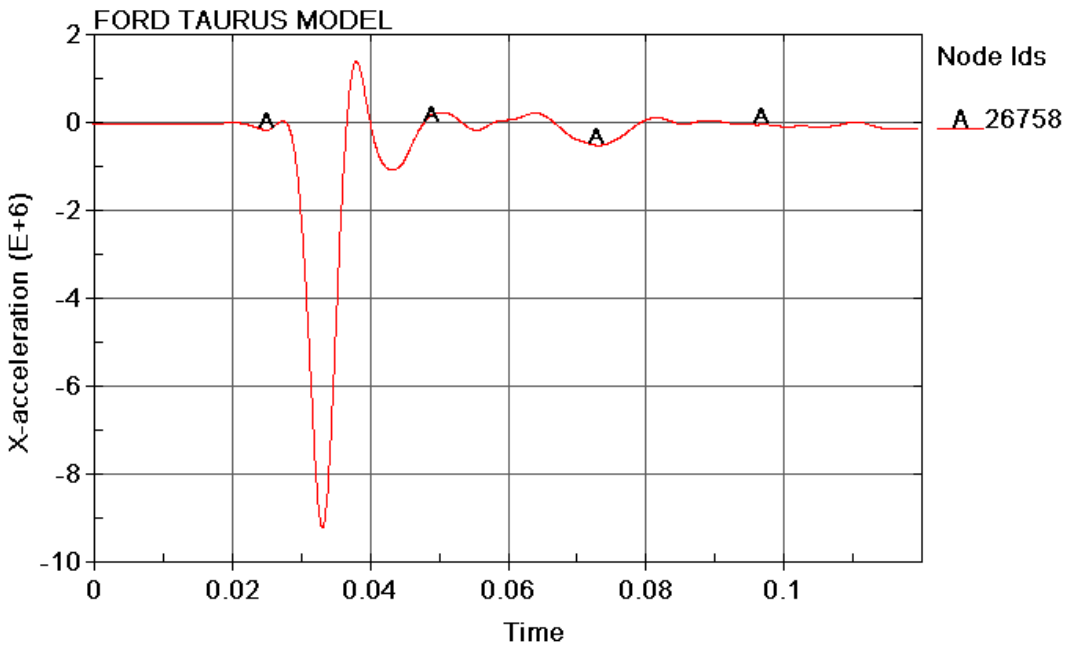

(a) Engine X-acceleration for full width rigid barrier test

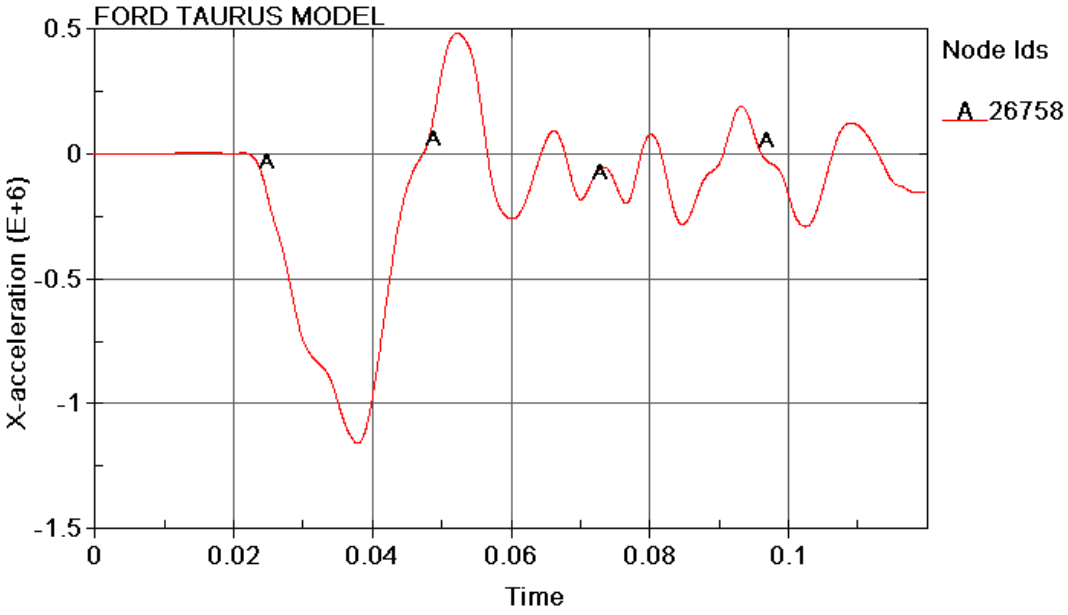

(b) Engine X-acceleration for offset test

Figure 25. Comparison of Engine X-acceleration for full width rigid barrier and offset test.

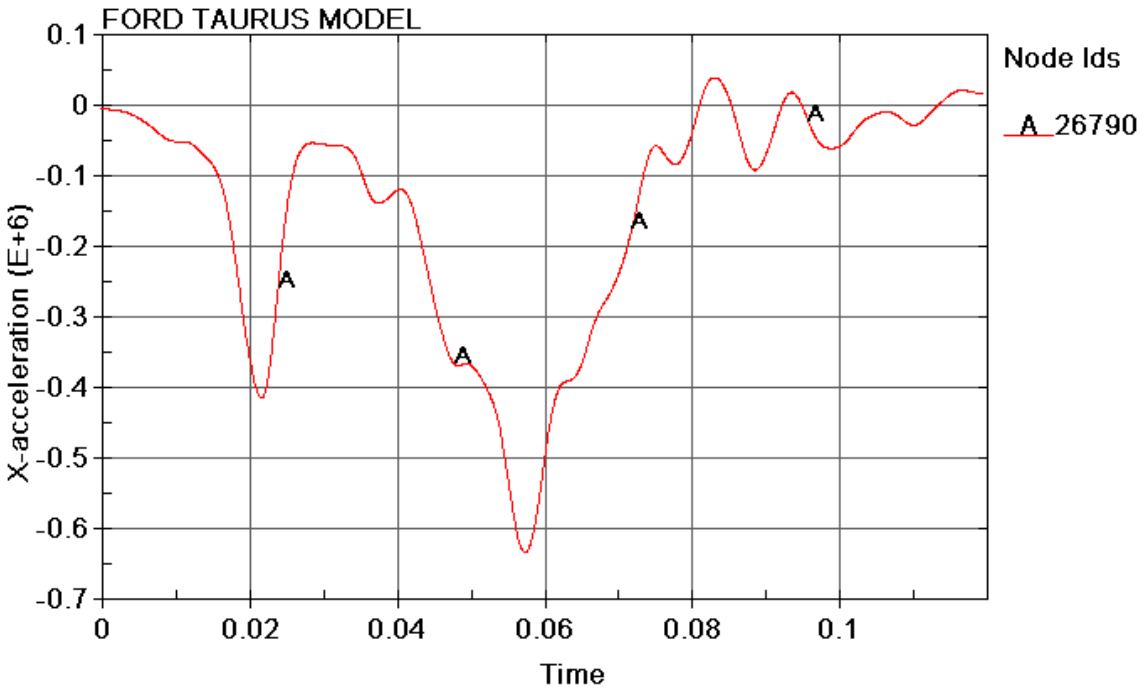

(a) Dashboard X-acceleration for full width rigid barrier test

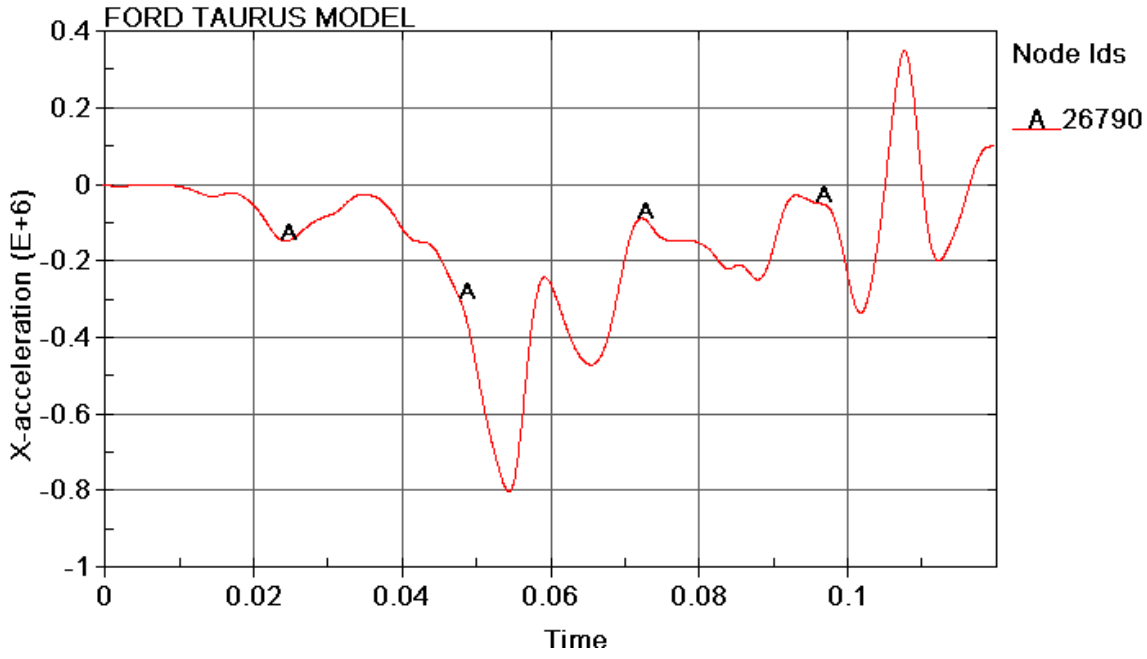

(b) Dashboard X-acceleration for offset test

Figure 26. Comparison of Dashboard X-acceleration for full width rigid barrier and offset test.

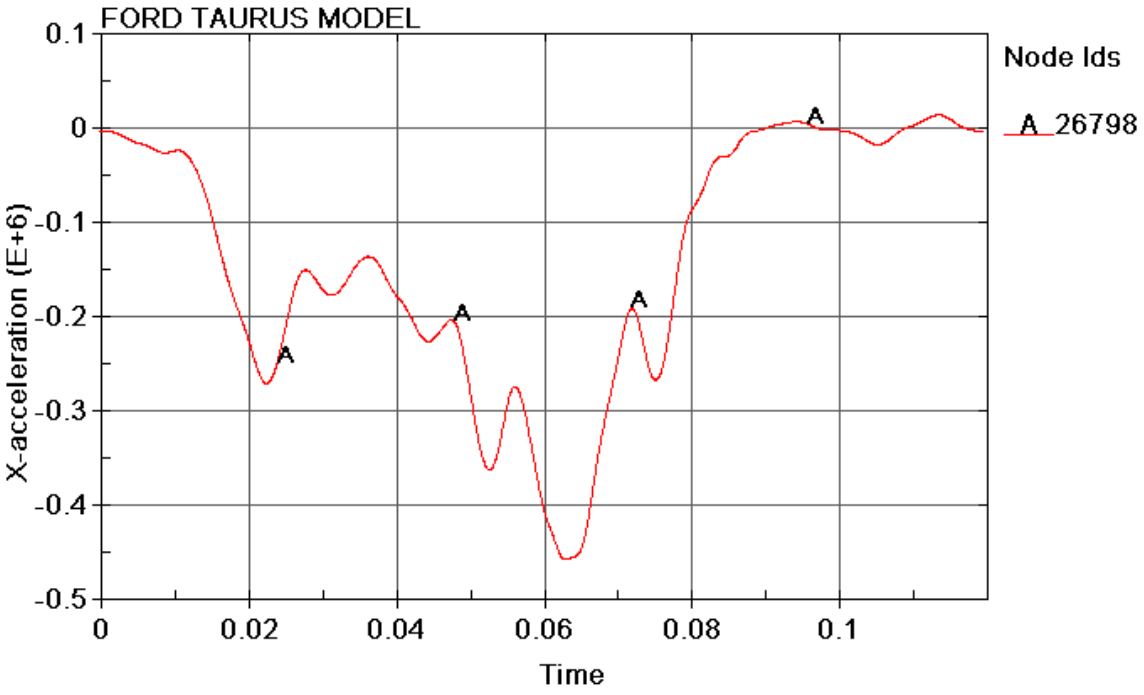

(a) Floor X-acceleration for full width rigid barrier test

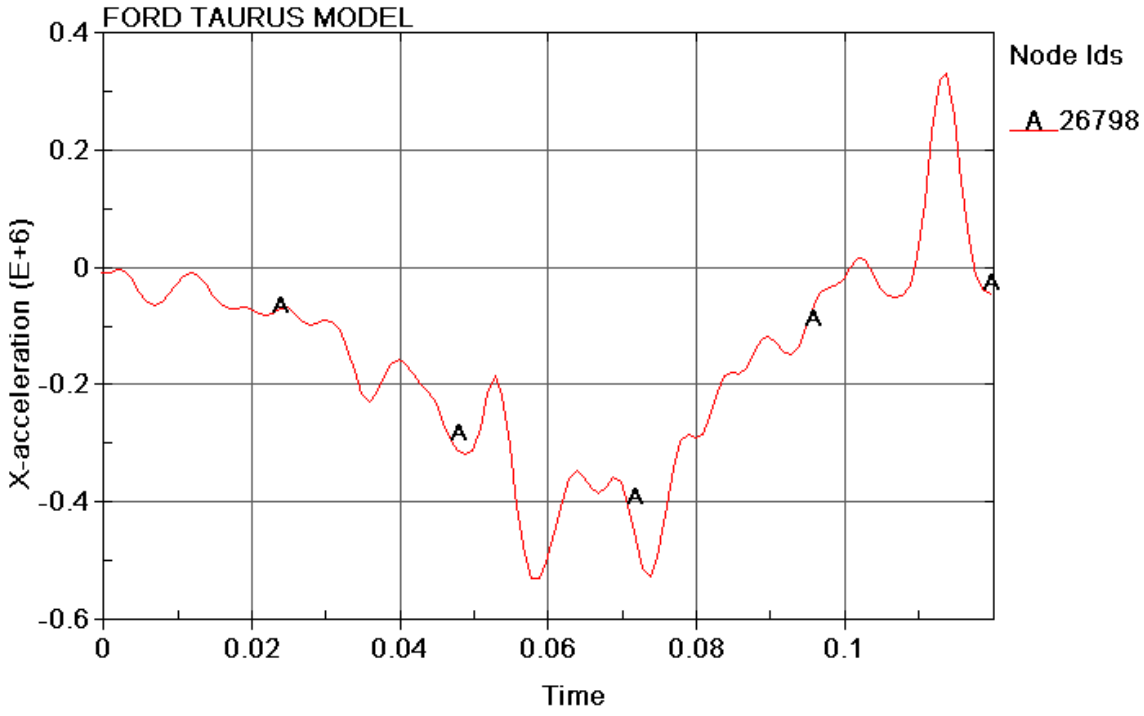

(b) Floor X-acceleration for offset test

Figure 27. Comparison of Floor X-acceleration for full width rigid barrier and offset test.

CHAPTER 6

DESIGN AND ANALYSIS OF CAR FRONT SUB-FRAME RAILS

6.1 Energy Management

The engine sub-frame rails are important contributors to crash energy management in frontal impact for automotive vehicles. Sub-frame design can enhance vehicle crash performance through energy management. In addition to energy management targets, the sub-frame must meet stiffness, durability and other vehicle engineering requirements. For any given vehicle crash we see that the amount of energy absorption is directly proportional to the amount of vehicle deformation. Thus more the amount of deformation more is energy absorbed. However the stiffness requirements cannot be neglected with respect to intrusions in the occupant compartment. The concept to improve the compatibility is to eliminate the influence of geometry to increase the crash energy absorption amount in the engine compartment.

6.2 Energy Absorption System for Collisions

The developed system has the capacity of transferring an outstanding part of energy from frontal impact to other area of the vehicle body in white.

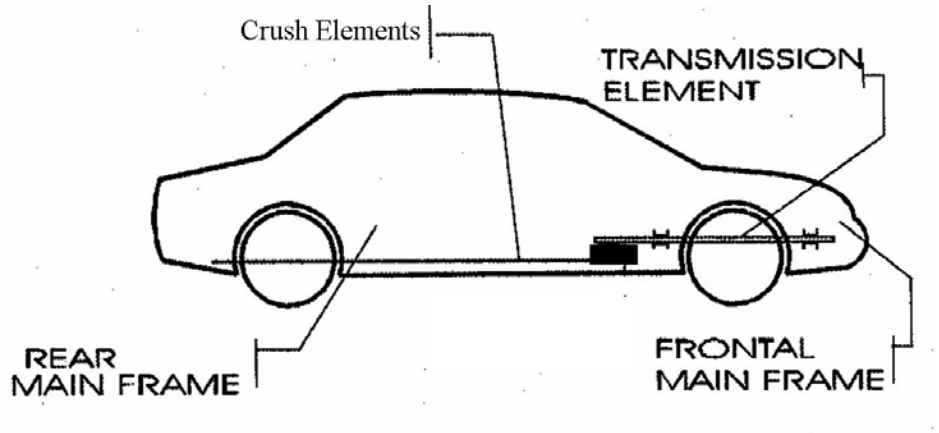

Figure 28. Energy absorption system for collisions [4].

As can be seen from figure 27, the system consists of longitudinal beam (flexible / translating frame) in the vehicles frontal part, connected to the crush elements placed below the floor of the vehicle. Therefore when the frontal crash occurs, the longitudinal beam is horizontally displaced behind, crushing the elements placed below the floor. When a frontal impact occurs, frontal mainframe is deformed, but the transmission element is displaced, transmitting the movement to the deformable additional element. In this way both the frontal main frame and the crush elements placed below the floor have the capacity to take up the frontal collision energy.

6.3 Section Modeling of Rails

The automotive mid rails are the main load carrying, energy-absorbing component during frontal and angled impacts. Mid-rails generally have non-uniform cross-sections contain crush initiators and include several holes. In this research, the frontal section is divided into several sections, where outer section is responsible for the most deformation. For that reason, frontal section is modeled with low-grade steel when compared to different section. Fig 28 shows how different grades of steel are used in the car for effective energy absorption.

This research concentrates more on the part, which absorbs most of the energy during frontal crashes, i.e. Rails. Here rails are divided into two sections, in which front portion of the rail are modeled with low strength steel and later part of the rail are modeled with high strength steel. The purpose is , in case of frontal crash first the front part comes in contact with rigid barrier or other vehicle , so the front part with low grade steel deforms faster than the later part with high grade steel which takes more time to deform, finally reduces the injury parameters of the occupants in the car.

Figure 29. Section Model in Volvo Model [4].

In this research the front section of the rail is modeled with low strength steel and later part is modeled with high strength steel

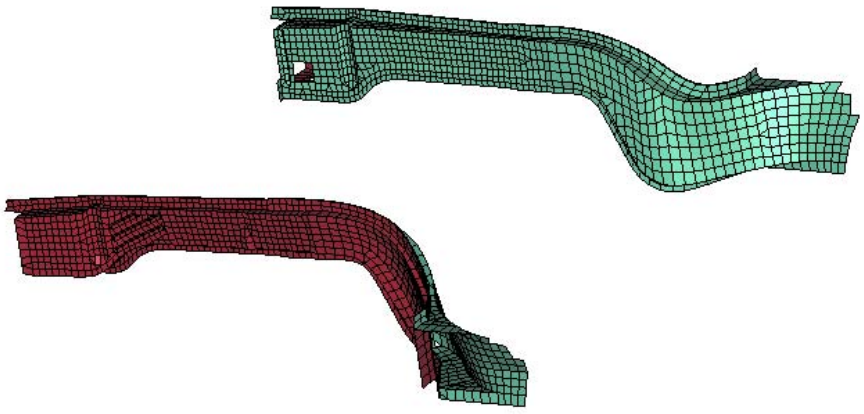

Figure 30. Rails in the Original Model.

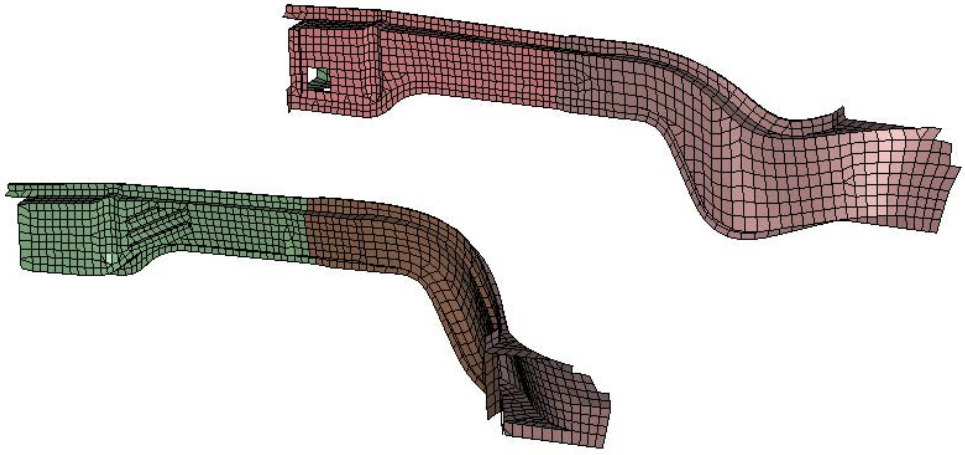

Figure 31. Rails in the Section Model.

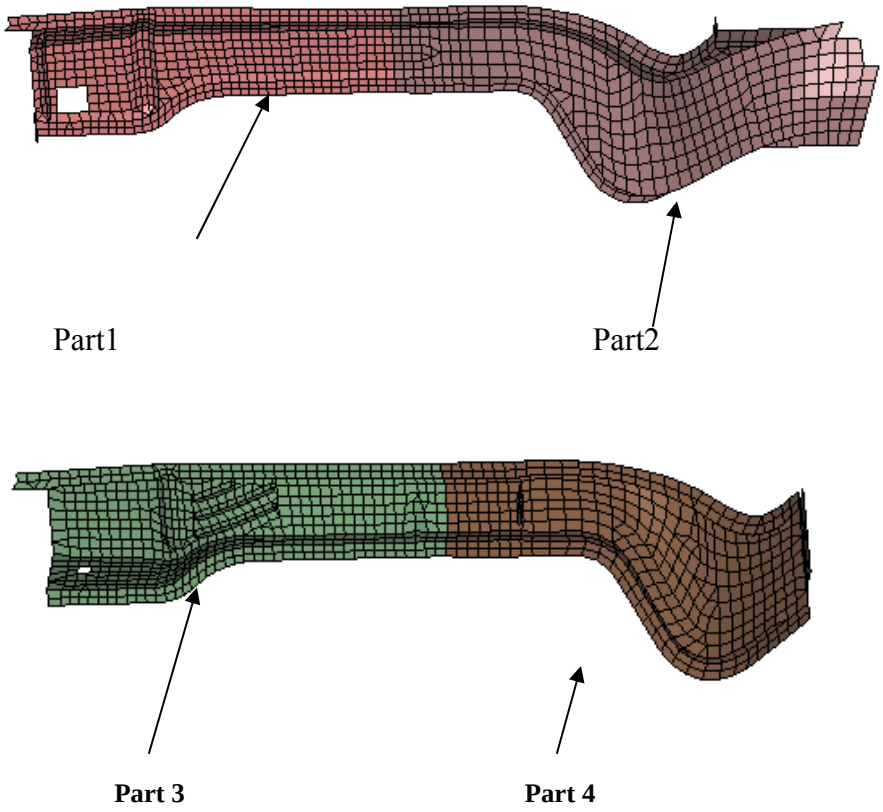

Figure 32. Exploded view of Rails in the Section Model.

Above fig 31 shows the section model of the rails. Here part 1 and 3 are modeled with low strength steel and part 2 and 4 are modeled with high strength steel. These parts are joined by spot welding. In LSDYNA analysis, CONSTRAINED_SPOTWELD chord is used to join different parts.

6.4 Analysis of the Section Model for full width rigid barrier tests

The vehicle with sectioned rails is shown in fig 32 and is then tested for full width rigid barrier test according to FMVSS 208 regulations at 30 mph speed

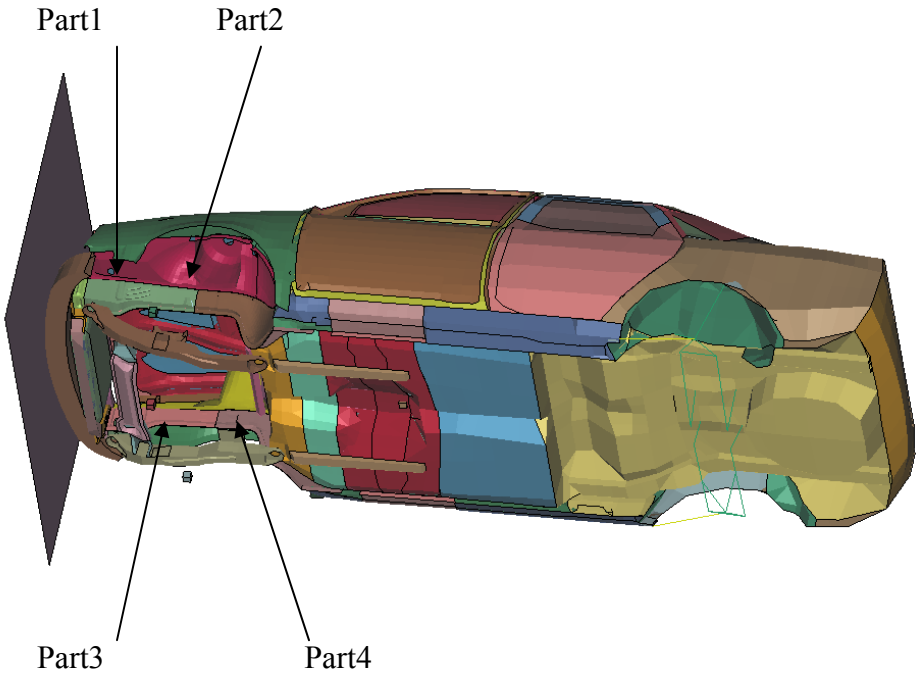

Figure 33. Section model of car.

During the development process of the Section Model, the Sub frame rails are modeled with different thickness. The thickness of the rails in the original model is 2 mm, here in section model we have considered 1.3mm for part 1 and part 3 and 2.6mm for part 2 and part 4. Here different thickness are considered for rails because in case of frontal crash when vehicle goes and it's a rigid barrier or other vehicle, part 1 and 3 starts deforming first and then part 2 and 4. All the parts are joined using Spot welding.

Due to lots of modifications of parts, the model remains no more validated model, however we need to check the performance of the vehicle after so many modifications and compare it with the validated model of the original vehicle.

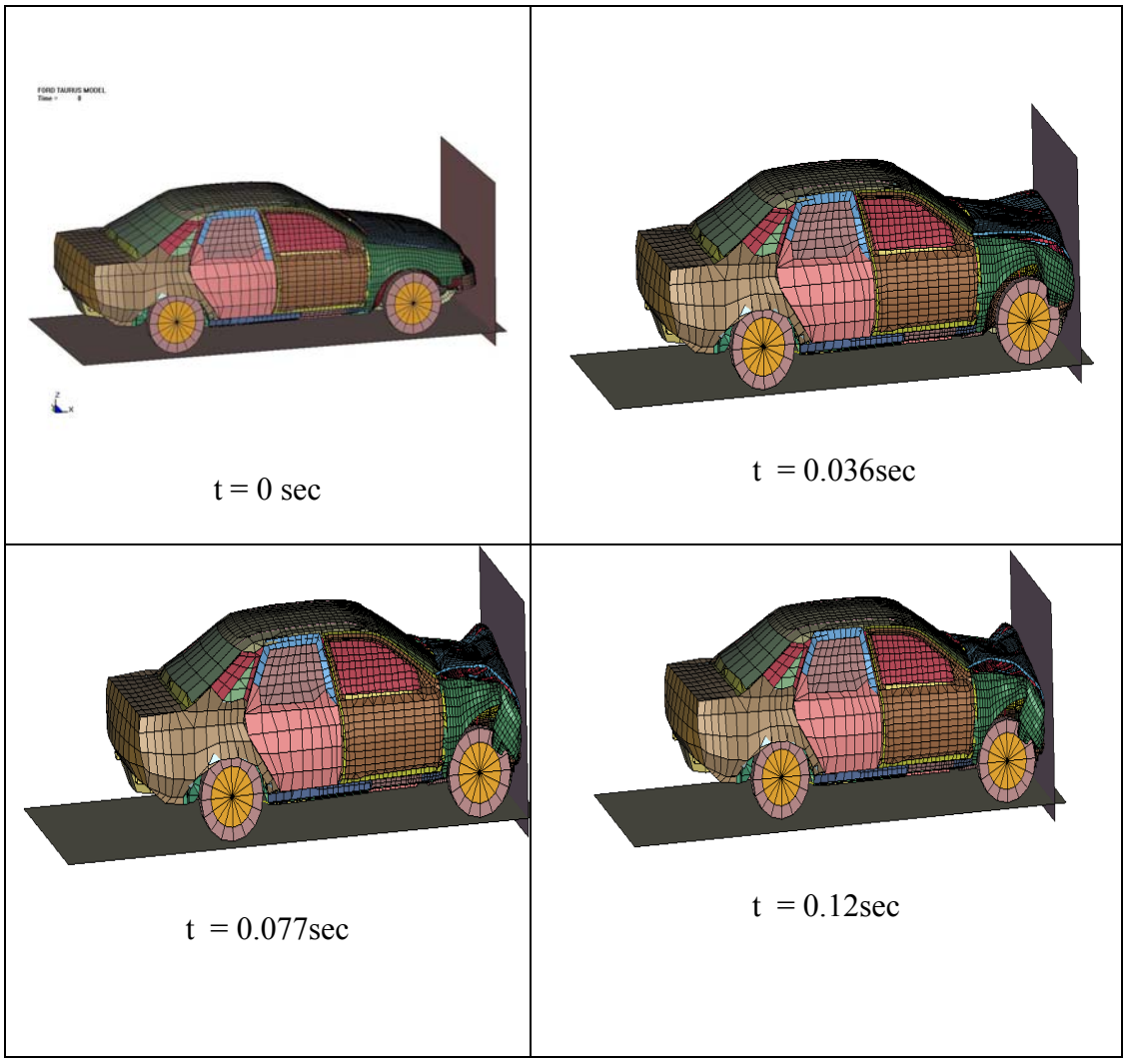

Figure 34. Animation sequence for the section model.

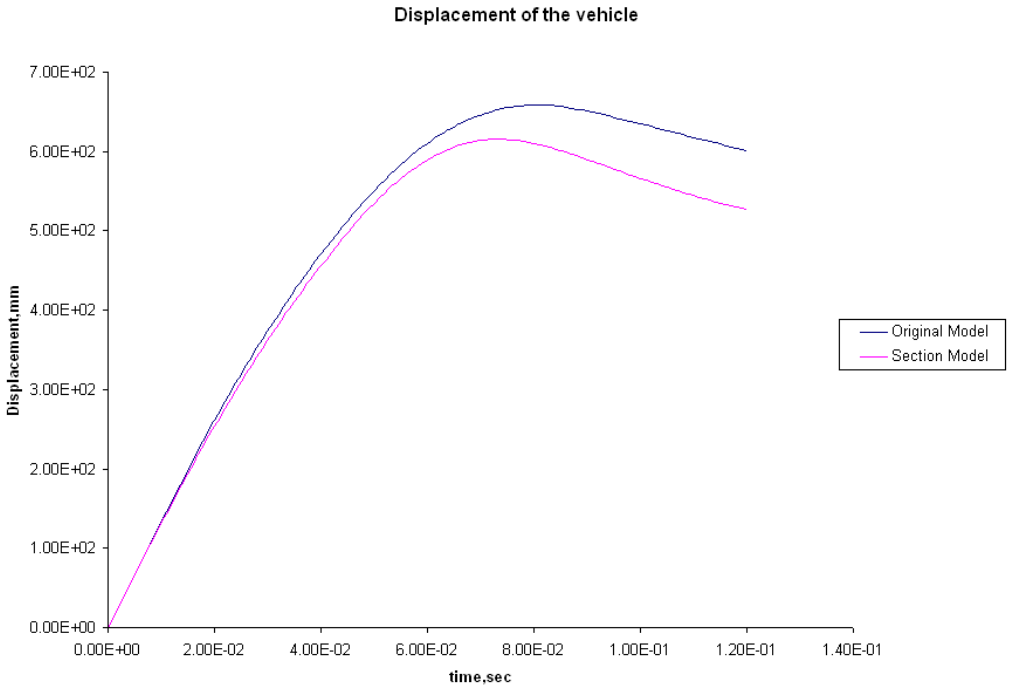

Figure 35. Comparison of vehicle displacement for the Original model and the Section model.

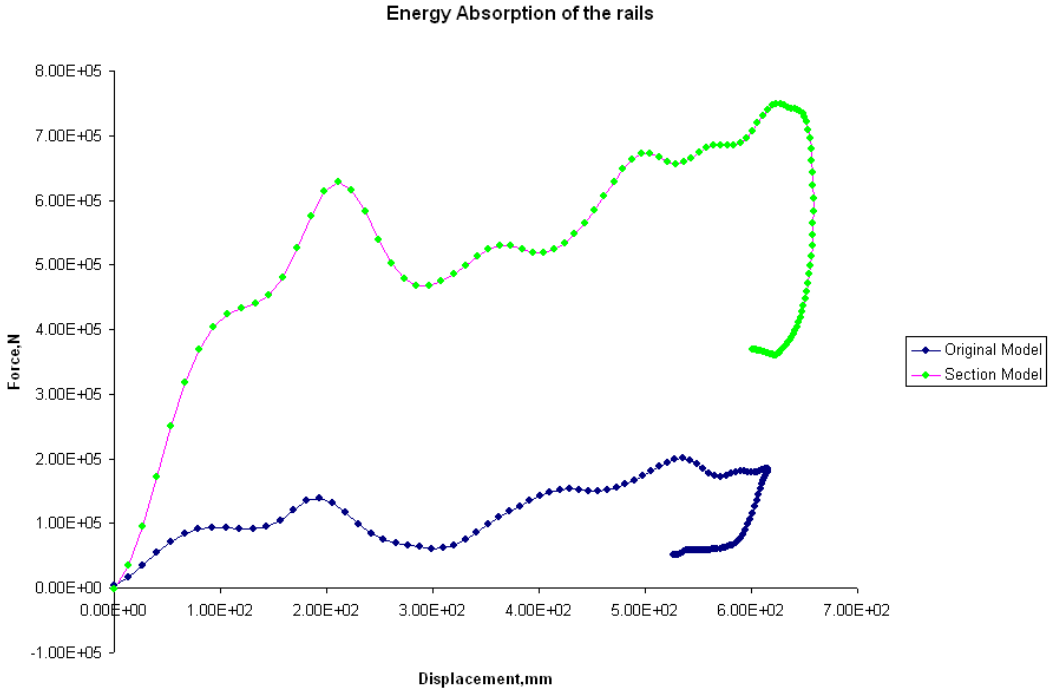

Figure 36. Comparison of Energy absorption of Rails in Original model and the Section model.

Figures 34 and 35 shows the comparison of vehicle displacement and Energy Absorption of the rail for the original Model and Section model. From the figures, we see that the pattern of curves for the vehicle displacements is less in case of section model when compared to original model. When Energy absorption curves are considered, section model absorbs more energy when compared to original model. This is possibly due to different in strengths of the steel used in the section model. Deformation is more at the frontal part of rail then later part ,which reduces the displacement of the vehicle.

6.5 Composite Modeling of Car Front Rails

Improved fuel mileage has become an important requirement of all new designs for automotive applications. As result, interest in lightweight composite materials has increased. Before composite structures can be incorporated in automotive structural applications, a body of FEM and experimental data must be assembled before adequate designs can be offered. One of the requirements of the front structures is the ability to absorb energy in predictable, consistent manner with progressive crush behavior [13]. A key characteristic in the study of the crushing behavior is the specific energy absorbed per unit mass of the material. [23]

Crush energy is a measure used to distinguish composite structures for their use in vehicles for improved crashworthiness. Crush energy absorption is not a materials property like strength or stiffness that can be definitively measured using coupon specimens. Instead, energy absorption is sensitive to the form of the structure in which the material is a part.

Specific Energy absorbed is calculated from the force-displacement curve generated during the crushing process. Figure 36 shows typical force-displacement curve.

From the curve it can be observed that it rises rapidly to an initial peak followed by a stable stage. For a material to have high-energy absorption, the sustained load has to be higher. The initial part of the curve, which is the peak load is controlled by the trigger mechanism or the degree of chamfering at the end where the crushing process is initiated. The peak load can be decreased by increasing the angle of the chamfer and in addition to this, stable crushing can be achieved sooner. Depending on the specimens, the initial peak load may be slightly greater or smaller than the average crushing load in the stable stage[23].

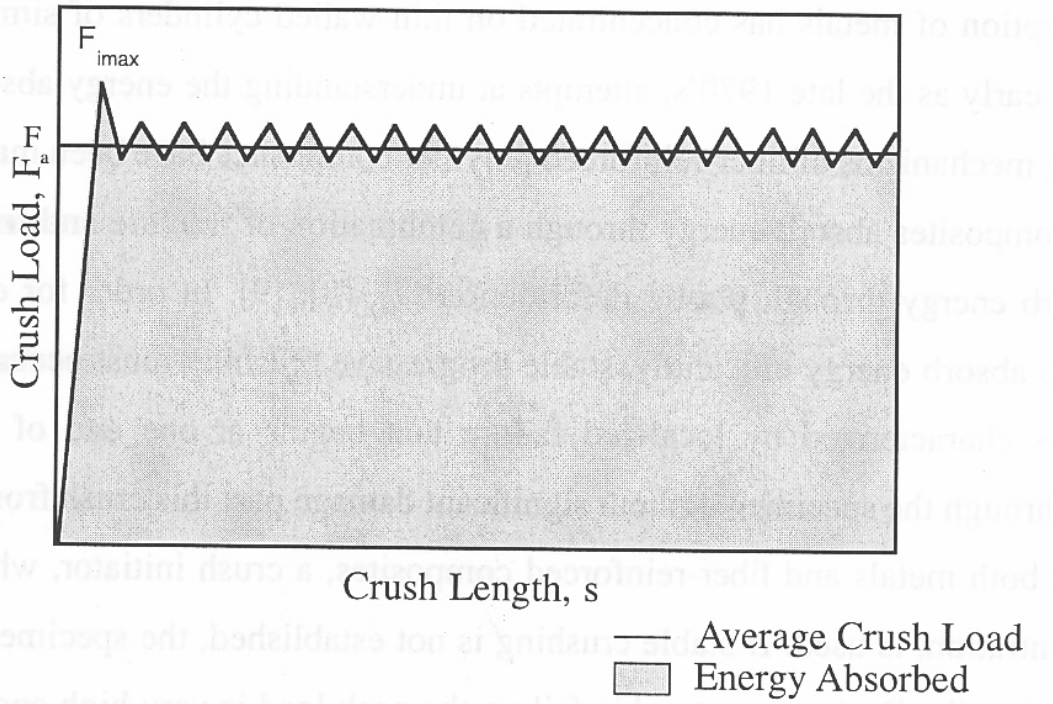

Figure 37. Force v/s Displacement curve [23].

6.5.1 Finite element modeling of the composite rails

Todays diamond shaped steel frames is an evolution by Intuition and trial-and-error process, which is very costly, slow and doesn't yield reliable results. Finite Element

Method is the best proved tool to solve these kinds of problems. FEM breaks the big problem into many small problems which are solved by computers.

In Today's FEM plays a major role in any new design or fine-tuning the existing design. This method can be used from the early stages of design to final stage of design.

When considering structural analysis applications, implicit FE methods can be used in static and dynamic analyses, where linear or moderate nonlinear effects are to be investigated. The implicit method formulates a group of matrices that allows the structural problem to be characterized by mathematical representation of key qualities of the structure, such as mass and stiffness.

The advantage of the explicit FE method is that due to the nature of the computational approach, extremely small time steps coupled with an iterative solving method, produce an unequaled ability to solve time-domain dynamic problems with extreme nonlinearities from material and geometrical effects. Less time is required by the explicit analysis. [17]

6.5.2 Composite modeling details

A Carbon fiber/epoxy model with a stacking sequence of $[(\pm 45°)_6/90°]$ is analyzed in . In this study the composite model is crushed at 30mph according to FMVSS 208 and the results are compared with the original model with steel has material for rails. In addition, parametric study is carried out on the composite model, to find out which configuration gives more energy absorption.

The composite rail is modeled with 13 layers and the thickness of each layer was 0.2 mm, which makes the total thickness of the composite rail to 2.6mm. Material used for the composite tube is Carbon fiber/epoxy and these properties are given in Table 5.

Enhanced Composite damage Material model that is Mat 54 in LS-DYNA is used to model carbon fiber. This card is based on lamination shell theory and used for composite failure analysis [25].

Tsai-Wu failure criterion or the Chang-Chang failure criterion can be used in Mat-54 material model . Tsai-Wu failure criterion is not suitable to study the composite failure modes. Hashin failure mode modified to get the chang-chang failure mode, which considers the tensile/compressive fiber mode, and tensile/compressive matrix mode.

Table 5. Carbon/Epoxy properties.

Property	**Value**	**Units**
Density	1.58E-06	Kg/mm^3
Ply longtitudinal modulus	142	Gpa
Ply transverse modulus	10.3	Gpa
Ply poisson's ratio	0.27	-
Ply shear modulus in plane	7.12	Gpa
Ply transverse modulus parallel to fiber direction	3.15	Gpa
Ply transverse modulus perpendicular to fiber direction	7.12	Gpa
Ply longitudinal tensile strength	1.83	Gpa
Ply longitudinal compressive strength	1.096	Gpa
Ply transverse tensile strength	0.057	Gpa
Ply transverse compression strength	0.228	Gpa
Ply shear strength	0.07	Gpa

Based on the above rule,Both minor poisson's ratio and transverse modulus are reduced to zero, if matrix shear failure and/or fiber breakage occurs in the composite lamina. On the other hand, Minor Poisson's ratio and transverse modulus reduce to zero if matrix tensile or compressive failure occurs first, but the shear modulus and longitudinal modulus remain unchanged. Below equations are based on Chang-Chang failure criterion. [25]

Fiber rupture occurs if

$\sigma_{11} \geq 0$: tensile fiber ……..……..5.5

$(e_f)^2 = (\sigma_{11} / Y_t)^2 + (\sigma_{12} / S_c)^2 - 1$ { ≥ 1 failed & < 0 elastic} ……5.6

Fiber buclking and kinking occurs if

$\sigma_{11} < 0$: Compressive fiber mode …….. 5.7

$(e_f)^2 = (\sigma_{11} / Y_t)^2 - 1$ { ≥ 1 failed & < 0 elastic } ……5.8

If $\sigma_{22} \geq 0$: tensile matrix mode (matrix cracking under transverse tension and shearing)

…….5.9

$(e_m)^2 = (\sigma_{22} / Y_t)^2 + (\sigma_{12} / S_c)^2 - 1$ { ≥ 1 failed & < 0 elastic} …….5.10

If $\sigma_{22} < 0$: Compressive Matrix mode (Matrix cracking under transverse compression and shearing) …… 5.11

$(e_d)^2 = (\sigma_{22} / 2S_c)^2 + (\sigma_{22} / Y_c) [(Y_c / 2S_c)^2 - 1)^2 - 1] + (\sigma_{12} / S_c)^2 - 1$ { ≥ 1 failed & < 0 elastic } ……5.12

MAT 54 material model (Enhanced Composite Damage Material) has the capability of deleting elements when there is a composite layer failure. Deletion of elements can be controlled by additional parameters in the material model

If the smallest time step goes lower than the defined time step, elements are set to fail [25]. Crushing process can be simulated when the elements adjacent to the failed elements allowed to reduction of strength. In the present model, only two percents of the elements were deleted and rest of the elements were intact.

6.6 Results and Discussion

Energy absorption is calculated by finding out the area under the load v/s displacement curve. This is calculated using the MATLAB software where in it calculates the area by plotting trapezoids in the region. It sums up all the trapezoidal area to obtain the area under the curve which is the energy absorbed. The carbon-fiber epoxy material model for this composite rail has energy absorption of 189.32 X 10^3 KN-mm..

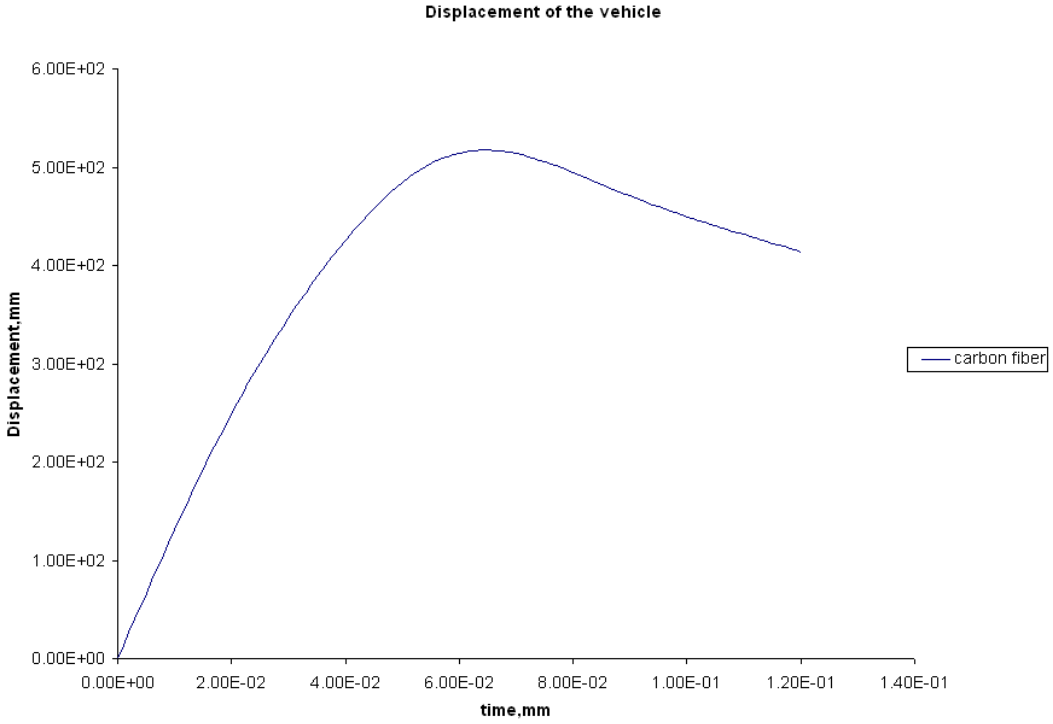

Figure 38. Displacement of the vehicle for the original model.

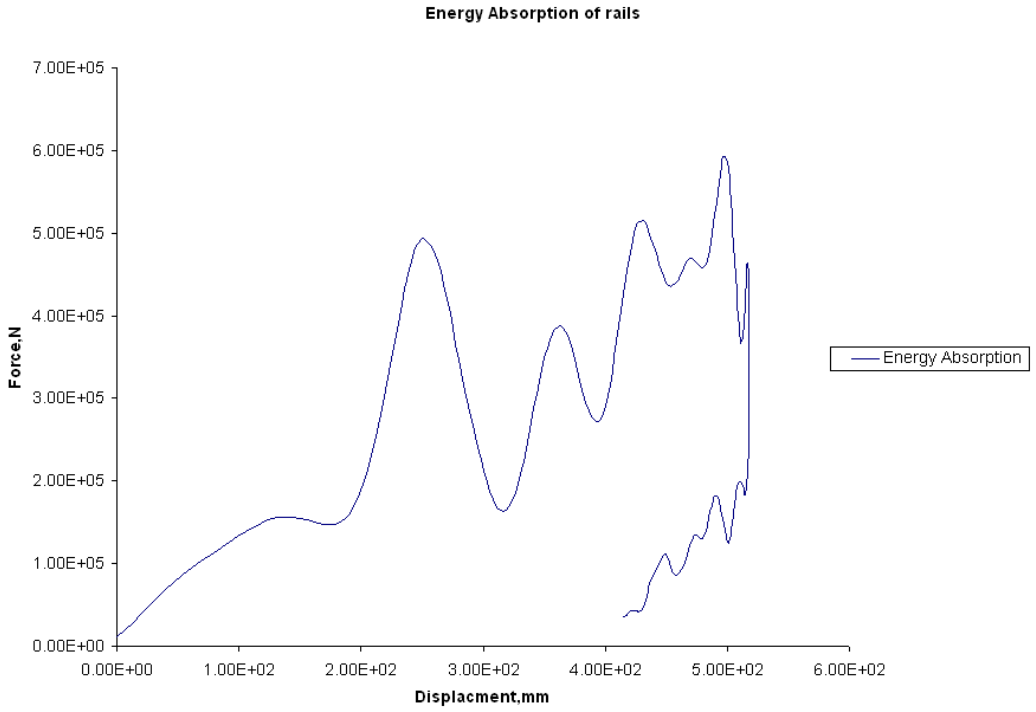

Figure 39. Energy absorption of rails for the original model.

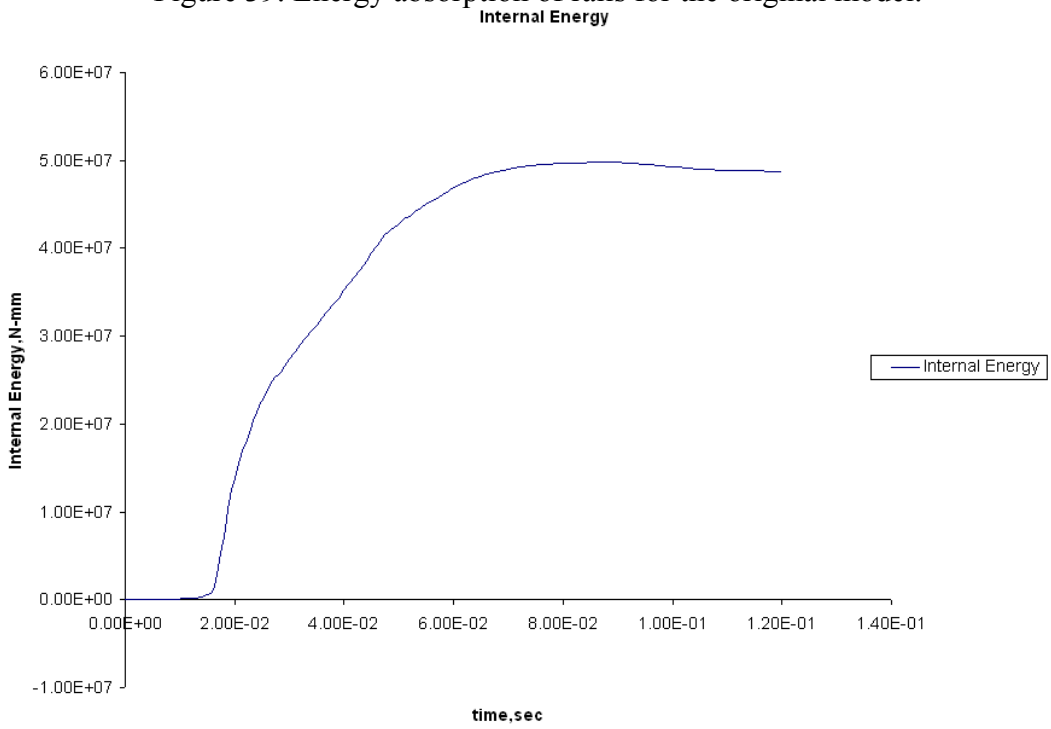

Figure 40. Internal Energy of rails for the original model.

Figure 37 & 38 depict the displacement of the vehicle and dissipated energy with the time in the original model respectively.

6.7 Parametric Study on Rails

The carbon-fiber/epoxy and Glass-fiber/epoxy composite models are tested according to FMVSS 208 at 30mph.

6.7.1 Orientation

The parametric study on the rail was carried out by starting with the variation in lay-up sequence. Four different lay-up sequences were analyzed and they are as follows.

1) $[(\pm 45°)_6/90°]$
2) 90,90,90,90,90,90,90,90,90,90,90,90,90
3) 45,-45,45,-45,45,-45,0,-45,45,-45,45,-45,45
4) 0,90,0,90,0,90,45,90,0,90,0,90,0

Finding out an orientation which is more energy absorbing is a complicated issue. Deciding the directions of lay-up for the specimen is very important. These above orientations are commonly used and were compared using the Force v/s Displacement curve.

6.7.2 Thickness

Thickness of the structure plays a vital role in energy absorption of a material. By increasing the thickness, the structure can be made to withstand more load and thus more energy absorption. However, the volume also increases when there is any increase in thickness and this in turn increases the mass of the structure. This not acceptable in the filed of crashworthiness as weight plays a very critical role in increasing the fuel efficiency of the vehicle.

In thus study, thickness were varied from 1.3 mm and 5.2 mm. When the 1.3 mm thickness was used, the deformation was very much and the deformation pattern was completely different. In addition, the energy absorption was very less. The 3.9 mm thickness yielded very good energy absorption than the 2.6 mm, but it constituted in increasing the weight of the structure. Therefore, in this study the thickness 2.6 mm was used in every composite part.

6.7.3 Material

Material of the structure also plays important role in energy absorption. Here two materials are used in this study carbon-fiber/epoxy and glass-fiber/epoxy.

From the figure 40 and table 6 it can be concluded that carbon fiber with orientation $[(\pm 45°)_6/90°]$ and thickness at 2.6 mm has higher energy absorption. Carbon fiber is the material used for designing of car front sub-frame rail in this study. It can also be seen that the displacement of the vehicle is lesser than other materials. This means that the injury sustained by the occupant in a vehicle is reduced considerably. Therefore, these are the parameters considered when analyzing the rails.

Table 6. Optimization of the Composite car front rail.

Orientation	No of Plies	Thickness of ply	Total Energy Absorption
$(\pm 45°)_6/90°$	13	0.2	1.890E+05 KN
0/90	13	0.2	0.940 E+05KN
+45/-45	13	0.3	1.120E+05 KN
+45/-45	13	0.4	1.024E+05 KN

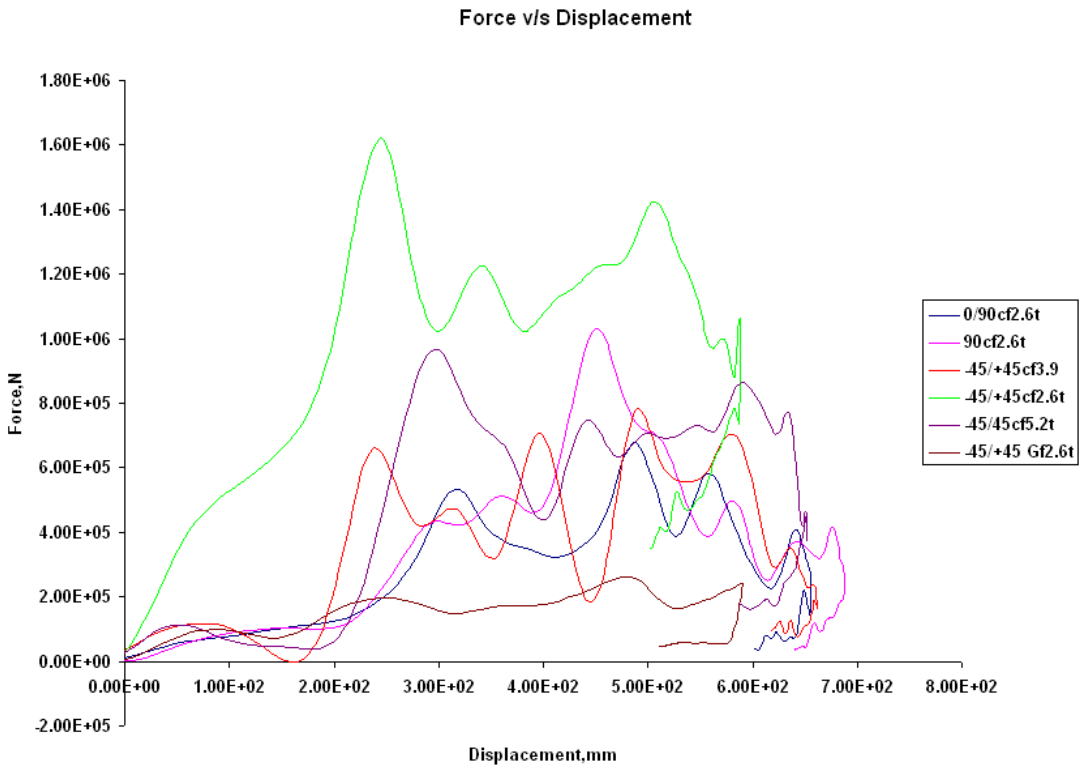

Figure 41. Force v/s Displacement for different orientations.

Table 7. Glass fiber/epoxy properties.

Property	Value	Units
Density	1.97E-06	Kg/mm^3
Ply longtitudinal modulus	45.847	Gpa
Ply transverse modulus	17.506	Gpa
Ply poisson's ratio	0.26	-
Ply shear modulus in plane	8.631	Gpa
Ply transverse modulus parallel to fiber direction	6.574	Gpa

Ply transverse modulus perpendicular to fiber direction	8.631	Gpa
Ply longitudinal tensile strength	1.12	Gpa
Ply longitudinal compressive strength	0.9	Gpa
Ply transverse tensile strength	0.039	Gpa
Ply transverse compression strength	0.134	Gpa
Ply shear strength	0.077	Gpa

CHAPTER 7

IMPACT ANALYSIS OF THE CAR FRONT RAILS

In the previous chapter, we discussed about composite modeling. Composite modeling of this new model should be able to reduce the displacements, accelerations and therefore, help in lowering the injuries sustained by the occupant. This chapter deals with the usefulness of new composite model and its effects on the injury criteria's.

This analysis is divided into three sections FMVSS 208, NCAP and IIHS standards. First of all FMVSS 208 standard is used to study the deformation sustained by the car when using the new model.

It has already been decided earlier in this study that carbon fiber composite is stronger and absorbs more energy. In this chapter, this is proved again by implementing the new composite model in the car. In addition, glass fiber results are also included to help in interpreting the results.

7.1 FMVSS 208 Test

7.1.1 LSDYNA simulations

The full frontal rigid barrier analysis is carried out in LS-DYNA for 120 milliseconds. The accelerometers are placed at eight locations in the vehicle. The contacts are defined by geometric interface. The distance between the vehicle and the barrier is kept to the minimum in order to minimize the simulation time. There is considerable deformation of hood, bumper and engine compartment as can be seen below.

7.1.2 Simulation of carbon fiber rail

The deformation sustained by the car when using the carbon fiber rail is as shown in figure 41

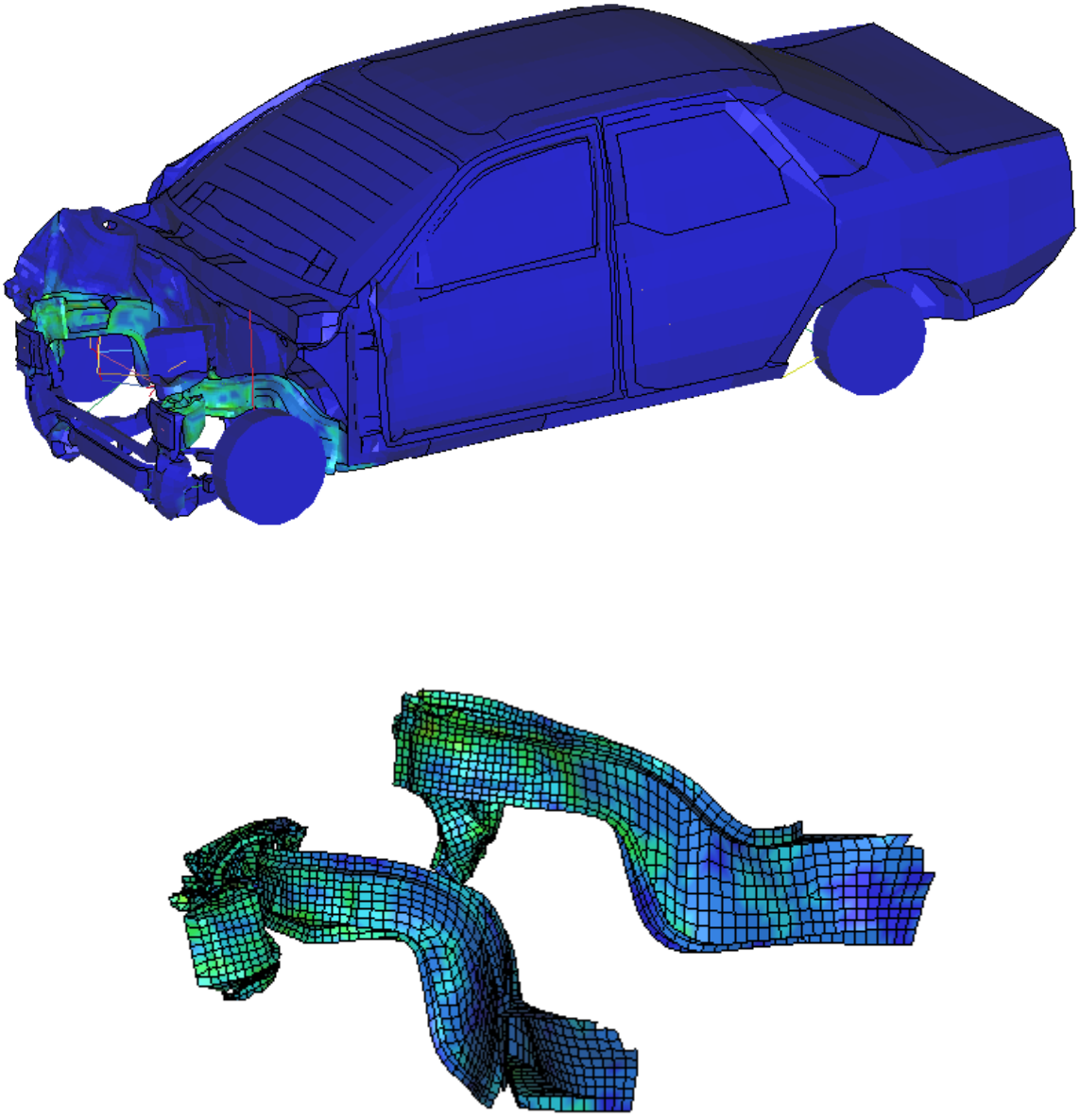

Figure 42. Deformation in the carbon fiber composite rail.

7.1.3 Simulation of glass fiber rail

Deformation sustained by the car while using the glass fiber reinforced composite rail is as shown in figure 42

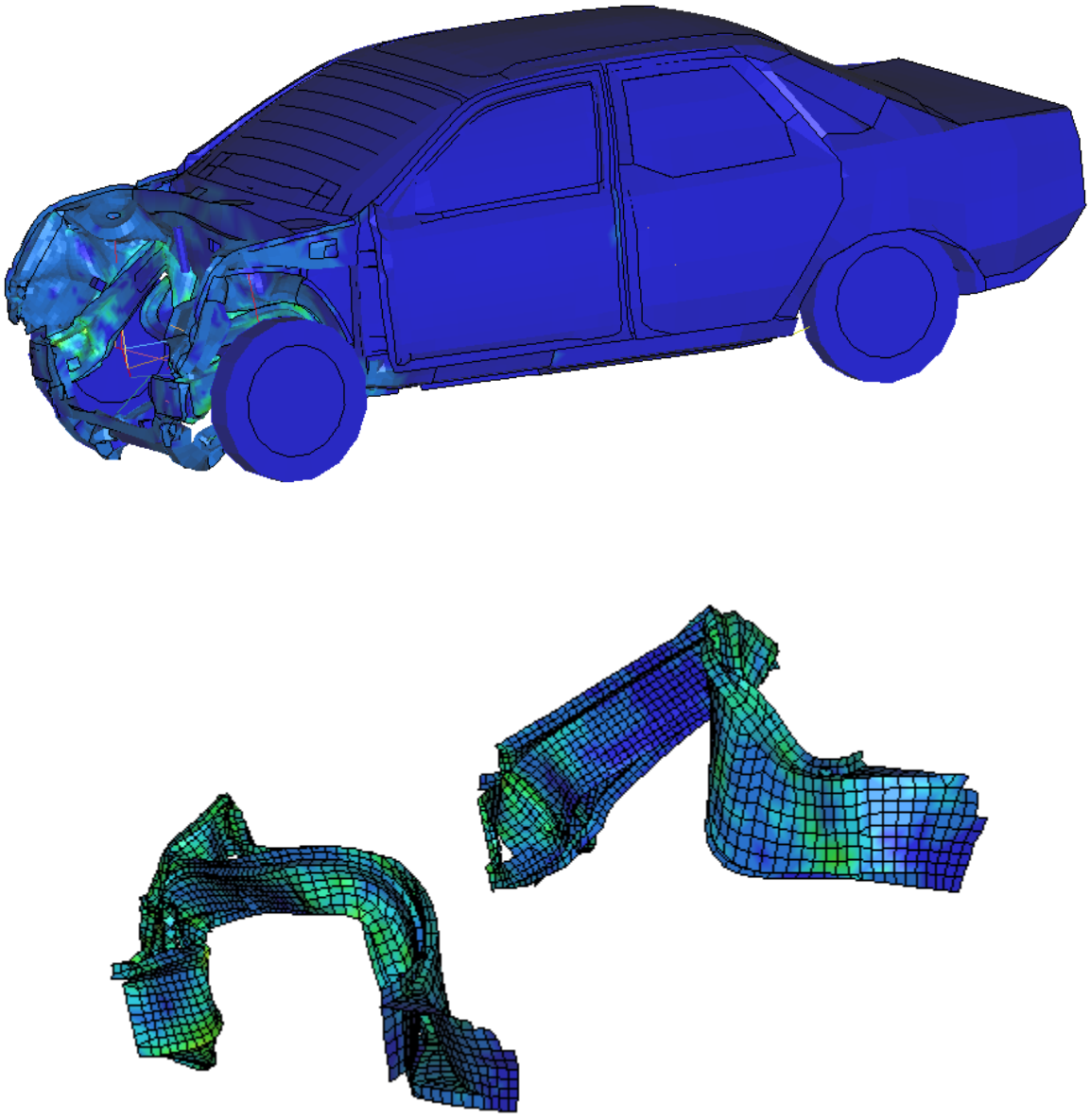

Figure 43. Deformation in the glass fiber rail.

From figure 41, it can be seen that the deformation of the car when the carbon fiber beam is used is very less. This indicates that the displacements and the accelerations

sustained by the car also reduces, hence reducing the injuries sustained by the occupant. In addition, it can be observed that the deformation on the composite carbon fiber beam is more, which means that the energy absorbed by the structure is high and it passes very less force onto other structures in the car. This helps in minimizing the injury criteria to as low as possible.

7.1.4 Results and discussion

Displacements and accelerations obtained in the frontal crash according to FMVSS 208 are shown in this section. In all of these displacements and accelerations curves, carbon fiber rail proves very useful.

7.1.4.1 *For Original Model*

a) CG Displacements and Energy absorption

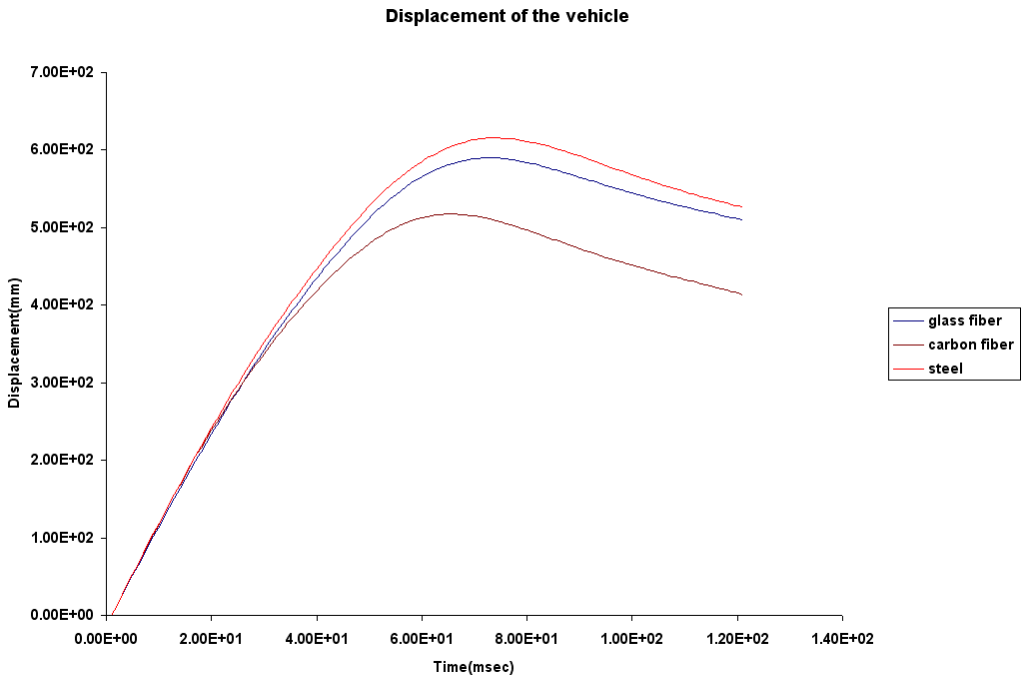

Figure 44. Displacement of the vehicle.

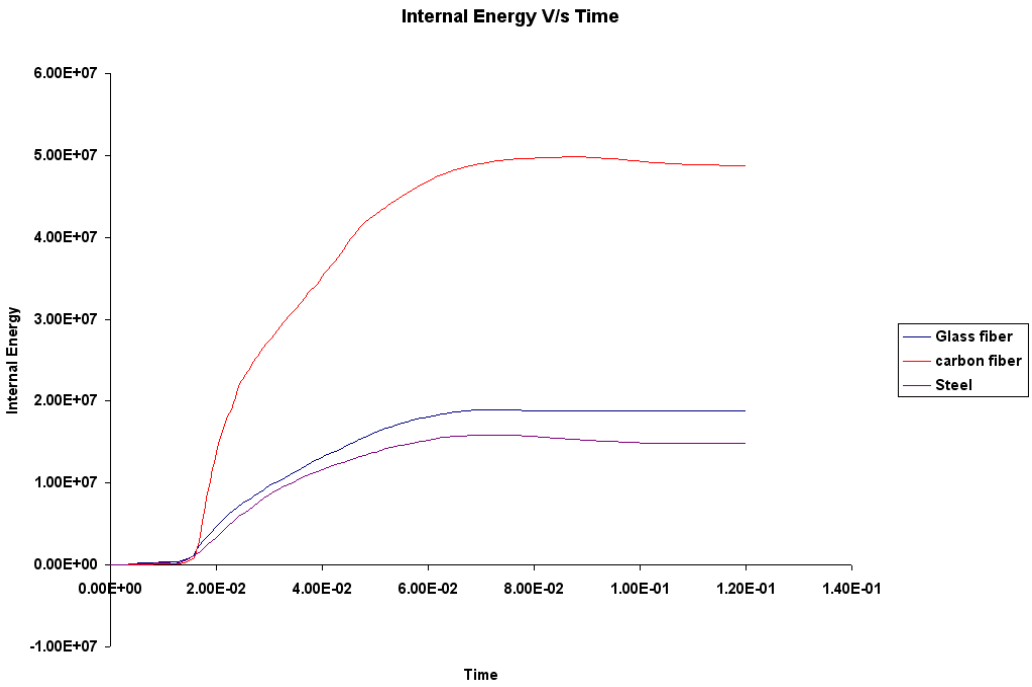

Figure 45. Internal Energy of rails.

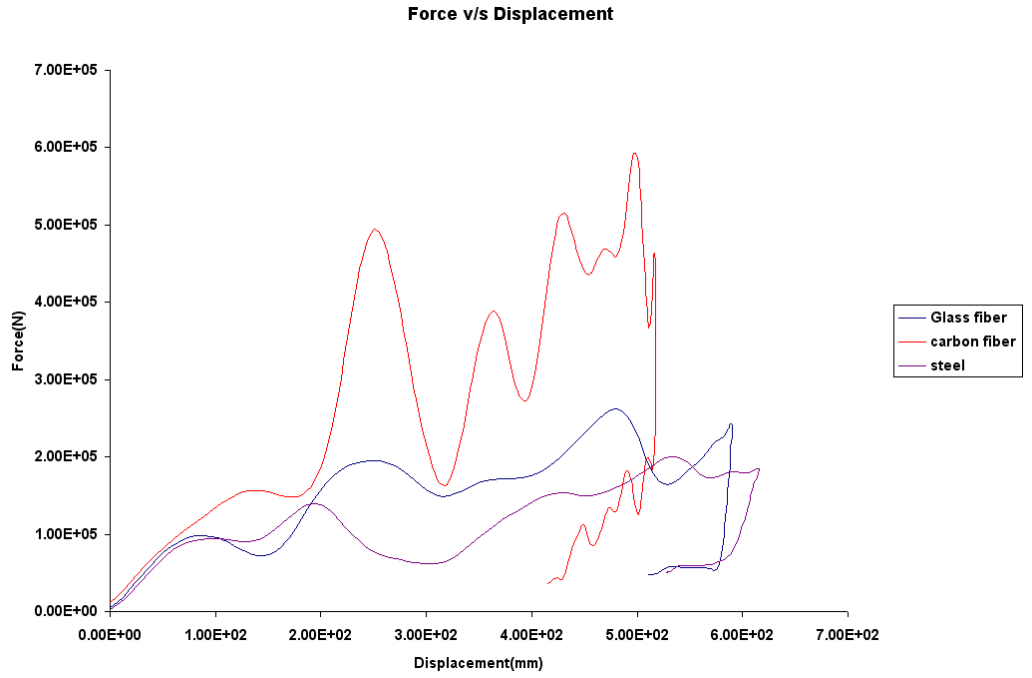

Figure 46. Load v/s Displacement for original model.

Figure 44 shows car's CG displacement with respect to time. Displacements in pertinent to the steel, Glass fiber (GF) and Carbon fiber (CF) are illustrated.

Table 8. Energy absorption for original model at 30mph.

	Steel	Glass fiber	Carbon fiber
Specific Energy Absorption	0.690E8	1.085E8	1.890E8

The curve is self-explanatory with the Glass fiber and the present beam having almost no difference in the displacement. However, Fig 45 depicts that the carbon fiber beam absorbs more energy and therefore the car's displacement reduces by almost 40%. This validates the fact that carbon fibers absorb more energy and thus reduces the displacement. Table 8 depicts that carbon fiber absorbs almost three times energy when compared to steel, which again validates the fact that by using carbon fiber, displacement of the vehicle reduces.

Figure 47. Comparison of acceleration curves of Centre of gravity for carbon fiber, glass fiber and steel.

In pertinent to the figure 46 it can be seen that the acceleration of the present beam is higher than the glass fiber and carbon fiber. The peak load in the present beam is around 45 g's whereas in the carbon fiber tube the CG's acceleration is around 15 g's. It can be seen that the acceleration decreases by 75%. This decreases the injuries affecting the occupant.

7.1.4.2 For Section Model

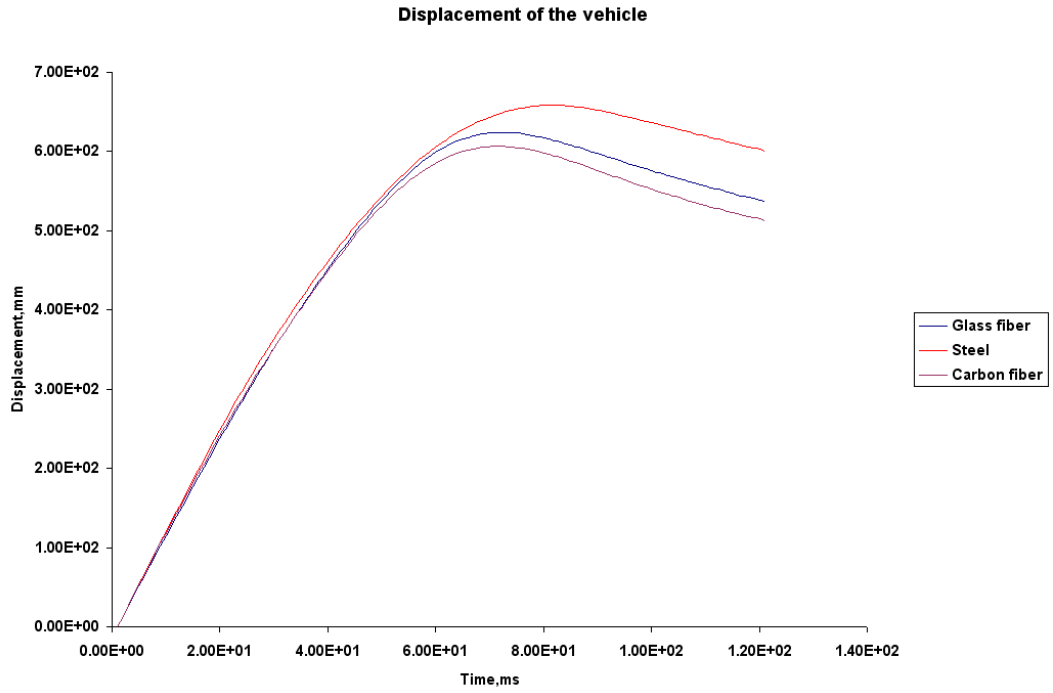

Figure 48. Displacement of the vehicle.

Figure 47 shows car's CG displacement with respect to time. Displacements in pertinent to the steel, Glass fiber (GF) and Carbon fiber (CF) are illustrated. The curve depicts that with carbon fiber displacement of the vehicle reduces when compared to glass fiber and steel.

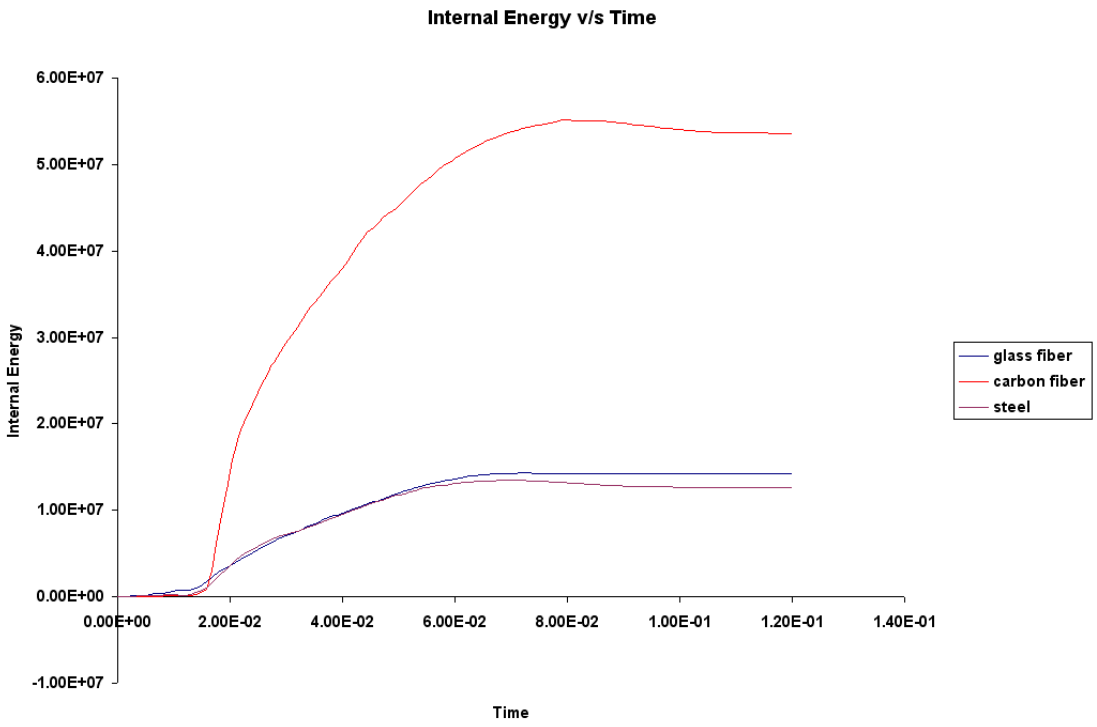

Figure 49. Internal Energy of rail.

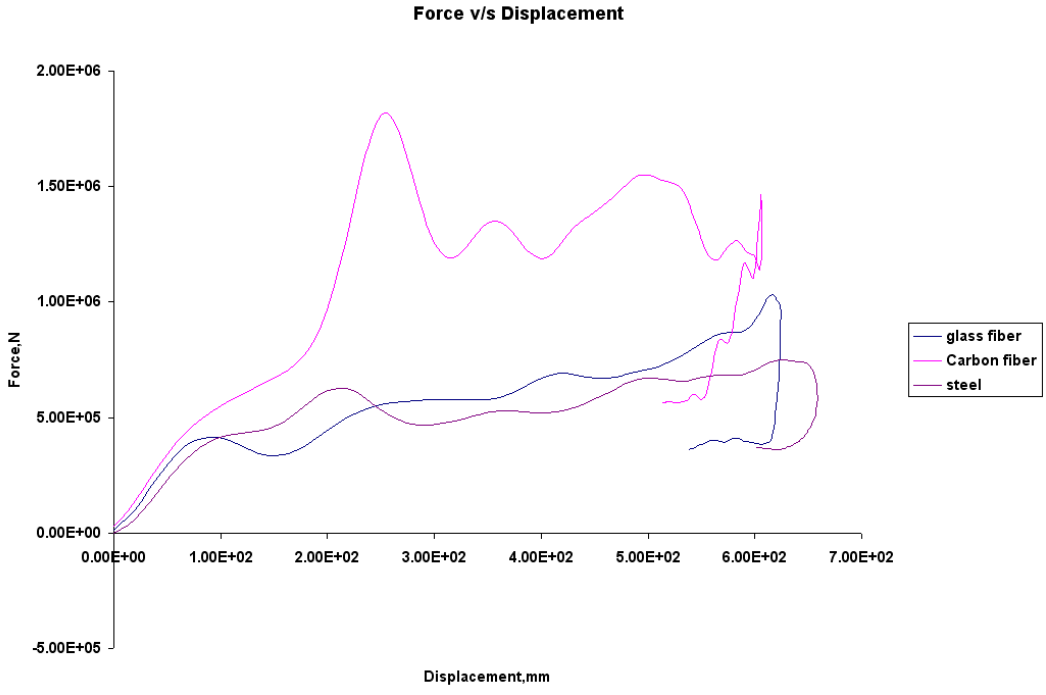

Figure 50. Load v/s Displacement for Section Model.

Table 9. Energy absorption for section model at 30mph.

	Steel	**Glass fiber**	**Carbon fiber**
Specific Energy Absorption	3.220E8	5.846E8	9.140E8

Fig 49 depicts that the carbon fiber beam absorbs more energy and therefore the car's displacement reduces by almost 30%. This validates the fact that carbon fibers absorb more energy and thus reduces the displacement. Table 9 depicts that carbon fiber absorbs almost three times energy when compared to steel, which again validates the fact that by using carbon fiber, displacement of the vehicle reduces.

Figure 51. Comparison of acceleration curves of Centre of gravity for carbon fiber, glass fiber and steel.

In pertinent to the figure 50 it can be seen that the acceleration CG for steel rail is higher than the glass fiber and carbon fiber. The peak load in case of steel is around 40 g's whereas in the carbon fiber tube the CG's acceleration is around 22 g's. It can be seen that the acceleration decreases by 45%. This decreases the injuries affecting the occupant.

7.2 NCAP Test

The NHTSA New Car Assessment Program (NCAP) uses a rigid barrier and the full width of vehicle is crashed into the rigid barrier at 35 mph.

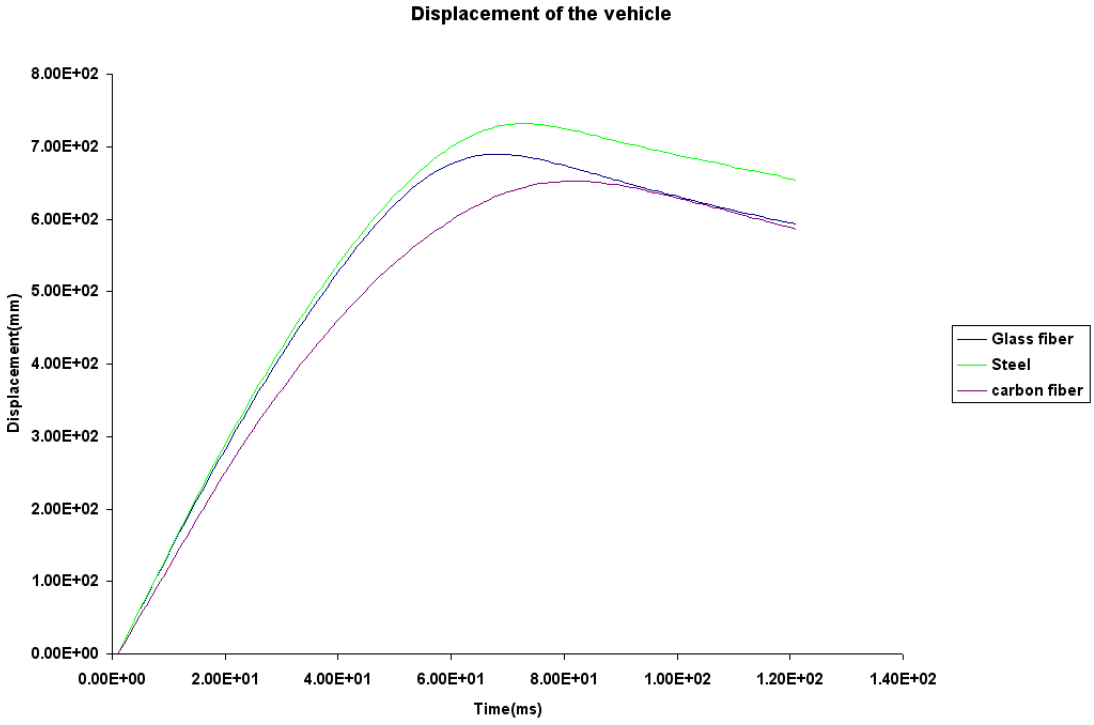

Figure 52. Displacement of the vehicle for NCAP test.

Figure 51 depicts that displacement of the car with carbon fiber is less when compared to steel or the glass fiber. The reduction in displacement is around 30%. This percentage reduction is more than what is required for reduction in the injury levels.

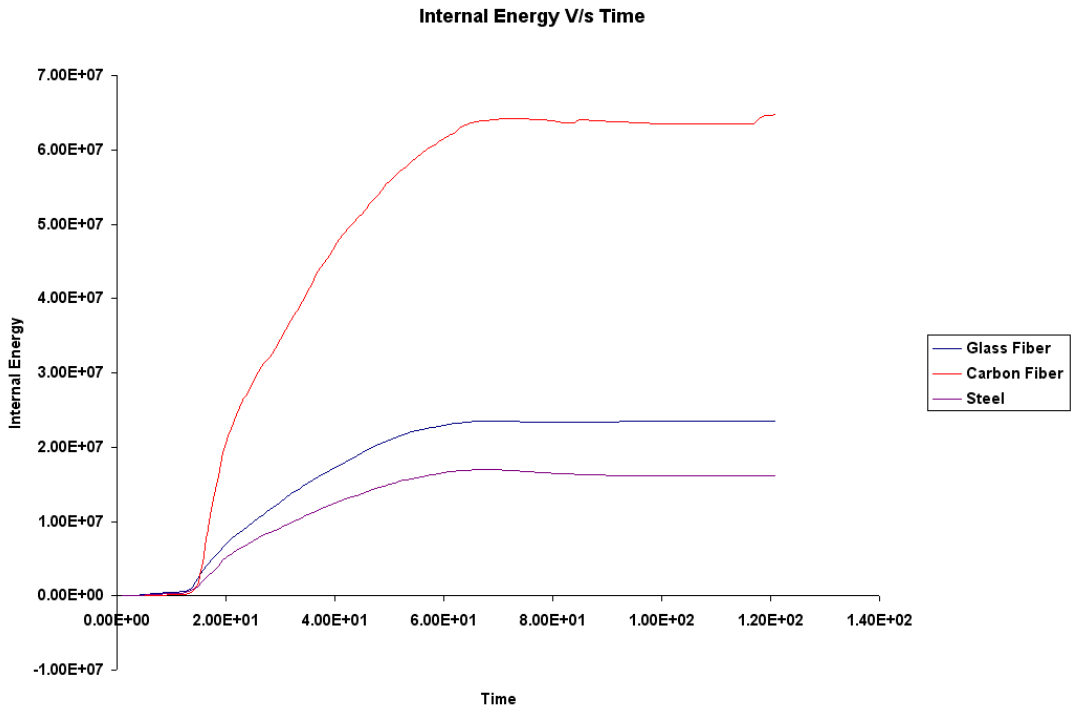

Figure 53. Internal energy of the structure for NCAP test.

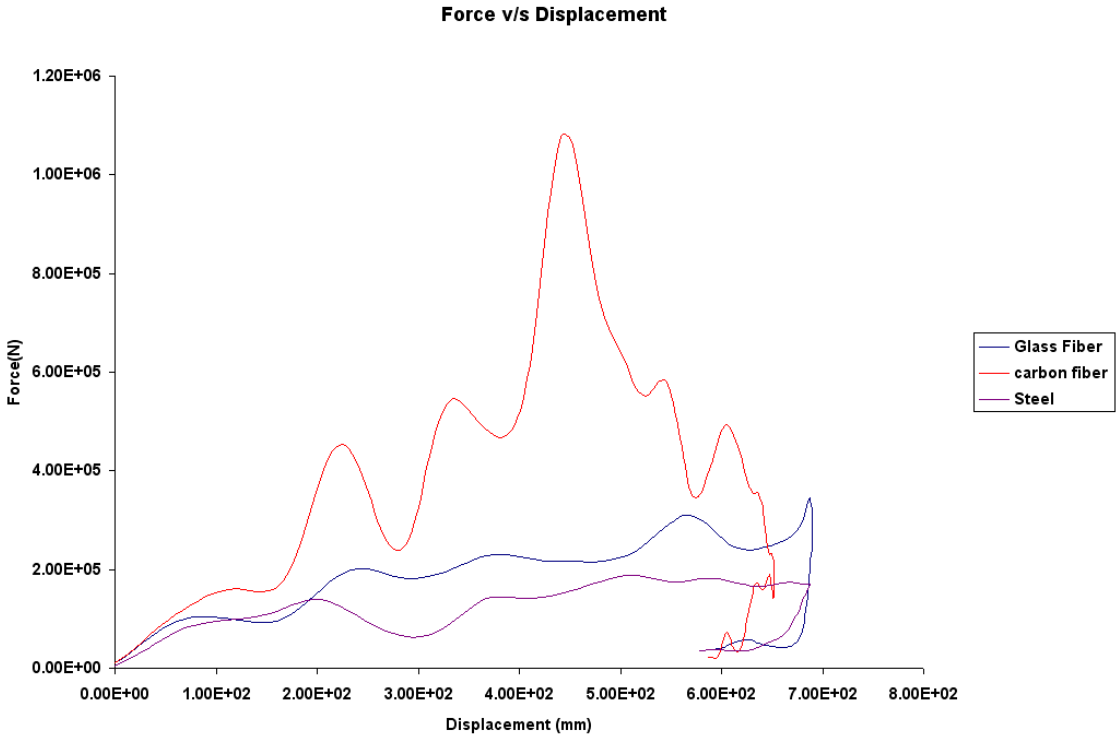

Figure 54. Energy absorption in the structure for NCAP test.

Table 10. Energy absorption for original model at 35mph.

	Steel	Glass fiber	Carbon fiber
Specific Energy Absorption	0.854E8	1.450E8	2.580E8

Table 10 depicts that carbon fiber absorbs almost three times energy when compared to steel, which again validates the fact that by using carbon fiber, displacement of the vehicle reduces.

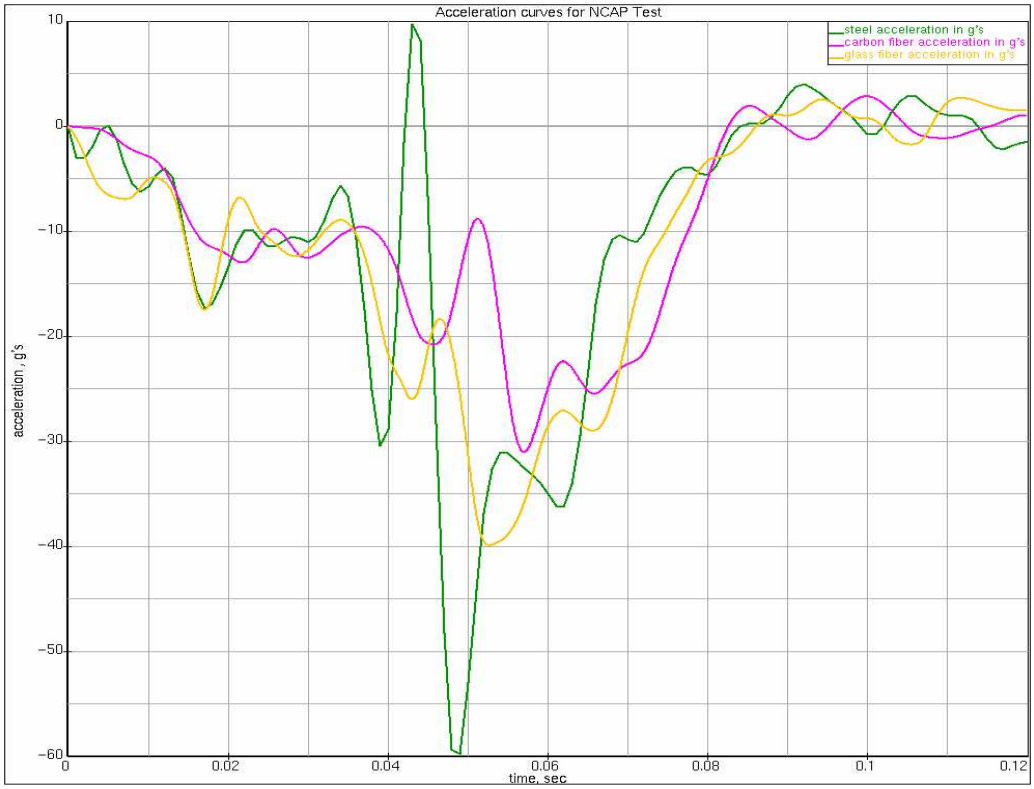

Figure 55. Comparison of acceleration curves of Centre of gravity for carbon fiber, glass fiber and steel.

From figure 55, it can be seen that the acceleration peak has decreased in case of carbon fiber and this shows that it absorbs more energy.

7.3 IIHS Test

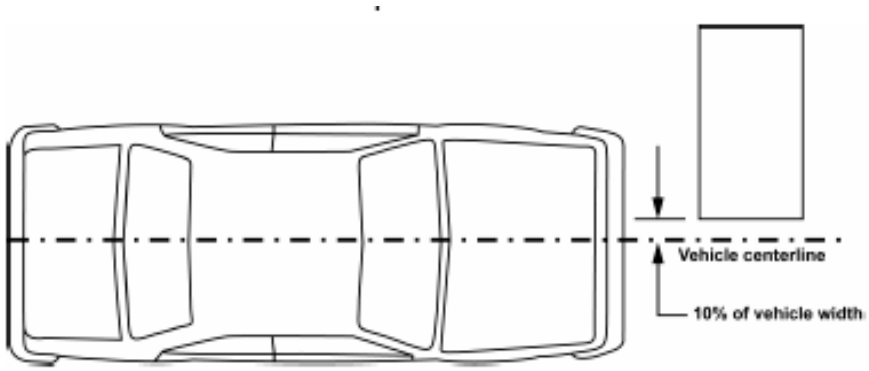

Figure 56. Offset test setup [9].

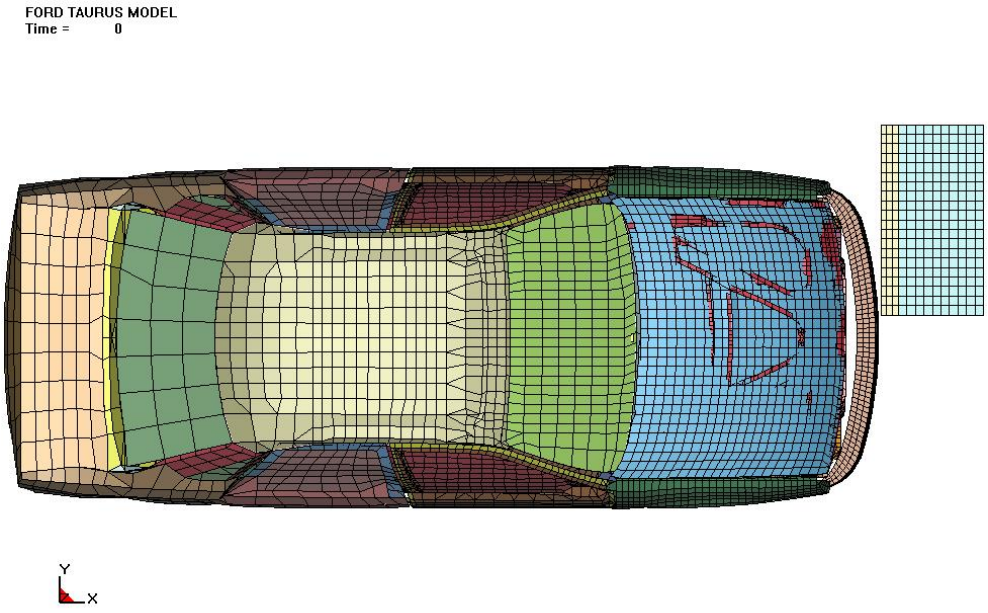

Figure 57. IIHS Offset Model.

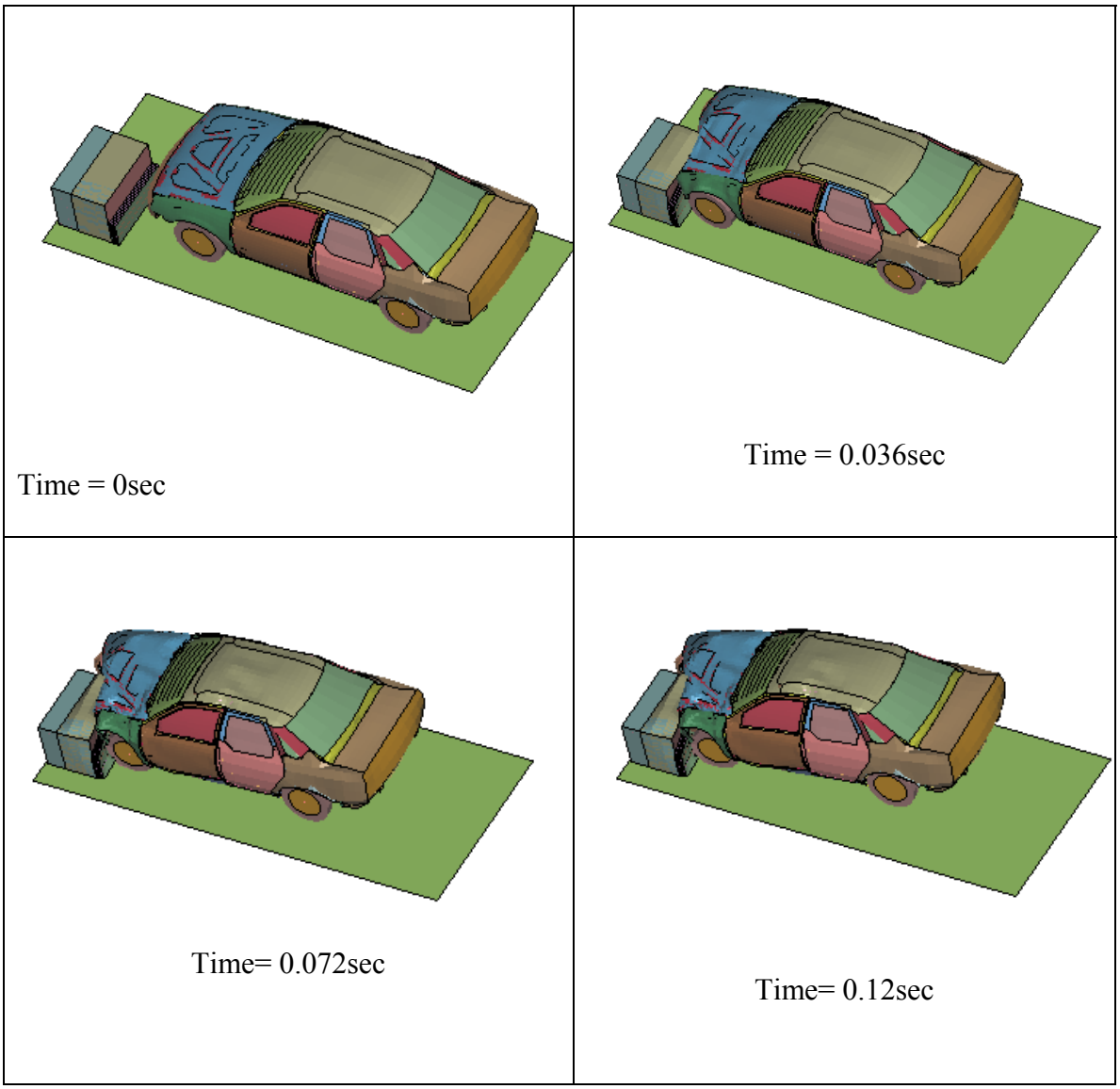

Figure 58. Animation sequence for IIHS 40 % offset test at 40mph.

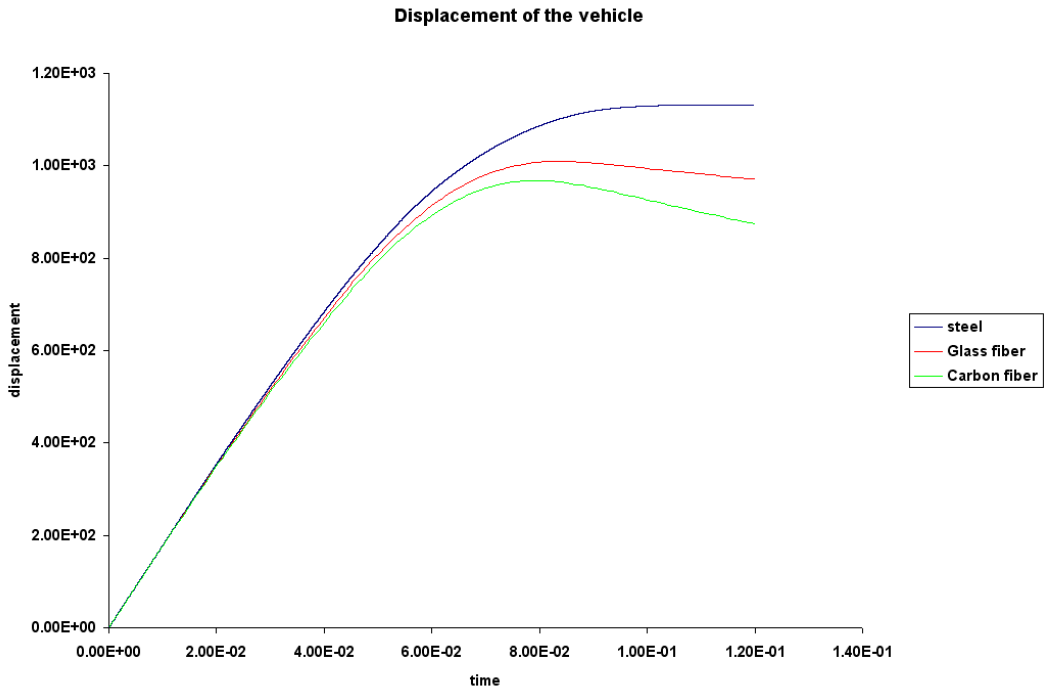

Figure 59. Displacement of the vehicle for IIHS test.

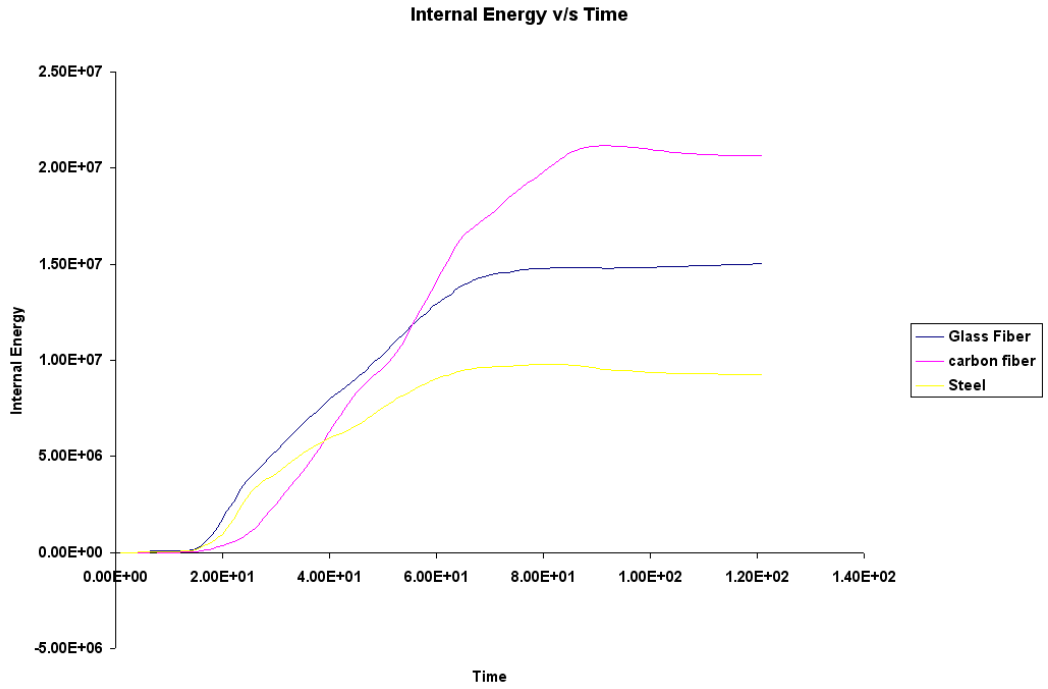

Figure 60. Internal Energy of the structure for IIHS test.

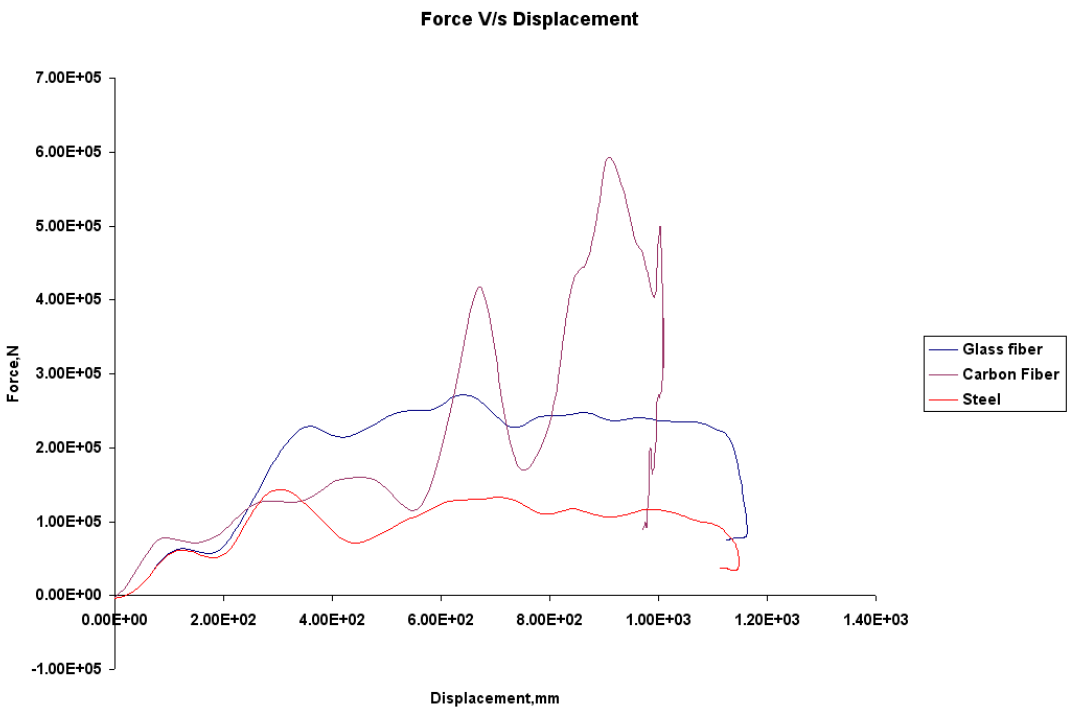

Figure 61. Energy absorption of the structure.

Table 11. Energy absorption for original model at 40mph.

	Steel	**Glass fiber**	**Carbon fiber**
Specific Energy Absorption	1.094E8	2.202E8	3.088E8

Figure 58 depicts that displacement of the car with carbon fiber is less when compared to steel or the glass fiber. The reduction in displacement is around 25%. This percentage reduction is more than what is required for reduction in the injury levels. Table 11 depicts that carbon fiber absorbs almost three times energy when compared to steel, which again validates the fact that by using carbon fiber, displacement of the vehicle reduces.

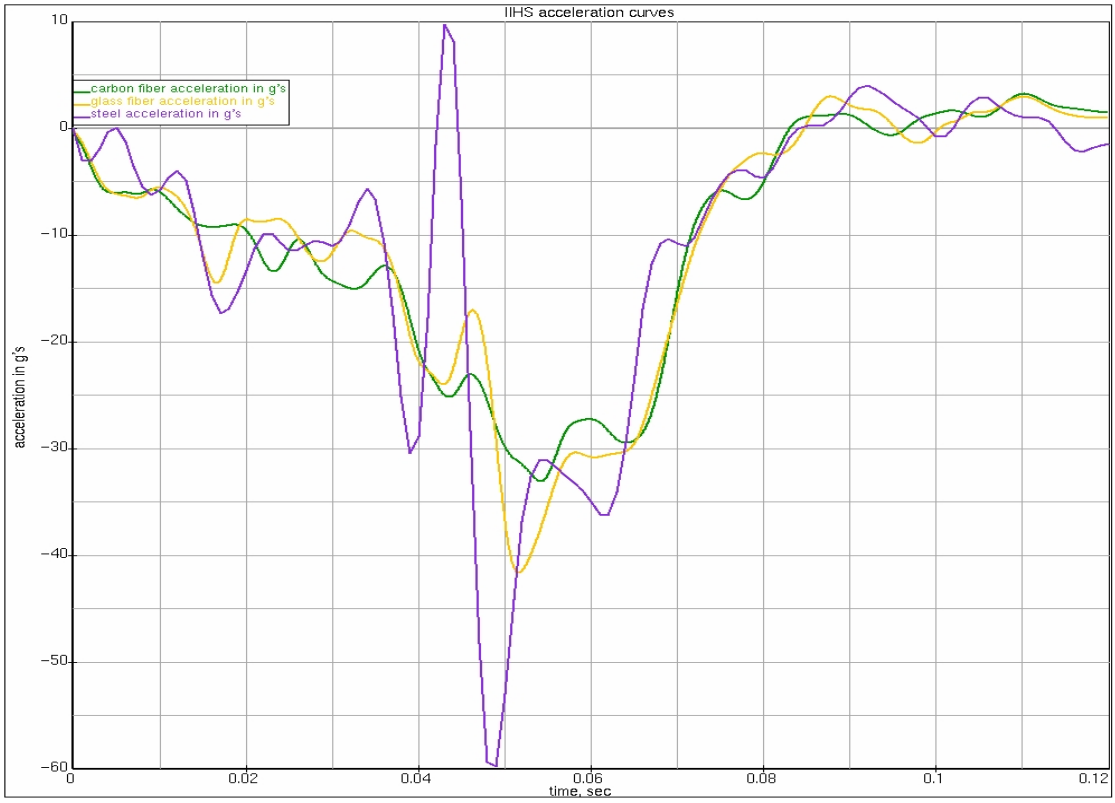

Figure 62. Comparison of acceleration curves of Centre of gravity for carbon fiber, glass fiber and steel.

From figure 61, it can be seen that the acceleration peak has decreased in case of carbon fiber and this shows that it absorbs more energy.

CHAPTER 8

MODELING OF OCCUPANT DYNAMIC RESPONSE USING MADYMO

With the improvements in computer simulations and vehicle FE models it has become possible for the car manufacturers to carry out testing in different test conditions. Also the car manufactures are able to launch vehicles at faster rate for they able to predict the design and performance of the vehicle at a very early stage. Safety of occupant is the most important issue that concerns during the design and development of vehicle. Depending on the occupant response the reliability and performance of the vehicle can be evaluated.

In this study hybrid III 50 percentile dummy is used as the reference model. Seat belts play a vital role in reducing the injuries of the occupant. Here the seat belts developed in MADYMO 601 are classified as FEM belts. These are basically the three-point belt restraint system. The width and thickness of the belt are equal to 40mm and 1mm respectively. Belts are modeled with 0.02 size tria-elements. HYSISO material is used for belts with density of 7850 kg/mm^3. Loading and unloading function for the FE belts are specified and they are as depicted in figure 62

The contact between the dummy and the belt is defined by kinematic contacts with coefficient of friction of 0.3. The belt section of the shoulder belt is in contact with the right clavicle, the right upper arm, the neck and the collar, the left and right upper torso, the ribs, the sternum, breasts and the abdomen. The FE belt section of the lap belt is in contact with the hips, abdomen, the bottom ribs and the lower torso of the dummy.

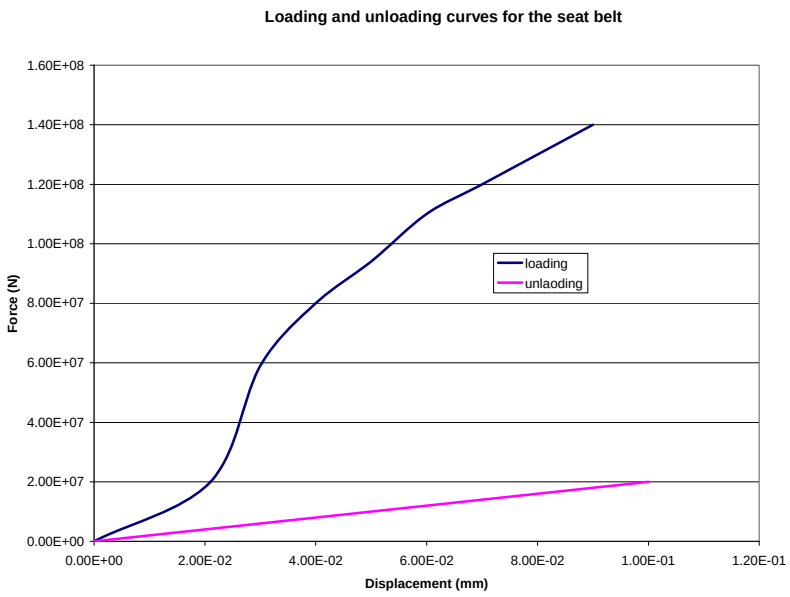

Figure 63. Loading and unloading curve for the FE belt.

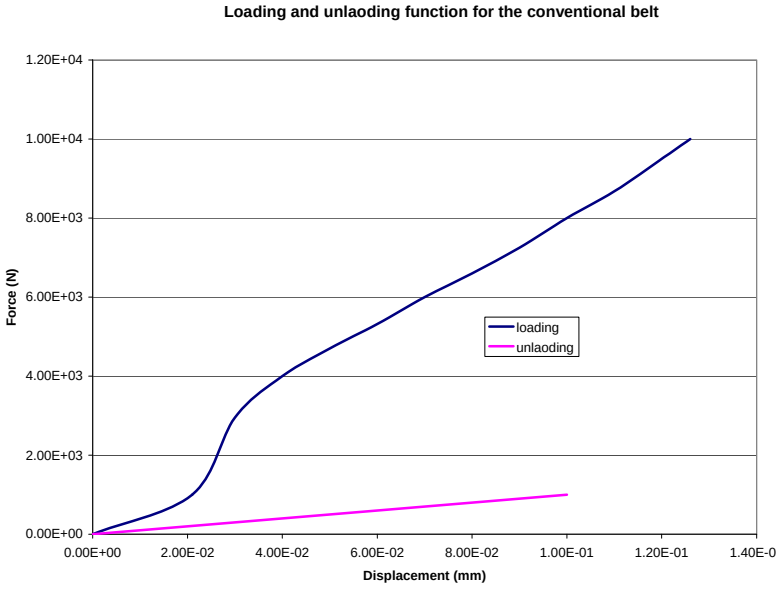

Figure 64. Loading and unloading function for the conventional seat belt.

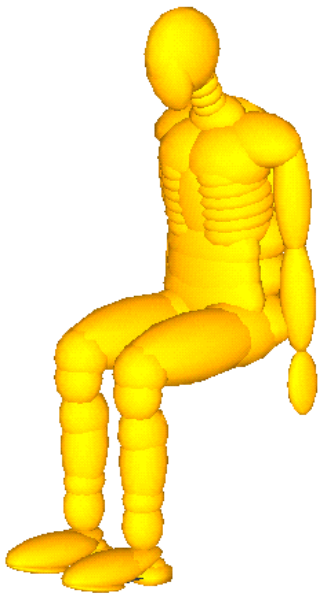

Figure 65. Hybrid III 50th percentile Dummy model.

8.1 Study of occupant kinematics in the event of impact

In order to study the effect of impact on the occupant, the acceleration pulse derived from the LS-DYNA is given to the occupant. Occupant responses are evaluated by using the injury criteria given by the MADYMO program. The simulations are done for original model and section model and composite model for 30 mph and 35 mph (NCAP) full frontal tests. In all the simulations, we have used 50-percentile Hybrid III dummy. Figure 65 shows the animation sequence for full width rigid barrier test at 30 mph.

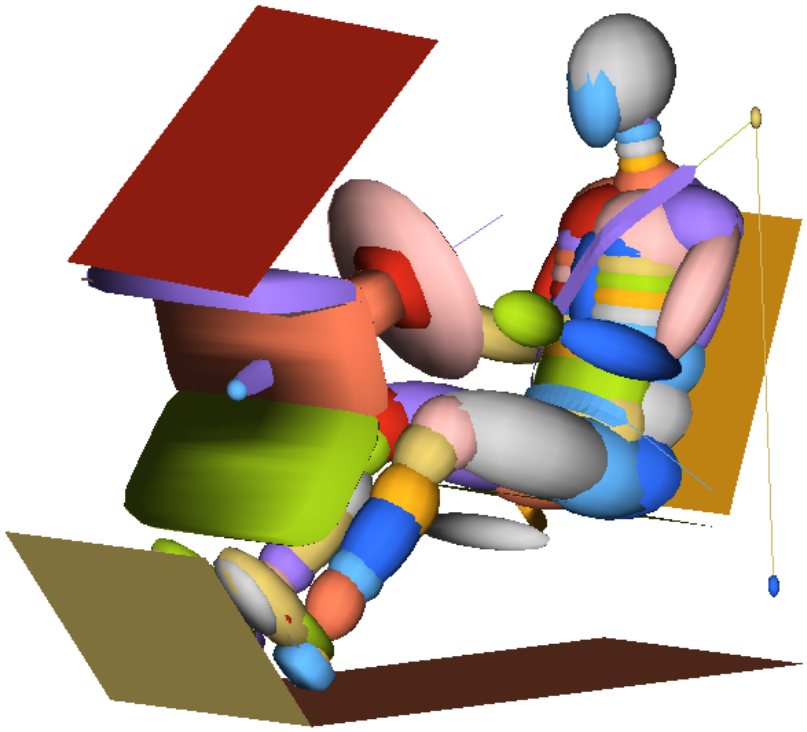

Time = 0 sec

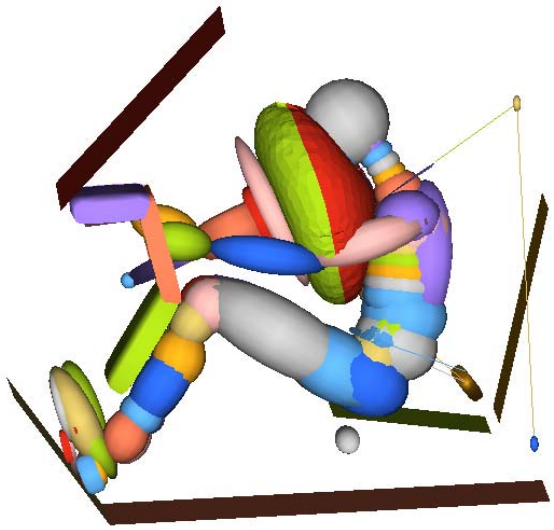

Time = 0.12 sec

Figure 66. Animation sequence of an impact analysis.

8.2 Results and Discussions

8.2.1 For original model

At 30 mph

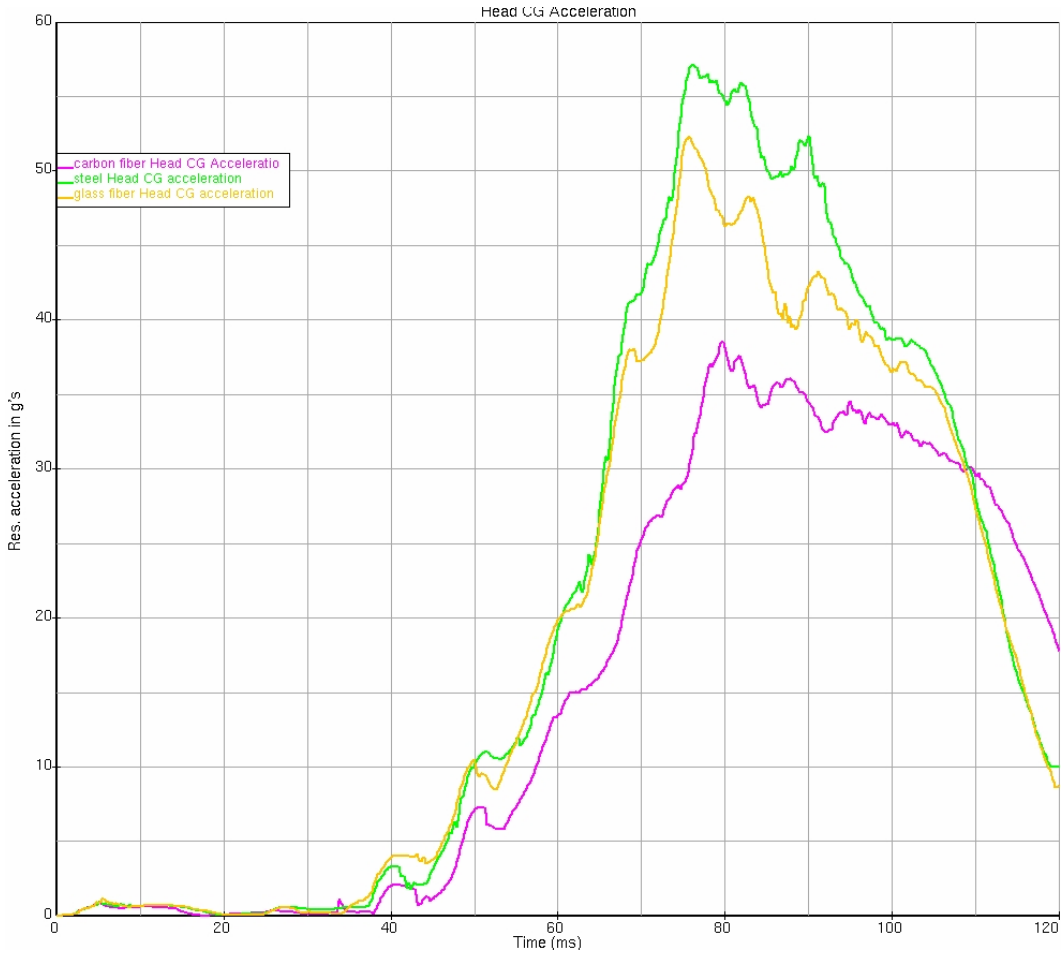

Figure 67. Head acceleration.

Figure 66 shows the comparison of Head CG acceleration of driver occupant for original model with steel, glass fiber and carbon fiber. From the figure, it can be observed that, head CG acceleration for the car with carbon fiber is lower as compared to the steel and the glass fiber model. Due to this, the injury criteria HIC, reduces tremendously.

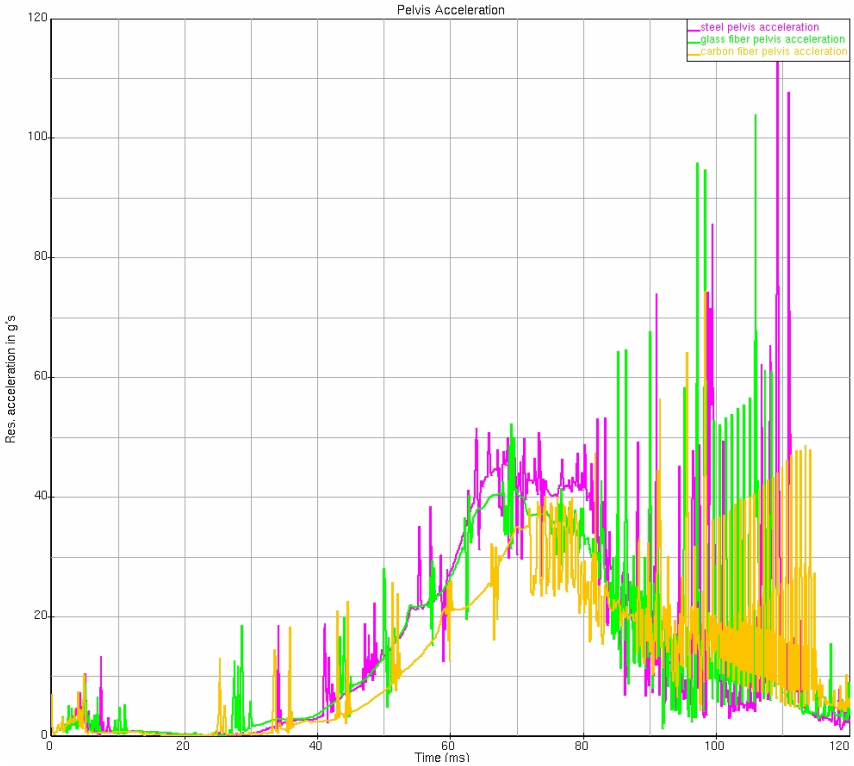

Figure 68. Pelvis Acceleration.

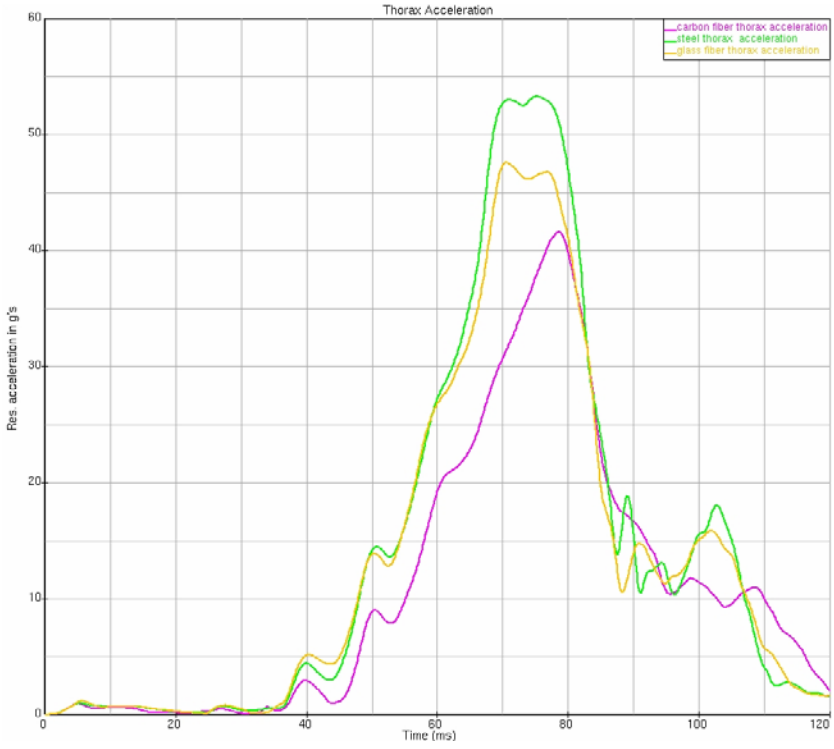

Figure 69. Thorax Acceleration.

Figure 67 and 68 illustrates the curve between acceleration of pelvis regions and Thorax region. It can be seen that the carbon fiber dominates in having lesser acceleration than the other models. This also indicates that the energy absorption of the carbon fiber beam is higher and thus it helps in reducing injuries to the occupant.

Table 12. Injury Criteria's calculated for the Frontal Impact of the original model at 30 mph (FMVSS 208).

	Steel Model	**Carbon Fiber Model**	**Glass Fiber Model**
HIC(1000)	561	234	417
Head Peak Acceleration (g's)	56	37	51
Chest Deflection	0.050	0.042	0.47
VC	0.295	0.192	0.250
Combined Thoracic index	0.500	0.438	0.480

Table 13. Injury Criteria's calculated for the Frontal Impact of the original model at 35 mph (NCAP).

	Steel Model	**Carbon Fiber Model**	**Glass Fiber Model**
HIC(1000)	710	391	777
Head Peak Acceleration (g's)	65	50	65
Chest Deflection	0.053	0.048	0.053
VC	0.370	0.282	0.336
Combined Thoracic index	0.548	0.478	0.554

Table 12 and 13 shows the injury criterias calculated during a Frontal impact crash test at 30 mph (FMVSS 208) and 35 mph (NCAP). It can be seen that the HIC, Head CG acceleration value for the carbon fiber is less and this is very much accepted in the field of crashworthiness.

8.2.2 For section model

At 30mph

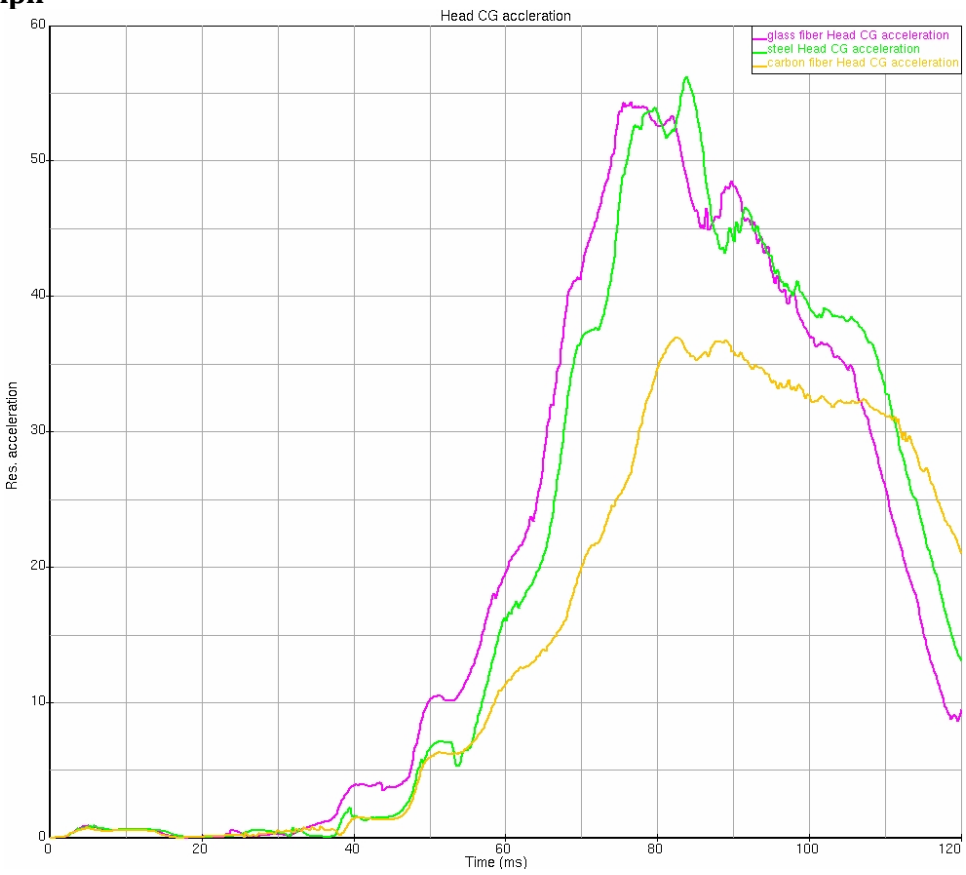

Figure 70. Head Acceleration.

Figure 69 shows the comparison of Head CG acceleration of driver occupant for section model with steel, glass fiber and carbon fiber. From the figure, it can be observed that, head CG acceleration for the car with carbon fiber is lower as compared to the steel and the glass fiber model. Due to this, the injury criteria HIC, reduces tremendously.

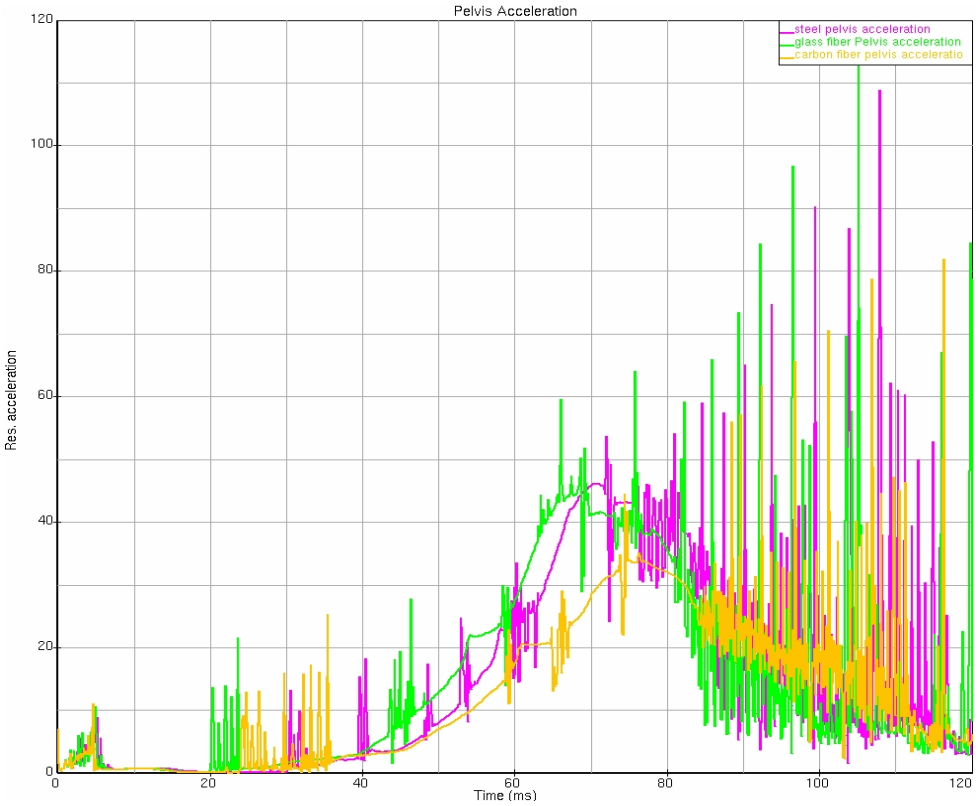

Figure 71. Pelvis Acceleration.

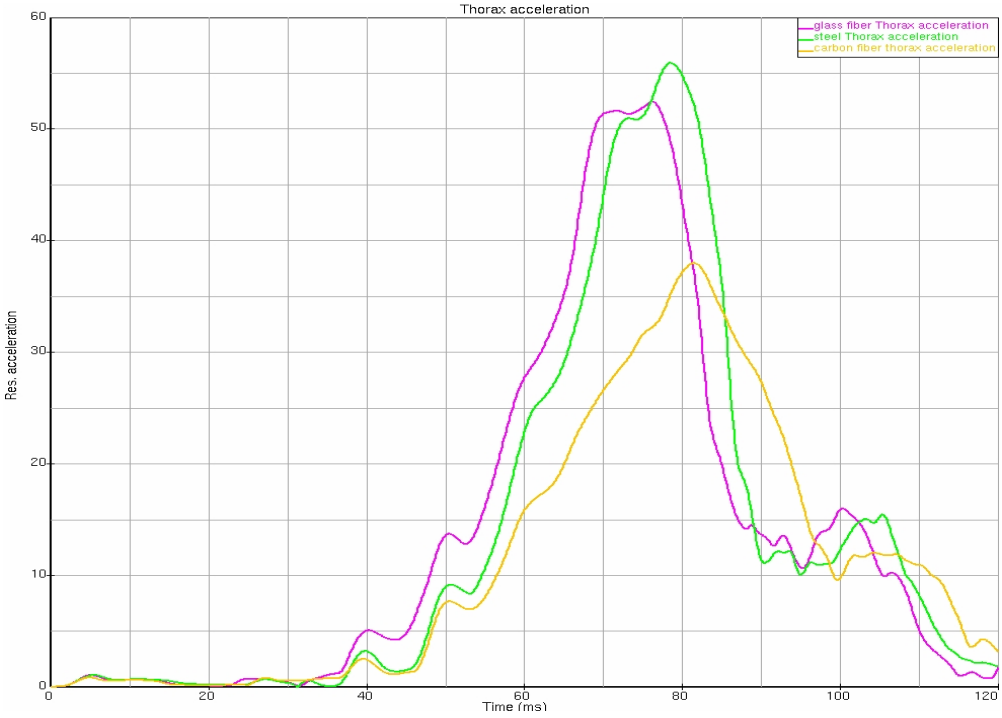

Figure 72. Thorax Acceleration.

Figure 70 and 71 illustrates the curve between acceleration of pelvis regions and Thorax region. It can be seen that the carbon fiber dominates in having lesser acceleration than the other models. This also indicates that the energy absorption of the carbon fiber beam is higher and thus it helps in reducing injuries to the occupant.

Table 14. Injury Criteria's calculated for the Frontal Impact of the section model at 30 mph (FMVSS 208).

	Steel Model	**Carbon Fiber Model**	**Glass Fiber Model**
HIC(1000)	489	236	507
Head Peak Acceleration (g's)	55	36	53
Chest Deflection	0.048	0.044	0.049
VC	0.320	0.164	0.284
Combined Thoracic Index	0.496	0.456	0.494

Table 15. Injury Criteria's calculated for the Frontal Impact of the section model at 35 mph (NCAP).

	Steel Model	**Carbon Fiber Model**	**Glass Fiber Model**
HIC(1000)	703	406	695
Head Peak Acceleration (g's)	65	51	65
Chest Deflection	0.052	0.048	0.052
VC	0.325	0.264	0.332
Combined Thoracic index	0.532	0.478	0.540

CHAPTER 9

CONLCUSIONS AND FUTURE WORK

The Automotive mid rail is the main load carrying/energy-absorbing component in a frontal vehicle crash. The objective of this study was to investigate the use of composites as an alternative in the car front sub-frame rails and thus help in reducing the injuries on the occupant. The composite rail was tested to find out the maximum possible energy absorption by changing the material, orientation and thickness. Section modeling of rails is also studied here. The validated FE Ford Taurus model is studied for the crashworthiness by using LS-DYNA. Two different models, one original model and other section model are tested for FMVSS full width rigid barrier test at 30mph, NCAP full width rigid barrier test at 35 mph and IIHS 40 percent offset test at 40 mph. FMVSS, NCAP and IIHS tests are conducted to find out the accelerations and the intrusion sustained by the vehicle, occupant kinematics is studied and discussed in detail.

By implementing the composite rail into the vehicle, the acceleration, displacement and the injuries sustained by the occupant was eventually reduced.

In addition, the following conclusions can be made:

- Composite rails are more effective for both FMVSS,NCAP and IIHS standards
- Composite absorbs more energy then steel and hence, the deformation sustained by the composite rails is more, which leads to decrease in the displacement and acceleration of the car to about 45%.
- By using composite in place of steel, there is considerable reduction in weight of the rails of about 58%.

- Injury level reduces drastically assuring the composite rails are stronger than the steel rails.
- Composite materials are replaceable where high strength and high stiffness are required

Although the composites rails fail by buckling during impact loading, by proper design, fiber orientation and fiber matrix combination buckling failure can be reduced.

Future Recommendations

The following recommendations for future work can be noted:

- Experimental validation can be done before practically implementing the composite rail in automobile industry.
- Materials other than carbon fiber/glass fiber can be used or a combination of different composite materials can be used to strengthen the beam.
- Design of Experiments can be used to optimize the composite rails by finding out the correct orientation, exact material, thickness that absorbs more energy.
- Thirty Degree angled impact can done to verify how composite rails behave during angled impact
- Extensive MADYMO analysis dealing with the Head injuries, Neck Injuries, viscous injury response, Thoracic index and so on can be studied to know the effectiveness of the composite rail.
- Filters other than SAE 60 can be used for different materials to find out which filter is suitable for impact analysis.

- Extensive study on Delamination of composite materials can be done to know the effectiveness of rails during frontal and angled impacts.
- Study on Material Degradation can be done during impact analysis.

REFERENCES

REFERENCES

[1] Miracle, D.B., and Donaldson, S.L., "Introduction to composites" Journal of Composite Materials , Vol. 34, pp. 200-215, 1995.

[2] Farley, G.L., and Jones, R.M., "Crushing Characteristics of Continuous Fiber-Reinforced Composite Tubes," *Journal of Composite Materials*, Vol.26, No.1, pp. 37-50, 1992.

[3] Matzenmiller, A., and Schweizerhof, K., "Crashworthiness Simulaions of Composite Structures-A First Step with Explicit Time Integration," *Nonlinear Computational Mechanics- a State of the Art*, Springer Verlag, New York, 1991.

[4] Han.J., and Yamazaki. K., "Crashworthiness Optimization of S-shape square tubes". International Journal of Vehicle Design, Vol 31, No.1, pp 72-85, 2003.

[5] Reid, J.D., "Crashworthiness of Automotive Steel Mid rails: Thickness and Material Sensitivity". Thin-Walled structures Vol. 26, No. 2, pp. 83-103, 1996.

[6] Philipps, M., Patberg, L., Dittmann, R., Henrik, A., "Structural analysis and testing of composites in automotive crashworthiness application", *SAE Special publications*, Vol 1320, 981140, *Safety and Material Test Methodologies*, pp 97-101, Feb, 1998.

[7] Jacob, C.G., Fellers, F.J, Simunovic, S., and Starbuck, J.M., "Energy Absorption in polymer composites for automotive crashworthiness", 1996.

[8] Fleming, D.C., "The Energy Absorption of Graphite/Epoxy Truncated Cones," M.S. Thesis, Department of Aerospace Engineering, University of Maryland, College Park, 1991.

[9] "Federal Motor Vehicle Safety Standards And Related Regulations", U.S department of Transportation**.** 1995.

[10] Farely, G.L., "Energy Absorption of Composite Materials", Journal of composite Materials, Vol. 17, pp. 267-279, 1983.

[11] Mamalis, A.G., Robinson, M., Manolakos, D.E., Demosthenous, G.A., Ioannidis, M.B., and Carruthers, J., " Crashworthy capability of composite material structures". 1996.

[12] Kum Cheol Shin, Jung Ju Lee, Ku Hyun Kim, Min Cheol Song, Jeung Soo Huh, "Axial crush and bending of an aluminum/GFRP hybrid square tube and its energy absorption capability", Vol 57, pp. 279-287, 2002.

[13] Thomas Brimhall, Hasetetsion G. Mariam., “Dynamic Crush Test of Subcompnent Composite Front Frame Rails”. Proceedings of 2001 ASME International Mechanical Engineering Congress and Exposition, AMD-Vol.250/MD-Vol.96, New York, NY, November 11-16, 2001.

[14] Ramiro Tarazona and Luis Castejon, “An Innovative Concept of Energy Absorption System for Automotive Collisions”, Taexpa S. A., Univerisity of Zaragoza, SAE transactions 2004.

[15] David R. Cramer, David F. Taggart, “Design and Manufacturing of an Affordable Advanced-Composite Automotive Body Structure, 1998.

[16] Joseph N. Kanianthra , Glen C. Rains and Thomas J. Trella. “Strategies for passenger car design to improve Occupant protection in real world side crashes”, 1994.

[17] Nguyen, Q.M.,Elder J.D., Bayandor, J., Thomson, S.R., Scott, L.M., "A review of explicit finite element software for composite impact analysis", 1999.

[18] S. Ramakrishna and H. Hamada, “Energy Absorption Characteristics of Crash worthy Structural Composite Materials”, Engineering Materials, Vol 141-143 pp.585-620, 1998.

[19] Thornton, P.H., “Energy Absorption in Composite Structures”, *Journal of CompositeMaterials*, Vol. 13, pp. 247-262, 1979.

[20] Mamalis, A.G., Robinson, M., Carruthers, J., “The energy absorption properties of composite materials: A literature survey”. Composite Structures 37, pp 109-134, 1997

[21] LS-Dyna User's Manual Version 970, 2002.

[22] MADYMO User Manual Version 6.0.1,1999.

[23] Tay, T.E., Lee, K.H., Ramakrishna, S., Shen, F. "Modelling the crushing behavior of composite tubes", Key Engineering Materials, Vols. 141-143 , pp. 777-790, 1998.

[24] Schweizerhof, K., Weimar, K., Th. Munz, Rottner, T., “Crashworthiness Analysis with Enhanced Composite Material Models in LS-DYNA - Merits and Limits, 1999.

[25] www.crashtest.com,US NCAP (NHTSA**)** Crash testing procedures, cited 2006.

[26] Sheshadri, A., “Design and Analysis of a composite beam and its use in reducing the side-impact injuries in a sedan”, M.S. Thesis, Department of Mechanical Engineering, Wichita State University, Wichita, 2006.